คาร์บอนไดออกไซด์รีฟอร์มมิงของมีเทนบน Al_2O_3-H-Beta ซึ่งมี
นิกเกิล โคบอลต์ ที่เตรียมด้วยวิธีโซลเจล

นางสาวพรธิชา กาทอง

วิทยานิพนธ์นี้เป็นส่วนหนึ่งของการศึกษาตามหลักสูตรปริญญาวิศวกรรมศาสตรมหาบัณฑิต
สาขาวิชาวิศวกรรมเคมี ภาควิชาวิศวกรรมเคมี
คณะวิศวกรรมศาสตร์ จุฬาลงกรณ์มหาวิทยาลัย
ปีการศึกษา 2557

CO_2 REFORMING OF METHANE ON Ni, Co-CONTAINING Al_2O_3-H-BETA PREPARED BY SOL-GEL METHOD

Miss Pornthicha Katong

A Thesis Submitted in Partial Fulfillment of the Requirements
for the Degree of Master of Engineering Program in Chemical Engineering
Department of Chemical Engineering
Faculty of Engineering
Chulalongkorn University
Academic Year 2014

Thesis Title	CO_2 REFORMING OF METHANE ON Ni, Co-CONTAINING Al_2O_3-H-BETA PREPARED BY SOL-GEL METHOD
By	Miss Pornthicha Katong
Field of Study	Chemical Engineering
Thesis Advisor	Assistant Professor Suphot Phatanasri, D.Eng.

Accepted by the Faculty of Engineering, Chulalongkorn University in Partial Fulfillment of the Requirements for the Master's Degree

.....Dean of the Faculty of Engineering

(Professor Bundhit Eua-arporn, Ph.D.)

THESIS COMMITTEE

.....Chairman

(Associate Professor Joongjai Panpranot, Ph.D.)

.....Thesis Advisor

(Assistant Professor Suphot Phatanasri, D.Eng.)

.....Examiner

(Associate Professor Bunjerd Jongsomjit, Ph.D.)

.....External Examiner

(Assistant Professor Soipatta Soisuwan, D.Eng.)

พรธิชา กาทอง : คาร์บอนไดออกไซด์รีฟอร์มมิงของมีเทนบน Al_2O_3-H-Beta ซึ่งมี นิกเกิล โคบอลต์ ที่เตรียมด้วยวิธีโซลเจล (CO_2 REFORMING OF METHANE ON Ni, Co-CONTAINING Al_2O_3-H-BETA PREPARED BY SOL-GEL METHOD) อ.ที่ปรึกษาวิทยานิพนธ์หลัก: ผศ. ดร.สุพจน์ พัฒนะศรี, 158 หน้า.

ในงานวิจัยนี้ได้ทำการศึกษาผลของโลหะชนิดเดี่ยว (10%โดยน้ำหนักของนิกเกิล และ 10% โดยน้ำหนักของโคบอลต์) และโลหะชนิดผสม (5%โดยน้ำหนักของโคบอลต์) บนตัวรองรับต่างชนิดกัน ซึ่งประกอบด้วยตัวรองรับชนิด H-Beta-Al_2O_3, Al_2O_3-SiO_2 ที่ถูกเตรียมด้วยวิธีโซลเจลและตัวรองรับชนิดอะลูมินาทางการค้า นอกจากนี้ยังศึกษาผลของความแตกต่างของอัตราส่วนการเติมโลหะชนิดผสมนิกเกิล-โคบอลต์ในอัตราส่วนของโลหะนิกเกิลต่อโคบอลต์ที่ 1:3, 1:1 และ 3:1 บนตัวรองรับชนิด H-Beta-Al_2O_3 โดยการทดสอบความว่องไวในการเกิดปฏิกิริยาในการทำปฏิกิริยาคาร์บอนไดออกไซด์รีฟอร์มมิงของมีเทน ที่อุณหภูมิ 700°C ความดันบรรยากาศ ซึ่งจากผลการศึกษาพบว่า อัตราส่วนการเติมโลหะชนิดผสมนิกเกิล-โคบอลต์ที่เหมาะสมคือ ในอัตราส่วนของโลหะนิกเกิลต่อโคบอลต์ที่ 1:1 บนตัวรองรับชนิด H-Beta-Al_2O_3 ที่ถูกเตรียมด้วยวิธีโซลเจล ให้ค่าความว่องไวสูงที่สุดในปฏิกิริยาคาร์บอนไดออกไซด์รีฟอร์มมิงของมีเทน โดยความสามารถที่ดีกว่าตัวเร่งปฏิกิริยาชนิดอื่นนั้น สามารถอธิบายได้เนื่องจากตำแหน่งที่ว่องไวของตัวเร่งปฏิกิริยาที่เหมาะสมของโลหะนิกเกิลและโคบอลต์และขนาดของ NiO และCoO ที่เล็กกว่าตัวเร่งปฏิกิริยาชนิดอื่น ซึ่งปัจจัยดังกล่าวจะส่งผลทำให้โลหะมีการกระจายตัวที่สูงซึ่งจะทำให้ความสามารถในการรีดิวซ์ตัวเร่งปฏิกิริยาที่ง่ายขึ้นและอุณหภูมิในการรีดิวซ์ของตัวเร่งปฏิกิริยาที่ต่ำลง นอกจากนี้อัตราส่วนการเติมโลหะชนิดผสมนิกเกิล-โคบอลต์ที่เหมาะสมคือ ในอัตราส่วนของโลหะนิกเกิลต่อโคบอลต์ที่ 1:1 สามารถที่จะปรับปรุงการกระจายตัวของโลหะนิเกิลทำให้สามารถลดการเกิดการรวมตัวของโลหะนิกเกิลได้ ซึ่งคุณสมบัตินี้จะสะท้อนให้เห็นถึงความต้านทานการลดการคาร์บอนที่สูงในตัวเร่งปฏิกิริยาที่มีการเติมโลหะโคบอลต์

ภาควิชา วิศวกรรมเคมี ลายมือชื่อนิสิต .....

สาขาวิชา วิศวกรรมเคมี ลายมือชื่อ อ.ที่ปรึกษาหลัก .....

ปีการศึกษา 2557

5670291721 : MAJOR CHEMICAL ENGINEERING
KEYWORDS: CARBON DIOXIDE REFORMING OF METHANE / BIMETALLIC CATALYST / CO CATALYST / HYDROGEN PRODUCTION / H-BETA ZEOLITE

PORNTHICHA KATONG: CO_2 REFORMING OF METHANE ON Ni, Co-CONTAINING Al_2O_3-H-BETA PREPARED BY SOL-GEL METHOD. ADVISOR: ASST. PROF. SUPHOT PHATANASRI, D.Eng., 158 pp.

In the present research, the effect of monometallic (10%wt.Ni, 10%wt.Co) and bimetallic (5%wt.NiCo) on different supports are H-Beta-Al_2O_3, Al_2O_3-SiO_2 prepared by sol-gel method, and Gamma-alumina commercial catalysts. In addition, to study the effect of bimetallic catalysts with different loading ratio of nickel metal and cobalt metal on H-Beta-Al_2O_3 supports. Loading ratios of nickel and cobalt indicates as followed 1:3, 1:1, and 3:1. The catalytic activity tests for carbon dioxide reforming of methane at 700°C and atmospheric pressure. It was found that the optimize bimetallic (5%wt.Ni5%wt.Co) which contained Ni:Co in a ratio of 1:1 supported on H-Beta-Al_2O_3 catalyst prepared by Sol-gel exhibit highest methane and carbon dioxide conversion in carbon dioxide reforming of methane reaction. The superior catalytic performance can be explain by the optimize amount of nickel and cobalt active sites and the smaller with NiO and CoO particles due to higher dispersion implied an easier reducibility and a shift the reduction temperature toward lower temperature. In Addition, the optimize cobalt addition which contained Ni:Co in a ratio of 1:1 has improving nickel metal dispersion of catalysts due to reduce the agglomerate of nickel particles. These features mirror a substantially higher resistance to carbon deposition of cobalt-containing catalysts.

Department: Chemical Engineering Student's Signature .....
Field of Study: Chemical Engineering Advisor's Signature .....
Academic Year: 2014

ACKNOWLEDGEMENTS

First of all, the authors would like to express my sincere gratitude and appreciation to my advisor, Assistance Professor Suphot Phatanasri for their valuable suggestions, stimulation, support, encouragement and useful discussions throughout this research and devotion to revise this thesis. The author would also be grateful to Associate Professor Joongjai Panpranot, as the chairman, Associate Professor Bunjerd Jongsomlit, and Assistance Professor Soipatta Soisuwan as the members of the thesis committee.

Besides, the author would like to be thankful her parents who always pay attention to her all the times, suggestions for each problems and encouragements. The most success of graduation is invested to her parents.

Finally, the author wishes to thank the member of the Center of Excellence on Catalysis and Catalytic Reaction Engineering, Department of Chemical Engineering, Faculty of Engineering, Chulalongkorn University for their advices and nice friendship. To the many others, not specifically named, who have provided her with support and encouragement I would like to thank you sincerely.

CONTENTS

Page

Page

Page

Page

Page

Page

LIST OF TABLES

LIST OF FIGURES

CHAPTER I

INTRODUCTION

1.1 Motivation

Global warming and greenhouse effect are the most of serious issues that the world is facing today. The greenhouse effect is a natural process that keeps the earth at temperatures that viable temperature condition [1,2]. Energy from the sun warms the earth when its heat rays are absorbed by greenhouse gasses and became trapped in the atmosphere [3,4]. Some of the most common greenhouse gasses are carbon dioxide and methane. Carbon dioxide, which comes from deforestation and fuel combustion, is the predominant factor resulting in the CH_4, although it has no direct effect on the climate change, it is more heat-trapping and it was oxidized capacity in the atmosphere than a molecule of CO_2. Moreover, the damage of ozone layer comes from several sources; first the most problematic are those coming from the burning of fossil fuels in power plants [5,6]. Second is the burning of gasoline in transportation, which continues to increase because of our increasing demand for cars and also increasing in worldwide consumption [7]. Third, deforestation results in larger amounts of CO_2 remain in the atmosphere [8]. Global warming leads to many problems that affect our environment.

Therefore, in recent years many attempts in industrial processes have been made to efficiently convert CO_2 to useful and non-pollution compound. Specifically, the CO_2 reforming of methane (DRM, Eq. (1)) [9] is an attractive way to utilize CO_2 and CH_4 emissions that contributes to the greenhouse gas reduction [10]. The reaction is important to increasing the hydrogen production that was used in ammonia synthesis fuel cell and hydrogenation reaction [10]. Moreover, carbon dioxide reforming of methane reaction used produce syngas ($CO+H_2$), which can be utilized as feedstock for methanol, dimethyl ether production and/or Fischer-Tropsch synthesis.

$$CH_4 + CO_2 \leftrightarrow 2H_2 + 2CO \qquad \Delta H^{o} = 247 \text{ kJ /mol} \qquad (1)$$

$$CO_2 + H_2 \leftrightarrow H_2O + CO \qquad \Delta H^{o} = 41.2 \text{ kJ /mol} \qquad (2)$$

Because of this reaction is highly endothermic character (Eq.1) [1]. It requires a high reaction temperature [11]. This reaction accompanied by secondary reaction of the reverse water gas shift (RWSG, Eq.2) [4]. This reaction is highly endothermic reaction at high temperature. However, the problems are deactivation and carbon composition of catalyst by side reactions; partial Oxidation of CH_4, Boudouard reaction and reverse carbon gasification are shown in Eq (3)-(5), respectively [12]. It produces carbon composition on catalysts.

$$CH_4 \leftrightarrow C + 2H_2 \qquad \Delta H^{o} = 75 \text{ kJ /mol} \qquad (3)$$

$$2CO \leftrightarrow C + CO_2 \qquad \Delta H^{o} = -172 \text{ kJ /mol} \qquad (4)$$

$$CO + H_2 \leftrightarrow H_2O + C \qquad \Delta H^{o} = -131 \text{ kJ /mol} \qquad (5)$$

Catalysts contain noble metals such as Pt, Ru and Rh, have high activity and selectivity for the DRM reaction because of good stability towards coke depositions. However they are expensive which limit the industrial application [4]. From a point of economy, Nickel is the popular choice because of its high activity which is similar to those noble metal [13]. Moreover, a major problem is the carbon decomposition on the surface of Nickel catalyst, which leads to agglomerate of catalyst's active sites and to deactivate at high temperature [4,9]. To solve this problem, some researches have suggested about cobalt metal because of its behavior towards the protection of carbon deposition and the better dispersion on support [5,8]. Thus, comparing metal, which consist of Ni, Co and NiCo catalysts are important to investigate their catalytic performance. Beside the addition of the metal, the catalyst support also plays on important role in the reaction [3,5]. Several research groups have studied effect of the support to catalytic activity. Amorphous solids (such as SiO_2 [1], MgO [14], TiO_2 [15], α-Al_2O_3 [5]) and crystalline solids (such as zeolite [16], γ-alumina [14]) have been reported as attractive support for DRM reaction. Alumina support was brought in exhibits high initial activity, despite its low coke resistance [6]. Therefore, in this study modify catalyst support, H-Beta zeolite, is used. H-Beta support has well-

defined structure, high surface area, high thermal stability and potential to deliver high metal dispersion [17].

In this work to investigate the effect of monometallic (10%wt.Ni, 10%wt.Co) and bimetallic (5%wt.NiCo) on different supports which are H-Beta-Al_2O_3, Al_2O_3-SiO_2 prepared by sol-gel method, and Gamma-alumina commercial catalysts was studied. Moreover, to study the effect of bimetallic catalysts with different loading ratio of nickel metal and cobalt metal on H-Beta-Al_2O_3 supports. Loading ratios of nickel and cobalt indicate as followed 1:3, 1:1, and 3:1. All catalysts were prepared by the incipient wetness impregnation method. The catalytic performances were tested in carbon dioxide reforming of methane

1.2 Objective of Research

1. To study the effect of different supports (i.e. H-Beta zeolite, Al_2O_3-SiO_2 prepared by sol-gel method and alumina commercial) on their catalytic activity and coke formation in carbon dioxide reforming of methane reaction.

2. To compare between monometallic (Ni,Co) and bimetallic (NiCo) and various ratios of Ni:Co loading which are 3:1, 1:1 and 1:3 to see their catalytic performance and coke formation in carbon dioxide reforming of methane.

1.3 Scope of Research

1.3.1 Study about the relating research and summary toward the interesting literature reviews.

1.3.2. Prepare monometallic (Ni, Co) approximately 10 wt % and bimetallic (5 wt% Ni5%wt.Co) on supports (i.e. H-Beta zeolite, Al_2O_3-SiO_2 prepared by sol-gel method and alumina commercial, respectively)

1.3.3. Preparation of bimetallic catalysts various ratio of Ni/Co loading of H-Beta support with 1:3, 1:1 and 3:1. Catalysts were prepared by incipient wetness impregnation method.

1.3.4 Characterize physical properties of catalysts by using various techniques using X-ray diffraction (XRD), Nitrogen physisorption, Temperature program reduction (H_2-TPR), Temperature-programmed desorption (NH_3-TPD), Scanning Electron Microscopy (SEM-EDX), H_2-chemisorption, and Thermogravimetric analysis (TGA)

1.3.5 Investigation the performance of the prepared catalysts with carbon dioxide reforming of methane reaction under the following condition:

Before the DRM testing, the catalysts were heated to 600°C at heating rate 10°C/min with pure hydrogen (50 ml/min), and then reduced the catalysts for 1 hour with pure hydrogen (50ml/min). The synthesized catalysts were tested in dry methane reforming reaction (DRM) at 700°C in a fixed-bed continuous-flow quartz reactor. Feed mixture composing of CH_4:CO_2 50:50 Vol% was used as a reactant. Reactant gas was continuously supplied by mass flow controller at the rate 60 ml/min. The exit gas was analyzed by Thermal Conductivity Detector-type gas chromatograph.

1.4 Research Methodology

1.4.1 Part I: effect of monometallic (10%wt.Ni, 10%wt.Co) and bimetallic (5%wt.NiCo) on different supports which are H-Beta-Al_2O_3, Al_2O_3-SiO_2 prepared by sol-gel method and Gamma-alumina commercial.

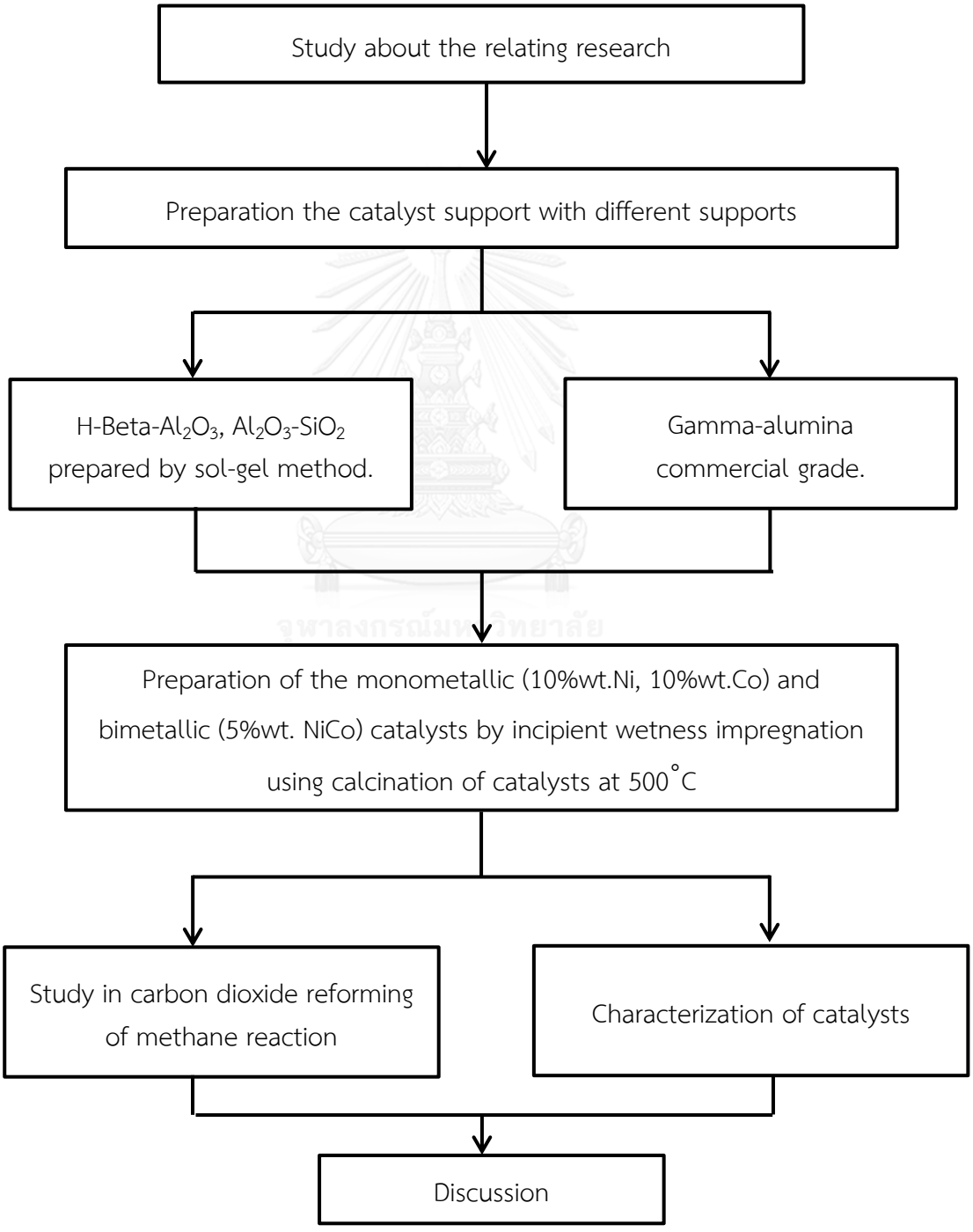

1.4.2 Part II: effect of 5%wt.NiCo catalysts on different supports, which are H-Beta-Al_2O_3, Al_2O_3-SiO_2 and Gamma-alumina commercial support.

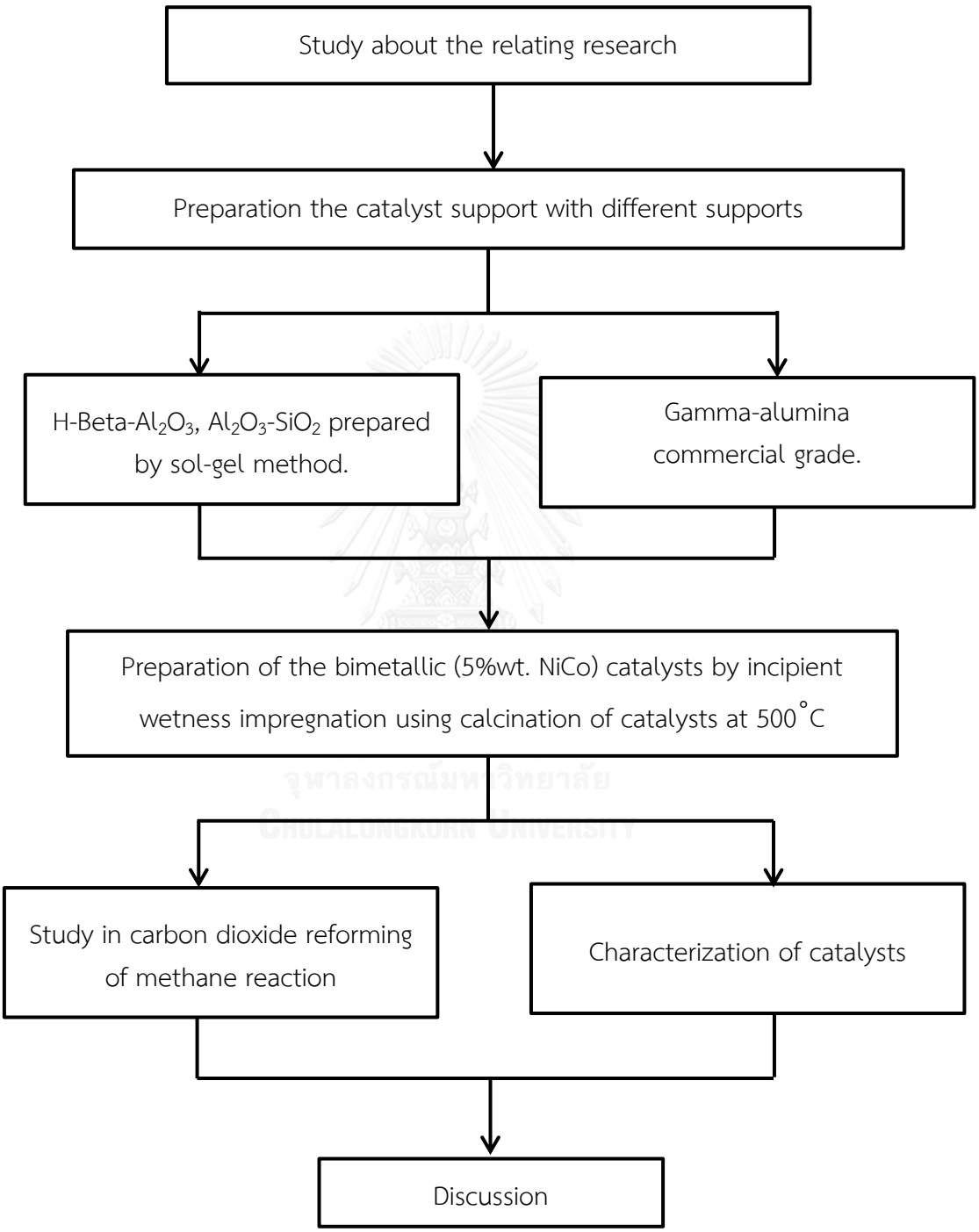

1.4.3 Part III: effect the catalysts were loading with nickel metal and cobalt metal of H-Beta-Al_2O_3 supports with 1:3, 1:1 and 3:1 various ratios between nickel and cobalt loading.

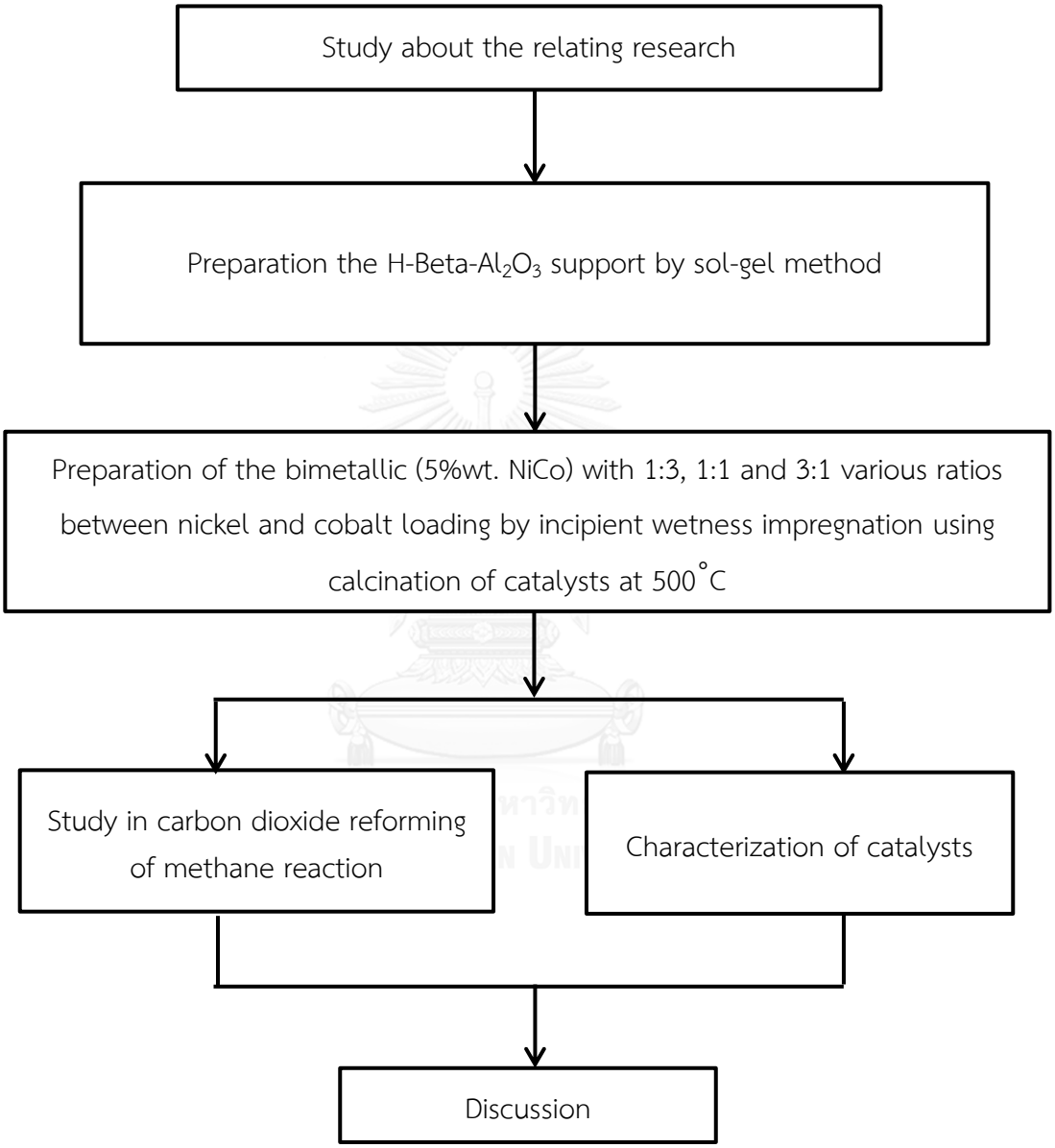

CHAPTER II

LITERATURE REVIEWS

2.1 Effect of metal catalyst

Z. Jianguo et al. (2008) [11] studies of Ni-Co bimetallic on MgO support prepared by co-precipitation method, effect of bimetallic loading, carbon formation on carbon dioxide reforming of methane. The catalysts were prepared with Ni:Co loadings ranging between 1.83Ni14.5Co by wt.% and 2.76Ni12.9Co by wt.%, respectively. They studied the catalyst's performances on carbon dioxide reforming of methane at 750 °C and 1 atm using a high GHSV of 180,000 ml/gcat h. The result showed the lower loading of Ni-Co (1.83–3.61 wt.% for Ni and 2.76–4.53 wt.% for Co) had higher activity and stability than Ni-Co loading (5.28–14.5 wt.% for Ni and 7.95–12.9 wt.% for Co). The research discovered 1.) Cobalt has smaller particle which leads to better dispersion than Nickel. Thus, Co improved the dispersion on catalyst. 2.) Loading content influence coke formation. The lower bimetallic loading to complete eliminate carbon dispersion of the catalysts because the lower Ni-Co loading (<10 nm) is believed to complete the suppression of the carbon formation during reaction.

S. In et al. (2014) [8] applied Ni/γ-Al_2O_3, CoNi/γ-Al_2O_3, and MgCoNi/γ-Al_2O_3 catalysts in the carbon dioxide reforming of methane reaction and then studied effect of the promoter, Co and Mg, on coke formation. MgCoNi/γ-Al_2O_3 exhibited the highest catalytic performance. The research found also a promoting effect of MgO in CoNi/γ-Al_2O_3 catalyst [18]. The addition of MgO helps accelerating the decomposition/dissociation of CH_4 and CO_2. Moreover, bimetallic Ni-Co reduces coke formation in CDR [13]. However, the coke formation on the 3Mg3Co3Ni catalyst mainly consisted of the amorphous carbon species which is easily oxidizable.

Moreover, there is no fatal encapsulating carbon species, which causes the deactivation of the catalyst.

D. San Jose´-Alonso et al. (2013) [3] studied effect of Co and Ni loading on alumina supported catalysts (4.0, 2.5 and 1.0 wt%) have been prepared by excess solution impregnation using aqueous solutions of $Ni(NO_3)_2.6H_2O$ and $Co(NO_3)_2.6H_2O$. This research found that the low metal loading of Co and Ni on alumina supported catalysts produce very low amount of carbon in the dry reforming of methane at 700 °C and 1 atm. The lower metal loading is due to the presence of small particles of catalysts. It hinders the growing of carbon filaments. While as, Co loading has less, is deactivated during the first minutes of reaction due to the formation of $CoAl_2O_4$ as inactive of this reaction.

S. Siddhartha et al. (2014) [7] synthesized Alumina supported nickel (Ni/Al_2O_3), nickel-cobalt ($Ni\text{-}Co/Al_2O_3$) and cobalt (Co/Al_2O_3) catalysts amount of 15% metal for dry methane reforming at 600°C 1 atm. The research found that added Co to catalyst improves its activity and stability because of the following reasons: 1.) Co has smaller metal particles also the addition of Co helps better metal dispersion. 2.) Interaction of Co with the supported Ni [16] resulting in the formation of a stable Ni-Co alloy and a synergy between Ni and Co. 3.) Co prevents the oxidation of metal and leads to higher activity for methane decomposition. In addition, synthesized catalyst contained Ni:Co in a ratio of 3:1 resulted in improved catalytic performance and decreased carbon formation because Co retards carbon formation between Ni particle.

K. Takanabe et at. (2013) [18] studied the effect of reduction temperature on the catalytic behavior of $10\%Co/TiO_2$ catalysts in carbon dioxide reforming of methane. The result shown that the Co/TiO_2-anatase catalysts reduce at lower

temperature (<1073K) had stable activities. On the contrary, the catalysts reduced at higher temperature, the crystal phase of TiO_2 is convert from anatase to rutile, cause almost no activity. Moreover, it does not found the carbon deposition for any of the Co/TiO_2 catalysts.

E. Ruckenstien et al. (2012) [19] studied the reaction behavior and carbon deposition during the carbon dioxide reforming of methane of Co over the γ-Al_2O_3 catalysts with varied Co content loading between 2 and 20%wt. which are calcination temperature between 500°C and 1000°C. The results found that the stability of Co/γ-Al_2O_3 were strongly dependent on the calcinations temperature and Co content loading. The stable activities have been shown at 6%wt.Co/γ-Al_2O_3, T=500°C and 9%wt.Co/γ-Al_2O_3, T=1000°C. However, the catalysts with high Co loadings (>12%wt.), remarkable amounts of carbon deposited during reaction, and deactivation was occurred. Moreover, the 2%wt. Co/γ-Al_2O_3 also found serious deactivation, caused by both the carbon deposition for T=500°C or the oxidation of metallic sites for T= 1000°C. Therefore, the mechanisms of deactivation have two different, carbon deposition and oxidation of metallic site.

J. Juan-Juan et al. (2015) [20] studied the Ni, Co and Ni-Co alumina supported catalyst (9%wt. nominal metal content) in carbon dioxide reforming of methane. The result showed that the catalysts with the highest cobalt content, Co(9) and Ni-Co(1-8) catalysts are the most active and stable, but produced a large amount of carbon. The higher activity shows by cobalt rich catalysts is related with the higher activity of this metal for methane decomposition reaction, which is the rate limiting step of overall reaction. Moreover, the stability of cobalt rich catalysts also related with the appeared of large particles involved in long term conversion, due to they produce non-deactivating carbon.

2.2. Effect of catalyst support

S. Damyanova et al. (2012) [21] prepared Ni catalysts on different supports δ,θ-Al_2O_3,$MgAl_2O_4$, SiO_2-Al_2O_3 and ZrO_2-Al_2O_3. The catalyst samples were tested in the reaction of reforming of methane with CO_2 at 700 °C. This work was shown different supports influence the catalyst's structure, catalytic activity and stability of the reaction. Ni/$MgAl_2O_4$ catalyst showed the highest catalytic performance due to the presence of small well dispersed of Ni particles, with size of 5.1nm. Which absence filamentous carbon because Ni/$MgAl_2O_4$ was strong interaction between Ni oxide species and $MgAl_2O_4$ support block the metal Ni sintering and the coke formation that leads to the high stability of reaction. However, Ni on SiO_2-Al_2O_3 catalyst showed the lowest activity because the agglomeration of nickel particles and filamentous carbon under reaction conditions.

A. Luengnaruemitchai et al. (2008) [22] synthesized Ni metal on different types of zeolite supports; zeolite A, zeolite X, zeolite Y, and ZSM-5. All supports were prepared by incipient wetness impregnation, and then reacted in the catalytic carbon dioxide reforming of methane into synthesis gas at 700 °C, and under atmospheric pressure. Firstly, researcher chose zeolites for reaction because it had well-defined structure, high surface area, high thermal stability, and high affinity for CO_2, which expected to enhance both catalytic activity and stability. The studies found that Ni/zeolite Y showed better catalytic performance than the other studied zeolites because zeolite Y support reduced carbon formation effect of catalysts. The research found the deactivation of catalyst not observed on catalyst. Finally, 7 wt.% Ni was the optimum value for all zeolites supported in dry methane reforming reaction.

S. Linping et al. (2010) [23] studied the effect of rhodium dispersion on catalytic activity and coke resistance on the catalyst. Researchers synthesized Rh/H-Beta zeolite with varied Rh metal loading from 0.5wt% to 4.0wt% in various reaction temperature range 600-900 °C. The results indicated the catalysts with Rh loading of 0.5 wt% and 1.0 wt% exhibiting high resistance to coke because H-Beta has high thermal stability with three-dimensional interlinking channels of 12-membered ring. They suggested that high dispersion of rhodium on H-Beta at low rhodium loading leads to the high activity for this reaction.

A. Fakeeha et al. (2013) [16] studied the stability of different supports on dry methane reforming reaction with varied reaction temperature (500, 600 and 700 °C). Ni/γ-Al_2O_3, Ni/Y-zeolite and Ni/H-ZSM-5 catalysts were prepared using the incipient wetness impregnation method. The research found that 5%wt Ni/H-ZSM-5 catalysts obtained lower carbon deposition for DRM reaction leading to high stability. In addition, reaction temperature was the main reason for this deactivation of the catalysts was carbon deposition after reaction test. Based on thermodynamics, at a high reaction temperature (>650 °C) coke was expected to be formed mainly via CH_4 decomposition.

M. Nagai et al. (2013) [24] studied the effect of catalyst pretreatment, the ratio of CH_4/CO_2 and compared Rh supported different support are CeO_2 and Al_2O_3 in carbon dioxide reforming of methane using micro-reactor. The oxidized or reduced Rh/Al_2O_3 catalyst had better activity and the addition CO_2 enhanced formation of H_2 during the carbon dioxide reforming of methane. Furthermore, decrease the catalyst deactivation due to high catalytic performance. Rh/CeO_2 catalyst is lower activity than Rh/Al_2O_3.

H.Y. Wang et al. (2013) [4] studied the carbon dioxide reforming of methane using Rh (0.5%wt.) over the reduced supported. Two group of oxide, reducible (CeO_2, Nb_2O_5, TaO_5, TiO_2, and ZrO_2) and no reducible (γ-Al_2O_3, La_2O_3, MgO, SiO_2, and Y_2O_3) were used as supports. The no reducible metal oxide, (γ-Al_2O_3, La_2O_3, and MgO gave stable activities during reaction, and the activity increased in sequence; La_2O_3 < MgO $\approx$ γ-Al_2O_3. The stability of catalyst was described as the long activity, ZrO_2 and CeO_2 showed a very long activation period, but deactivation occurred of TaO_5 and TiO_2. Hence, the reducible oxide supported group gave lower yields of CO and H2 than the no reducible oxide supported group. Conclude, MgO and γ-Al_2O_3 were the most ability supported because they gave high performance of catalysts

L. Ji et al. (2009) [25] studied three cobalt-based catalysts with 10%wt. cobalt were prepared by conventional impregnation of commercial γ-Al_2O_3 support ($Co/Al_{CO\text{-}IM}$), Sol-gel method ($Co/Al_{SG\text{-}IM}$), and direct Sol-gel processing from organometallic compounds (Co/Al_{SG}), respectively. The result showed all three catalysts had the same activity at 750°C. While as, Co/Al_{SG} showed low catalytic activity with low reaction temperature (550-650°C), because of the formation of $CoAl_2O_4$. Nevertheless, it had the best carbon resistivity. Rapid and large carbon deposition occurred on $Co/Al_{CO\text{-}IM}$ catalyst. Compared with the $Co/Al_{CO\text{-}IM}$ catalyst, the Co/Al_{SG} had smaller metallic Co particles, more surface OH^- species and stronger metal-support interaction. These properties may useful for resistant of carbon formation.

CHAPTER III

Theoretical

3.1 Syngas and Hydrogen production

Hydrogen can be produced from several of feedstock [26]. These include fossil resources (such as natural gas and coal), and renewable resources, such as biomass and renewable energy sources (e.g. sunlight, wind, wave or hydro-power) [27]. A variety of process technologies can be used, including chemical, biological, electrolytic, photolytic and thermo-chemical [21]. Moreover, syngas produced through the following catalytic processes: partial oxidation, steam reforming, dry reforming and oxy-reforming processes [14]. These processed represent a very versatile intermediate in several synthetic routes, lead to ultra-clean liquid fuels and valuable raw chemicals from alternative sources to petroleum. Syngas and hydrogen currently are produced from natural gas by means of three different chemical processes:

3.1.1 Steam reforming (steam methane reforming – SMR) [15] is an effective commercial process. Steam reforming involves the endothermic conversion of methane and water vapor into hydrogen and carbon monoxide. Heat is often supplied from the combustion of the methane feed-gas. The process typically occurs at high reaction temperatures [28]. The gas product contains CO, which can be further converted to CO_2 and H_2 through the water-gas shift reaction [26].

$$CH_4 + H_2O \leftrightarrow CO + 3H_2 \qquad (6)$$

$$CO + H_2O \leftrightarrow CO_2 + H_2 \qquad (7)$$

3.1.2 Partial oxidation of natural gas is the process whereby hydrogen is produced through the partial combustion of methane with oxygen gas to yield carbon monoxide and hydrogen [9]. This process is an exothermic reaction which

heat is produced. Hence, a compact design can be achieved because there is no need for external heating for the reactor. produced CO is further converted to H_2 as described in equation (8) [1].

$$CH_4 + 1/2O_2 \leftrightarrow CO + H_2 \qquad (8)$$

3.1.3 Carbon dioxide reforming of methane or dry methane reforming (DRM) [1] is a method to produce synthesis gas (mixtures of hydrogen and carbon monoxide) from the reaction of carbon dioxide with hydrocarbons such as methane. Synthesis gas is conventionally produced via the steam reforming reaction [14]. In recent years, there are increased concerns on the contribution of greenhouse gases to global warming [15]. Replacing reactant from steam to carbon dioxide is suggested.

$$CH_4 + CO_2 \leftrightarrow 2H_2 + 2CO \qquad (9)$$

$$CO_2 + H_2 \leftrightarrow H_2O + CO \qquad (10)$$

Moreover, hydrogen applied in ammonia synthesis process, hydrotreating, hydrogenation, and fuel cell power [21].

3.2. Carbon dioxide reforming of methane

Dry (CO_2) reforming of methane (DRM) or carbon dioxide reforming of methane is a well-studied reaction in both scientific and industrial importance [10]. This reaction produces syngas that used in produce wide range of products, such as higher alkanes and oxygenates by means of Fischer–Tropsch synthesis [16]. This reaction is highly endothermic reaction at high temperature. However, the problems DRM are inevitably accompanied by carbon deposition. DRM is a highly endothermic reaction and requires operating temperatures at 800–1000 °C. 1.) to attain high equilibrium conversion of CH_4 and CO_2 to H_2 and CO. 2.) to minimize the thermodynamic driving force for carbon deposition [29]. Products of this reaction, first, hydrogen could be applied as fuel cells and more, as mentioned above [6], second, the synthesis gas, a mixture of carbon monoxide and hydrogen can be used

a raw material in the production of methanol, dimethyl ether and Fischer-Tropsch synthesis [14].

3.2.1 Overall reaction for carbon dioxide reforming of methane.

$CH_4 + CO_2 \leftrightarrow 2H_2 + 2CO$	ΔH^o= 247 kJ /mol	(5) CO_2 reforming of CH_4
$CO_2 + H_2 \leftrightarrow H_2O + CO$	ΔH^o= 41.2 kJ /mol	(6) Reverse water-gas shift
$CH_4 \leftrightarrow C + 2H_2$	ΔH^o= 75 kJ /mol	(7) CH_4 decomposition
$2CO \leftrightarrow C + CO_2$	ΔH^o= -172 kJ /mol	(8) Boudouard
$CO + H_2 \leftrightarrow H_2O + C$	ΔH^o= -131 kJ /mol	(9) Reverse carbon gasification

The reaction equilibrium for carbon dioxide reforming of methane (5), usually occurs simultaneously with reverse water-gas shift reaction (6), result a H_2/CO ratio of less than unity. In addition to the side reaction, CH_4 decomposition (7) and Boudouard reaction (8) were involved with carbon deposition on the catalyst's surface. The equilibrium constant of the carbon dioxide reforming of methane is a strongly endothermic reaction which the conversion is increasing seriously with increasing reaction temperature [27]. However, methane decomposition (7), and reverse water-gas shift reaction, are moderately endothermic reaction. Hence, the raising in temperature increases the rate of reaction [7]. The Boudouard reaction (8) and the reverse carbon gasification are exothermic reaction [8]. Therefore, the thermodynamic does not prefer at higher temperature. In conclusion, high temperature is more favorable for the carbon dioxide reforming of methane (5) than side reaction [12].

Because the carbon dioxide reforming of methane reaction is strongly endothermic it requires high temperature. Thus, the main drawback of this reaction is the rapid deactivation by carbon deposition on catalyst's surface, sintering of metallic particles, or metal oxidation. The selection of appropriate catalysts and supports are playing an important role to prevent the deactivation [6].

3.3 Sol-gel method

Sol-gel methods are synthesis materials from solutions, in which the gel formation is present at one of the process stages[30]. The most famous version of the sol-gel process is based on the processes of controlled hydrolysis of compounds, usually alkoxides $M(OR)_x$ (M = Si, Ti, Zr, V, Zn, Al, etc.) or corresponding chlorides, in an aqueous or organic medium, usually alcohol [18].

At the first stage of the sol-gel process the hydrolysis and poly-condensation reactions lead to the formation of a colloidal solution, i. e. sol, of hydroxide particles whose size does not exceed several dozen nm [24]. Increasing bulk concentration of the dispersed phase or other changes in external conditions (pH, solvent substitution) leads to the intense formation of contacts between particles and the formation of a monolithic gel, consists of a three dimensional continuous network, which encloses a liquid phase, In a colloidal gel, the network is built from agglomeration of colloidal particles. In a polymer gel the particles have a polymeric sub-structure made by aggregates of sub-colloidal particles [31]. Generally, the sol particles may interact by van der Waals forces or hydrogen bonds. A gel may also be formed from linking polymer chains. In most gel systems used for materials synthesis, the interactions are of a covalent nature and the gel process is irreversible. The gelation process may be reversible if other interactions are involved [32].

Sol-gel process is played by the processes of solvent removal from the gel (drying). Depending on the method the synthesis can result in various products (xerogels, ambigels, cryogels, aerogels), whose properties are described in the corresponding sections [33]. The common features of these products include the preservation of the Nano sizes of the structural elements and sufficiently high values of specific surface area (hundreds of m^2/g), although the bulk density can vary by hundreds of times. Most products of sol-gel synthesis are used as precursors in obtaining oxide Nano-powders, thin films or ceramics [11].

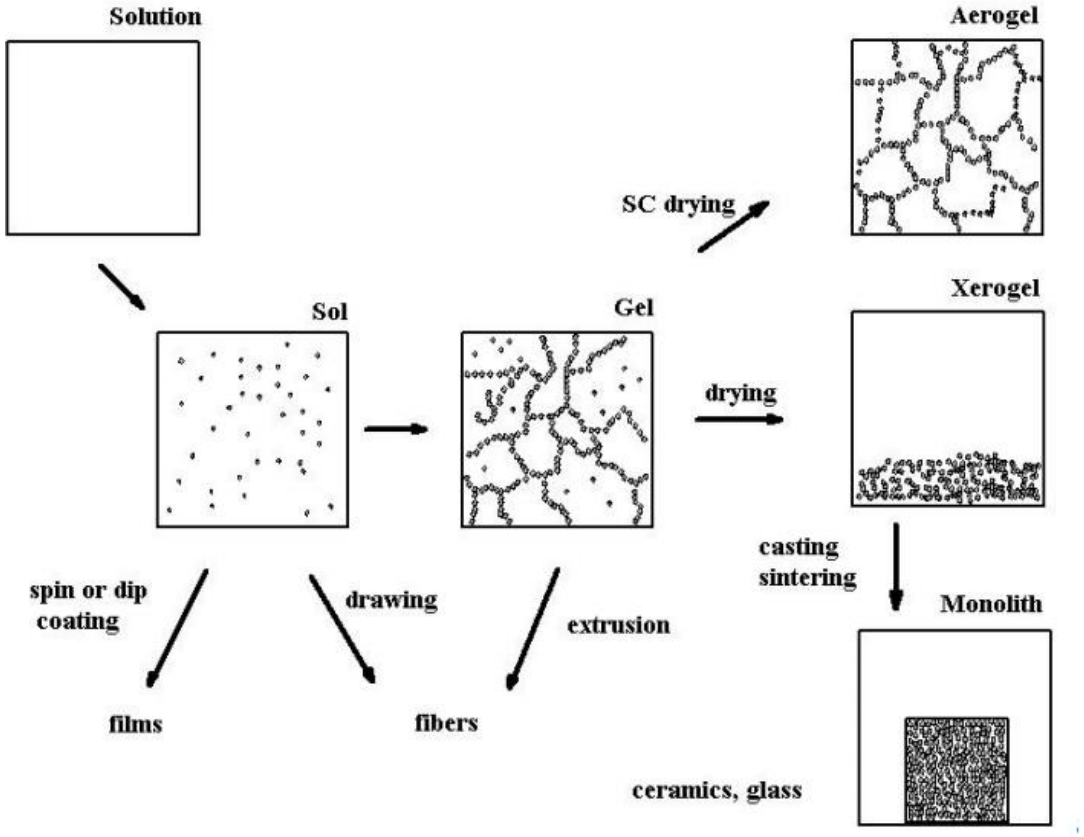

Figure 3.1 Sol-gel synthesis

3.4 Alumina

Alumina has been the most common commercial carriers because of their excellent thermal stability and wide range of chemical, physical, and catalytic properties. Alumina (Al_2O_3) or Aluminum Oxide is the only oxide formed by the metal aluminum and occurs in nature as the minerals corundum (Al_2O_3), diaspore ($Al_2O_3.H_2O$), gibbsite ($Al_2O_3.3H_2O$), and most commonly as bauxite [34], which is an impure form of gibbsite. The alumina consists of more than a dozen well-characterized amorphous or crystalline structures. It varies over wide range of surface area (0.5-600 m^2/g), pore size and pore distribution. Alumina is also the most important and wide-ranging use of alumina is in the field of ceramics [35].

The structures and properties of a given alumina depend on its preparation, purity, dehydration, and thermal treatment history [11]. The more acidic, high-surface-area alumina hydrate produced at relatively low temperature by precipitation from either acidic or basic solutions and are transformed by dehydration and treatment at high temperature to 'transitional' β, γ, η, χ, δ, and θ- alumina and ultimately α-alumina, all of lower surface area and acidity [36]. Some of the more well-known transformations are illustrated as a function of calcination temperature in Figure 3.2, and the physical and structural characteristics of important alumina phase formed at different calcinations temperatures are listed in Table 3.1 [8].

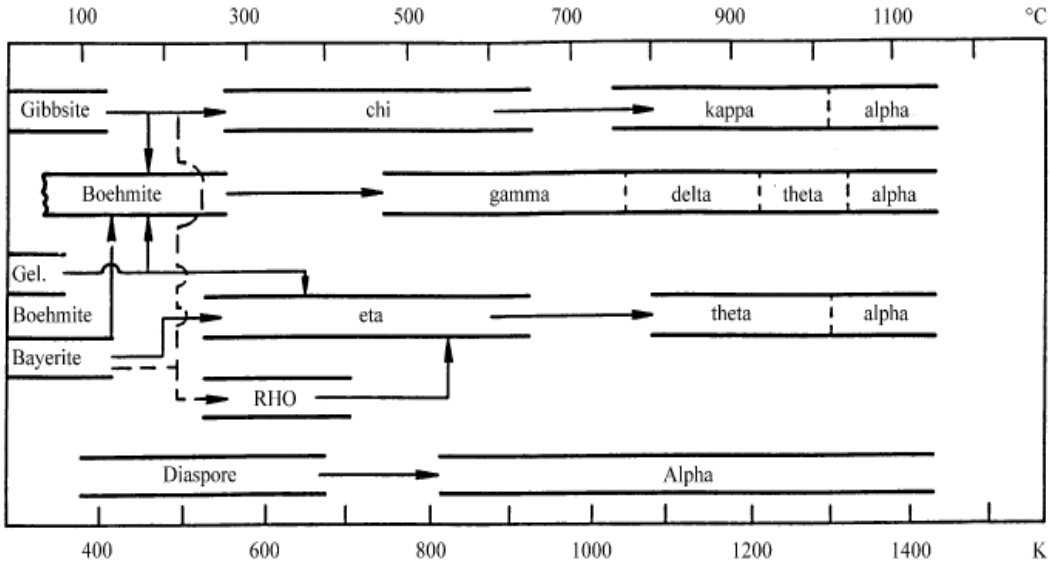

Figure 3.2 Alumina phase present at different temperatures

Table 3.1 Physical and structural characteristic of common aluminum oxides.

T_{calc}(°C)	Alumina phase	SA, (m^2/g)	V_{pore}, (cm^3/g)	$D_{pore,}$ (nm)
250	Pseudoboehmite	390	0.50	5.2
450	γ- alumina	335	0.53	6.4
650		226	0.55	9.8
850		167	0.58	14
950	δ- alumina	120	0.50	16.6
1050	θ- alumina	50	0.50	28
1200	α- alumina	1-5		

3.5 Zeolite

Zeolites are microporous, aluminosilicate minerals commonly used as commercial adsorbents and catalysts [28]. The term zeolite had been adsorbed by the material. Based on this, called the material zeolite, from the Greek *zein*, meaning "to boil" and líthos, meaning "stone" [37]. Zeolites are water-aluminosilicates of natural or synthetic origin with highly structures. They consist of SiO_4 and AlO_4^- tetrahedra, which are inerlinked through common oxygen atoms give a three dimensional network through which long channels run [38]. The interior characteristic of zeolites channels, which are characteristic of zeolites, are water molecules and mobile alkali metal ions, which can be exchanged with other cations. These compensate for the excess negative charge in the anionic framework resulting from the aluminum content [14]. The interior of the pore system, with its atomic-scale dimension, is the catalytically active surface of the zeolites. The inner pore structure depends on the composition, the zeolite type [39].

H-Beta Zeolite

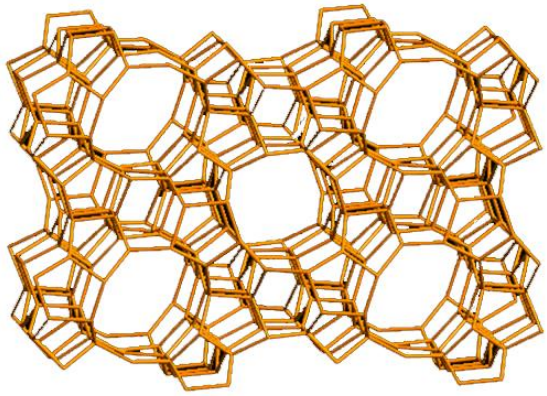

Figure 3.3 Structure of H-Beta zeolite

Zeolite beta (BEA) showed high catalytic activity. The structure of BEA was only recently determined, because the crystals of BEA always contains severe structure faulting and hence shows strong diffuse scattering in diffraction patterns [35]. The structure of BEA consists of an inter-grown hybrid of two distinct polytypic series of layers viz. polymorph A and B. Both the polymorphs have 3D network of 12-ring pores. The polymorph grows as two dimensional sheets and the sheets randomly alternate between the two [40]. BEA has two mutually perpendicular straight channels each with a cross section of 0.76 x 0.64 nm along the a and b direction and a helical channel of 0.55 x 0.55 nm along the c-axis. BEA is of great industrial interest because of its high acidity and larger pore size [40]. BEA has been successfully used for acid catalyzed reactions, catalytic cracking, aromatic and aliphatic alkylation. It has been shown that the acidity of BEA can be tuned by the incorporation of trivalent and tetravalent atoms (B, Al, V, Ti, Sn, Cr, Fe) into the framework positions of BEA [41]. In addition, H-Beta has well-defined structure, high surface area, high thermal stability , high affinities for carbon monoxide, and potential to deliver high metal dispersion [37].

3.6 Silica dioxide

Silica dioxide is a chemical compound that is an oxide of silicon with the chemical formula SiO_2. Silica is a group IV metal oxide, which has good abrasion resistance, electrical insulation and high thermal stability [42]. Silica occurs commonly in nature as sandstone, silica sand or quartzite. It is the starting material for the production of silicate glasses and ceramics. Silica is one of the most abundant oxide materials in the earth's crust [42]. It can exist in an amorphous form (vitreous silica) or in a variety of crystalline forms. Often it will occur as a non-crystalline oxidation product on the surface of silicon or silicon compounds [43].

3.7 Metal catalyst

Catalysts contain noble metal such as Pt, Ru and Rh, have high activity and selectivity for the DRM reaction in addition to good stability towards coke deposition, however there are still high cost [44]. From a point of economy, Industrial used Ni metal because Ni catalyst has high activity catalytic. Moreover, a major problem Ni catalyst is carbon deposition on surface, which leads to agglomerates of active site of catalyst and deactivation at high temperature [7, 8]. To solve this problem, some researches data reported about cobalt metal generally behavior towards the suppression of carbon deposition and cobalt has better dispersion on support.

3.7.1 Nickel

Nickel is a chemical element with symbol Ni and atomic number is 28. Nickel has high activity in chemical industrial such as a catalyst in carbon dioxide reforming of methane. Pure nickel shows a significant chemical activity that can be observed when nickel is powder to maximize the exposed surface areas on which reactions can occur, but larger pieces of the metal are slow to react with air at ambient conditions due to the formation of a protective oxide surface [7].

The nickel atom has two electron configurations, [Ar] $3d^8$ $4s^2$ and [Ar] $3d^9$ $4s^1$, which are transition metal The most common oxidation state of nickel is +2, but compounds of Ni^0, Ni^+, and Ni^{3+} are well known, as well as exotic oxidation states Ni^{2-}, Ni^{1-}, and Ni^{4+} [27].

Nickel(0) or Tetracarbonylnickel ($Ni(CO)_4$) is a volatile, highly toxic liquid at room temperature. On heating, the complex decomposes back to nickel and carbon monoxide:

$$Ni(CO)_4 \leftrightarrow Ni + 4CO \qquad (10)$$

The related nickel(0) complex bis(cyclooctadiene)nickel(0) is a useful catalyst in organonickel chemistry due to the easily displaced cod ligands [45].

Nickel(I) complexes are uncommon, however one example is the tetrahedral complex $NiBr(PPh_3)_3$. Many nickel(I) complexes feature Ni-Ni bonding, such as the dark red diamagnetic $K_4[Ni_2(CN)_6]$ [46]

Nickel(II) forms compounds with all common anions, i.e. the sulfide, sulfate, carbonate, hydroxide, carboxylates, and halides. Nickel(II) sulfate is produced in large quantities by dissolving nickel metal or oxides in sulfuric acid [47]. It exists as both a hexa- and heptahydrates. This compound is useful for electroplating nickel. Common salts of nickel, such as the chloride, nitrate, and sulfate, dissolve in water to give

green solutions containing the metal aquo complex $[Ni(H_2O)_6]^{2+}$. The structures of these solids feature octahedral Ni centers. Nickel(II) chloride is most common, and its behavior is illustrative of the other halides. Nickel(II) chloride is produced by dissolving nickel or its oxide in hydrochloric acid [48].

Nickel(III) and (IV) Numerous Ni(III) compounds are known, with the first such examples being Nickel(III) trihalophosphines [49]. Further, Ni(III) forms simple salts with fluoride or oxide ions, Ni(III) can be stabilized by **σ**-donor ligands. Ni(IV) is present in the mixed oxide $BaNiO_3$ [50].

.

3.7.2. Cobalt

Cobalt is a chemical element with symbol Co and atomic number 27. Like nickel, common oxidation states of cobalt include +2 and +3 [51], although compounds with oxidation states ranging from −3 to +4 are also known. A common oxidation state for simple compounds is +2 (cobalt(II)). These salts form the pink-colored metal aquo complex $[Co(H_2O)_6]^{2+}$ in water [8]. It is readily oxidized with water and oxygen to brown cobalt(III) hydroxide ($Co(OH)_3$). At temperatures of 600–700 °C, CoO oxidizes to the blue cobalt(II,III) oxide (Co_3O_4), which has a spinel structure. The reduction potential for the reaction [52]

$$Co^{3+} + e^- \longrightarrow Co^{2+} \qquad (11)$$

Several cobalt compounds are used in chemical reactions as oxidation catalysts. Cobalt acetate is used for the conversion of xylene to terephthalic acid, the precursor to the bulk polymer polyethylene terephthalate. Typical catalysts are the cobalt carboxylates [33]. They are also used in paints, varnishes, and inks as "drying agents" through the oxidation of drying oils. The same carboxylates are used to improve the adhesion of the steel to rubber in steel-belted radial tires [53].

Cobalt-based catalysts are also important in reactions involving carbon monoxide. Steam reforming, useful in hydrogen production, uses cobalt oxide-base catalysts. Cobalt is also a catalyst in the Fischer–Tropsch process [17], used in the hydrogenation of carbon monoxide into liquid fuels [54]. The hydroformylation of alkenes often rely on cobalt octacarbonyl as the catalyst, although such processes have been partially displaced by more efficient iridium- and rhodium-based catalysts [55].

CHAPTER IV

EXPERIMENTAL

In this chapter describes the experimental procedure used in this research, which can divide into three sections. Firstly, to explains support and catalysts preparation in this work in section 4.1. Secondly, the properties of the catalysts characterized by various techniques and discussed in section 4.2. Finally, the reaction studies in the carbon dioxide reforming of methane reaction explained in section 4.4.

4.1 Catalyst preparation

This research focuses on the monometallic and bimetallic catalysts on Al_2O_3-H-Beta and Al_2O_3-SiO_2 support, which are prepared by Sol-gel method and Gamma-alumina commercial support. Therefore, the details of preparation procedure are important.

4.1.1 Chemicals

The support and material precursor used for the catalysts preparation are listed in the Table 4.1

Table 4.1 Chemical used for the catalysts preparation

Chemical	Formula	Manufacturer
H-Beta-zeolites		TOSOH
aluminum isopropoxide >98%	$C_9H_{21}O_3Al$	Aldrich
Silica dioxide >98%	SiO_2	Aldrich
Alumina oxide >98%	Al_2O_3	Aldrich
Ethanol 99%	C_2H_5OH	Qrec New Zealand
Hydrochloric acid 37.7%	HCl	Sixma
Nickel (II) nitrate hexahydrate 98%	$Ni(NO_3)_2.6H_2O$	Fluka
Cobalt (II) nitrate hexahydrate 98%	$Co(NO_3)_2.6H_2O$	Carbo Erba

4.2 Material preparation

4.2.1 Support synthesis by sol-gel method

In this study H-Beta alumina and silica alumina were employed as support. Which were prepared by Sol-gel method. For this purpose, alumina isopropoxide used as precursor was first hydrolyzed in mixture of ethanol and deionized water with volume ratio by stirred at 80°C for 1 hr. Then, increase temperature of solution to 90°C for 15 min. After that H-Beta zeolite or silica powder was added into the solution with H-Beta zeolite or silica to Al_2O_3 weight ratio 1:3. Subsequently, added hydrochloric acid to solutions and controlled pH value equal to 2.5 with stirred at 90°C around 10 hr. After this step the sol was become viscous. The formed gel was dried overnight at 110°C and calcined at 550°C under air condition for 2 hr. 4.2.1 Catalysts synthesis by incipient wetness impregnation method

4.2.2 Catalysts synthesis by incipient wetness impregnation method

H-Beta zeolite alumina, silica alumina, and alumina commercial supported monometallic and bimetallic with varied compositions (10wt%Ni, 10wt%Co and 5wt%Ni5%wt.Co) were synthesized by the Incipient Wetness Impregnation (IWI) technique using nickel nitrate hexahydrate, and cobalt nitrate hexahydrate as Ni and Co precursors with appropriate concentration loading above. After impregnation, catalysts were kept at room temperature for 4 h in order to assure completely adequate distribution of metal. Then, the catalysts were dried at 110°C overnight and calcined at 500°C for 4 hr.

4.3 Catalyst characterization

4.3.1 X-Ray diffraction (XRD)

X-Ray diffraction (XRD) used to find the crystal structure of an unknown. Then XRD is used to investigate unknown material and determine of unknown solids. These features are critical to studies in geology, environmental science, material science, engineering and biology. Other applications include; characterization of crystalline materials, identification of fine-grained minerals. Thus this work, X-ray diffraction (SIEMENS D 5000), it was connected to a personal computer with Diffract AT version 3.3 program for fully control of XRD analyzer. The XRD is analyzer for the Cu Kα radiation between 20°-80° with a generator voltage and current of 30kV and 30mA respectively, to identify the crystallite phase. The step scan was 0.04°.

4.3.2 N_2-physisorption

Brunauer- Emmett-Teller Method (BET) method is the most widely used procedure to determine the surface area of solid materials and involve use of the

BET equation. BET is used to find specific surface area, pore volume and pore diameter of prepared catalysts. 0.1 grams of each samples were analyzed by N_2 adsorption desorption isotherm used micromeritics ASAP 2020 at liquid nitrogen temperature of -196°C. This research determined surface area and pore size distribution were calculated by BET and (BJH) methods respectively.

4.3.3 Scanning Electron Microscope (SEM-EDX)

A scanning electron microscope (SEM) is a type of electron microscope that produces images of a sample by scanning with a focused beam of electrons. SEM is the most widely used procedure to determine the morphology structure of sample. Other applications include the shape and size of the sample. The JEOL JSM-35 CF model at the Scientific was used for this work.

4.3.4 Thermogravimetric analysis (TGA)

The as-spun alumina fibers was subjected to the thermogravimetric and differential thermal analysis (Diamond Thermogravimetric and Differential Analyzer, TA Instruments SDT Q600) to determine the carbon content in the sample, as well as their thermal behaviors in the range of room temperature to 1000 °C. The analysis was performed at a heating rate of 10°C/min in 100ml/min flow air.

4.3.5 Hydrogen Temperature Programmed Reduction (H_2-TPR)

The reducing temperatures of prepared catalysts were observed by Temperature Programmed Reduction of Hydrogen (H_2-TPR) equipment by using Micromeritics chemisorp 2750 Pulse Chemisorption System. In experiment, 0.1g of the catalyst samples was placed in a quartz tube and the sample was pretreated in

flow of nitrogen at 500°C for 1 hr. The H_2-TPR profiles were obtained using 10%H_2 in Ar gas mixture flow rate of 25 ml/min from 40°C to 800°C. Hydrogen consumption during the TPR experiments was measured by the TCD as a function of temperature.

4.3.6 Temperature Programmed Desorption (NH_3-TPD)

Acid properties of prepared catalysts were observed by NH_3-TPD by using Micrometritics Chemisorb 2750 Pulse Chemisorption System. In experiment, 0.1g of the catalyst sample was place in a quartz tube and the sample was pretreated in a helium flow at 500°C for 1 h and then ammonia was introduced with helium. After that, the samples were heat from 40°C to 800°C while the temperature was elevated at a rate of 10°C /min. The desorbed ammonia was detected by a TCD.

4.3.7 Hydrogen Chemisorption

Hydrogen Pulse Chemisorption was performed by using Micrometritics Chemisorb 2750 and ASAP 2101CV.3.00 software unit fitted with a Thermal Conductivity Detector (TCD) to determine amount of H_2 chemisorption of catalyst. 0.1g of the catalyst sample was place in a quartz tube and the catalyst sample were reduced by H_2 at 600°C for 1 h at flow rate of 30 ml/min. H_2 was pulsed over reduced sample until TCD. The synthesized catalysts were tested in dry methane reforming reaction (DRM) at 700°C

4.4 Reaction in carbon dioxide reforming of methane

4.4.1 Material

In this reaction, the CH_4 in CO_2 feed was used to the reactant gas from Thai Industrial Gas Limited (TIG). The carbon dioxide reforming of methane was operated using 0.2 g catalyst packed in a fixed-bed continuous-flow quartz reactor feed mixture composition of CH_4:CO_2 50:50 Vol% the total gas flow rate was 60 ml/min. The catalyst was heat from ambient temperature to 600°C and reduced in flowing H_2 for 1h. under atmospheric pressure. Then, the synthesized catalysts were tested in dry methane reforming reaction (DRM) at 700°C. The exit gas was analyzed by Thermal Conductivity Detector-type gas chromatograph (Shimudzu, GC-8A) equipped with Porapak-Q and Molecular sieve 5A packed column.

4.4.2 Apparatus

The catalytic test was performed in a flow system as shown diagrammatically in Figure 4.1 The apparatus consisted of a fixed-bed continuous-flow quartz reactor, electrical furnace and temperature controller. The instruments used in this system are listed and explain flow;

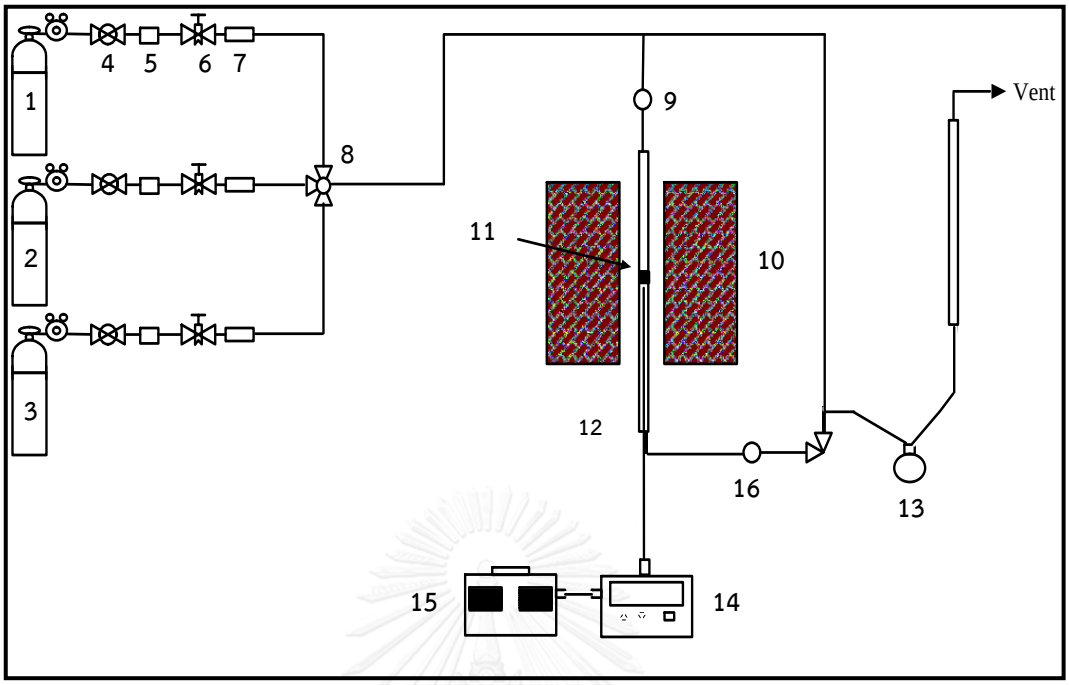

Figure 4.1 Flow Diagram of carbon dioxide reforming of methane

1. CH_4:CO_2 balance gas (1:1 ratio)
2. N_2 gas cylinder
3. H_2 gas cylinder
4. On-off valve
5. Filter
6. Mass flow controller
7. Check valve
8. 4-ways fitting
9. Inlet gas inject port
10. Furnace
11. Quartz tube
12. Thermocouple
13. Bubble flow
14. Temperature controller
15. Variable voltage transformer
16. outlet gas inject port

4.4.2.1 Reactor

The reactor was a quartz tube. Length of 47 mm and inner diameter of 12 mm. The catalyst was filled between quartz wool layers.

4.4.2.2 Temperature controller

There is a magnetic switch connected to a variable voltage transformer and a temperature controller this system included a thermocouple attached to the catalyst bed in reactor. A dial setting established a set point at any temperature within the ranged between 0°C to 1000°C

4.4.2.3. Electrical furnace

This supply required heated to the reactor for reaction. The reactor could be operated at 700°C

4.4.2.4 Gas controlling system

Gas was adjusted by a pressure regulator (0-120 psig), an on-off valve and needle valve were used adjust flow of gas.

4.4.2.5 Gas chromatographs

Gas composition in feed and product were analyzed by a Shimadzu GC8A gas chromatograph equipped with a TCD (Thermal conductivity detector). The operating conditions for each instrument are summarized in Table 4.2

Table 4.2 Operating condition of gas chromatograph in carbon dioxide reforming of methane

Gas Chromatograph	Shimazu, GC-8A	
Detector	TCD	TCD
Column	Porapack-Q	Molecular sieve 5A
Carrier gas	Ar	Ar
Carrier gas flow	50 ml/min	50 ml/min
Column temperature		
- Initial	70°C	70°C
- Final	70°C	70°C
Detector temperature	100°C	100°C
Injector temperature	100°C	100°C
Current (mA)	80	80
Analyzed gas	CO_2	H_2, CH_4, CO

4.4.3 Reaction method

The carbon dioxide reforming of methane was carried out at atmospheric pressure in fix-bed flow reactor (quartz tube, inner diameter 12 mm and length 47 mm) packed with 0.2 g catalyst. The reactor temperature was measured and controlled by K-type thermocouple positioned at the middle of catalyst bed. The catalyst was reduces in pure hydrogen (50ml/min) at 600°C for 1 h. Then, the hydrogen was replaced by pure nitrogen (50ml/min) and the system was heated (10°C/min) to the reaction temperature for 30 min. The catalytic performance test was carried out at 700°C. The feed gas consisted of methane and carbon dioxide (volume ratio 1:1), and feed flow rate 75 ml/min. The gas compositions of reactants and products were analyzed by TCD detector type gas chromatograph (Shimudzu, GC-8A) equipped with a Porapack-Q and Molecular sieve 5A packed column.

CHAPTER V

RESULTS AND DISCUSSION

The chapter is divided into three parts. Part (5.1) illustrates the effect of monometallic (10%wt.Ni, 10%wt.Co) and bimetallic (5%wt.NiCo) on different supports which are H-Beta-Al_2O_3, Al_2O_3-SiO_2 prepared by sol-gel method and Gamma-alumina commercial. Part (5.2) illustrates the effect of kinds of supports, which are H-Beta-Al_2O_3, Al_2O_3-SiO_2 and Gamma-alumina commercial support. All supports used 5%wt.Ni5%wt.Co which is prepared by incipient wetness impregnation. Part (5.3) illustrates the effect catalysts with different loading ratio of nickel metal and cobalt metal on H-Beta-Al_2O_3 supports. Loading ratios of nickel and cobalt indicates as followed 1:3, 1:1 and 3:1. Catalysts were prepared by incipient wetness impregnation method. The catalysts were characterized by XRD, N_2-physisorption, H_2-TPR, NH_3-TPD, H_2-chemisorption, TGA, SEM-EDX. The performance of the catalytic activity in the CO_2 reforming of methane also explained in this part.

5.1 Effect of monometallic (10%wt.Ni, 10%wt.Co) and bimetallic (5%wt.Ni5%wtCo) on different supports

5.1.1 Effect of monometallic (10%wt.Ni, 10%wt.Co) and bimetallic (5%wt.Ni5%wtCo) on H-Beta-Al_2O_3 support

5.1.1.1 Catalysts characterization

5.1.1.1.1 X-ray diffraction (XRD)

The XRD pattern show the monometallic (10%wt.Ni, 10%wt.Co) and bimetallic (5%wt.Ni5%wt.Co) on H-Beta-Al_2O_3 support. H-Beta-Al_2O_3 was prepared by sol-gel method. The monometallic and bimetallic catalysts which prepared by the incipient wetness impregnation were calcined at 500˚C. XRD result of each catalysts are shown in figure 5.1. The scans were recorded in the 2θ range of 20-80˚. The XRD diffraction peaks of all the Ni-loaded catalysts exhibit at 2θ degrees 32.6˚, 43.9˚and 64.1˚, which correspond to NiO or $NiAl_2O_4$ crystalline phase [20]. Also, the Co-loaded catalysts exhibit at 2θ degrees 26.3˚, 30.3˚, 36.4˚, 43.9˚, 58.1˚ and 64.1˚, which correspond to Co_3O_4 or $CoAl_2O_4$ crystalline phase [1]. The Co_3O_4 or $CoAl_2O_4$ and NiO and $NiAl_2O_4$ crystalline phase, there is no significant difference between phase structures [11]. This suggests that the Co_3O_4 or $CoAl_2O_4$ and NiO or $NiAl_2O_4$ may have similar morphology due to the detection limit of the XRD [41, 56]. In term of Ni and Co species, the XRD peaks corresponding to nickel oxide and cobalt oxide crystallite phase could not be separated because of their similar morphology [43]. The result showed H-Beta-Al_2O_3 has sharp peak, however, after added metal both in the monometallic (10%wt.Ni/H-Beta-Al_2O_3, (10%wt.Co/H-Beta-Al_2O_3) and bimetallic (5%wt.Ni5%wt.Co/H-Beta-Al_2O_3) catalyst can decrease the crystallite phases. The monometallic catalysts showed characteristic peaks of H-Beta-Al_2O_3 support with the corresponding peaks of metal oxides: Co_3O_4 and NiO, respectively. 5%wt.Ni5%wt.Co/H-Beta-Al_2O_3 was reported in the literature review that during the calcination Ni and Co tend to form $NiCo_2O_4$. However in bimetallic catalyst, no $NiCo_2O_4$ or Co_3O_4 were detected, most likely because of their small particle sizes [20, 43]. These features suggest the cobalt species have higher dispersion in the bimetallic system than in 10%wt.Co/H-Beta-Al_2O_3. The crystallite sizes of the catalysts calculated by Scherrer equation using XRD pattern. The average crystallite sizes after calcination at 500˚C are summarized in table 5.1 The size of the catalyst H-Beta-Al_2O_3 support was 30.9 nm and the sizes of catalysts containing 10wt%.Ni, 10wt%.Co and 5wt%.Ni5%wt.Co were 34.6 nm, 24.9 nm and 21.9 nm respectively.

The 10%wt.Ni/H-Beta-Al_2O_3 had the biggest size, 37.6 nm. It was reported in the literature review that the agglomerate of nickel particles [15].

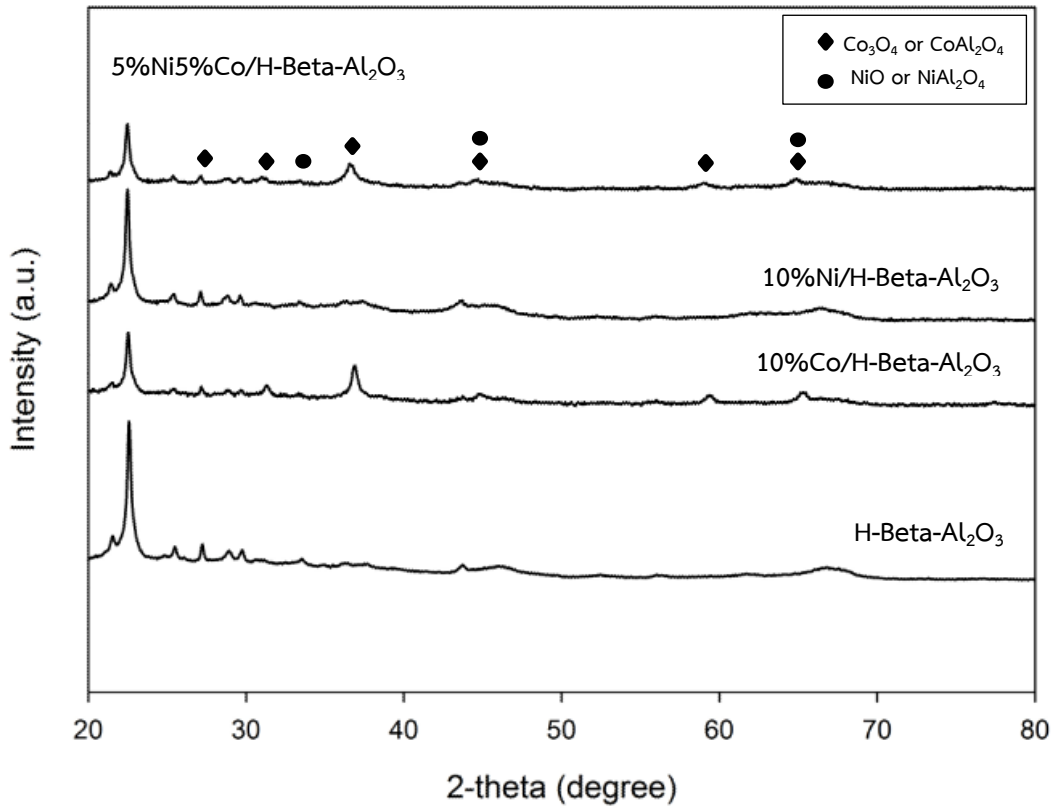

Figure 5.1 The XRD patterns to compare between monometallic (10%wt.Ni, 10%wt.Co) and bimetallic (5%wt.Ni5%wt.Co) on H-Beta-Al_2O_3 catalysts,

♦ = Co_3O_4 or $CoAl_2O_4$, ●= NiO or $NiAl_2O_4$.

Table 5.1 Average crystallite size of between monometallic and bimetallic on H-Beta-Al_2O_3 catalysts

Sample	Average crystallite size of catalysts from XRD (nm)
5%Ni5%Co/H-Beta-Al_2O_3	21.9
10%Ni/H-Beta-Al_2O_3	34.6
10%Co/H-Beta-Al_2O_3	24.9
H-Beta-Al_2O_3	30.9

5.1.1.1.2 N_2 physisorption

The nitrogen adsorption-desorption isotherm of the monometallic and bimetallic on H-Beta-Al_2O_3 catalysts are displayed in Fig. 5.2. All samples exhibited type IV isotherms and H2-shaped hysteresis loops that are typical of mesoporous structure. The H2-shaped hysteresis loops are associated with a more complex pore structure such as interparticle porosity or irregular tube-like porosity

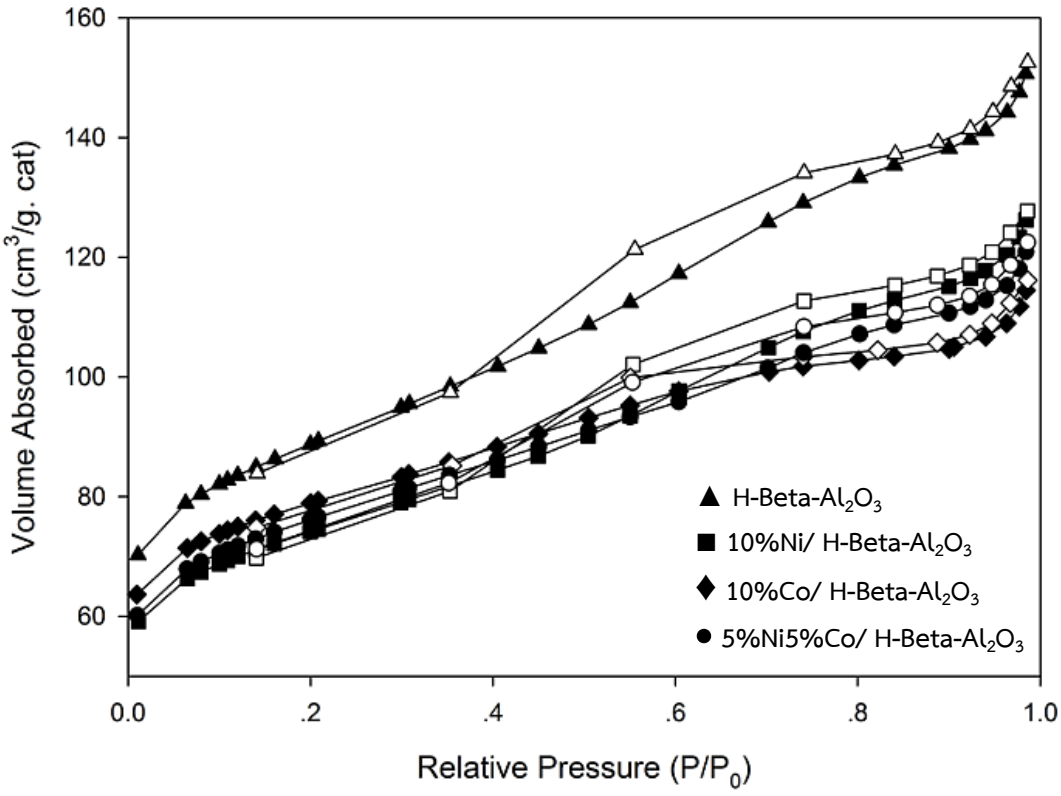

Figure 5.2 Nitrogen adsorption-desorption isotherm of the monometallic and bimetallic on H-Beta-Al_2O_3 catalysts

The surface areas of catalysts were characterized by BET (Brunauer-Emmett-Teller) method [57]. BET surface area, pore volume, and pore size of the monometallic (10%wt.Ni, 10%wt.Co) and bimetallic (5%wt.Ni5%wt.Co) on H-Beta-Al_2O_3 catalysts were summarized in Table 5.2. The surface areas of monometallic and bimetallic catalysts were ranged between 255-306 m^2/g. 5%wt.Ni5%wt.Co/H-Beta-Al_2O_3 has higher surface area than 10%wt.Ni/H-Beta-Al_2O_3 and 10%wt.Co/H-Beta-Al_2O_3. However, BET surface areas of catalysts were decreased compare to that of support. This suggests that some pore of H-Beta-Al_2O_3 support may be blocked by Ni-metal and Co-metal loaded particles [56]. Moreover, pore volume of 10%wt.Ni/H-Beta-Al_2O_3, 10%wt.Co/H-Beta-Al_2O_3 and 5%wt.Ni5%wt.Co/H-Beta-Al_2O_3 catalysts and catalyst support were ranged between 0.12-0.14 cm^3/g. There is no significant difference between catalysts and catalyst support. In term of Ni and Co species, this suggests that the particles size of the Ni and Co metal may be small and their

dispersion on support catalysts [54]. Then, the pore size of 10%wt.Ni/H-Beta-Al_2O_3, 10%wt.Co/H-Beta-Al_2O_3, 5%wt.Ni5%wt.Co/H-Beta-Al_2O_3 catalysts and catalyst support were ranged between 3.56-3.90 nm. The monometallic and bimetallic catalysts indicated the decrease of pore size compare to H-Beta-Al_2O_3 support, illustrating that the some pores of H-Beta-Al_2O_3 were blocked by Ni and Co loaded particles [54, 55].

Table 5.2 N_2 physisorption illustrate BET surface areas, pore volume and pore size of monometallic and bimetallic on H-Beta-Al_2O_3 catalysts

Sample	BET surface area (m^2/g)	Average pore volume (cm^3/g)	Average pore size (nm)
5%Ni5%Co/H-Beta-Al_2O_3	270	0.14	3.78
10%Ni/H-Beta-Al_2O_3	262	0.12	3.56
10%Co/H-Beta-Al_2O_3	255	0.15	3.81
H-Beta-Al_2O_3	306	0.18	3.90

5.1.1.1.3 Hydrogen temperature program reduction (H_2-TPR)

Hydrogen temperature program reduction technique was carried out to determine the reduction behaviors of the monometallic (10%wt.Ni, 10%wt.Co) and bimetallic (5%wt.Ni5%wt.Co) on H-Beta-Al_2O_3 catalysts samples prepared by the incipient wetness impregnation method by nickel nitrate and cobalt nitrate. In general, the TPR profiles depend on the metal support interaction, variance in metal particle size, and support porous structure which; resulted in different reducibility of nickel and cobalt species on the H-Beta-Al_2O_3 support [42]. The TPR profile for the monometallic (10%wt.Ni, 10%wt.Co) and bimetallic (5%wt.NiCo) on H-Beta-Al_2O_3 catalysts samples are shown in Figure 5.2.

Table 5.3 TPR data of monometallic and bimetallic on H-Beta-Al_2O_3 catalysts

Sample	T_m (°C)		
	1° peak	2° peak	3° peak
5%Ni5%Co/H-Beta-Al_2O_3	**284**	**308**	**457**
10%Ni/H-Beta-Al_2O_3	**520**	**-**	**-**
10%Co/H-Beta-Al_2O_3	**344**	**437**	**560**

According to the TPR profiles, the reducibility of NiO particles could be classified into one sharp peak, which was assigned to NiO to Ni^0 species reduction [20]. The TPR-profiles of 10%Co/H-Beta-Al_2O_3 and 5%Ni5%Co/H-Beta-Al_2O_3, in both cases, three reduction peaks can be observed. It is estimated that the first reduction peak is the bulk Co_3O_4, the second reduction peak means the reduction of Co_3O_4 to CoO and the third peak represents the reduction of CoO to metallic cobalt [58, 59]. A similar result was also reported by Bouarab et al [60]. The reduction temperature of bimetallic catalyst is attribution to the formation of Ni-Co alloy as similar result reported by Wang et al [8]. The TPR results of the monometallic (10%wt.Ni, 10%wt.Co) and bimetallic (5%wt.Ni5%wt.Co) supported on H-Beta-Al_2O_3 catalysts were compared the peak temperature summarized in Table 5.3. The reduction temperature of 5%wt.Ni5%wt.Co/H-Beta-Al_2O_3 decreased compared to 10%wt.Ni/H-Beta-Al_2O_3 and 10%wt.Co/H-Beta-Al_2O_3 catalysts (10%wt.Ni/H-Beta-Al_2O_3 reduction temperature: 520°C, 10%wt.Co/H-Beta-Al_2O_3 reduction temperature: 344°C, 437°C and 560°C, 5%wt.Ni5%wt.Co/H-Beta-Al_2O_3 reduction temperature: 289°C, 308°C and 457°C). The decreased reduction temperature means in part that Ni and Co atoms in the 5%wt.Ni5%wt.Co/H-Beta-Al_2O_3 catalyst are more easily accessible than that in 10%wt.Ni/H-Beta-Al_2O_3 and 10%wt.Co/H-Beta-Al_2O_3 catalysts [61]. A shift in the reduction peaks to lower temperatures implied an easier reducibility of the 5%wt.Ni5%wt.Co/H-Beta-Al_2O_3 samples [52]. This result indicates that the addition of Co improves the dispersion of Co, leading to the surface enrichment of cobalt in 5%wt.Ni5%wt.Co/ H-Beta-Al_2O_3 [59].

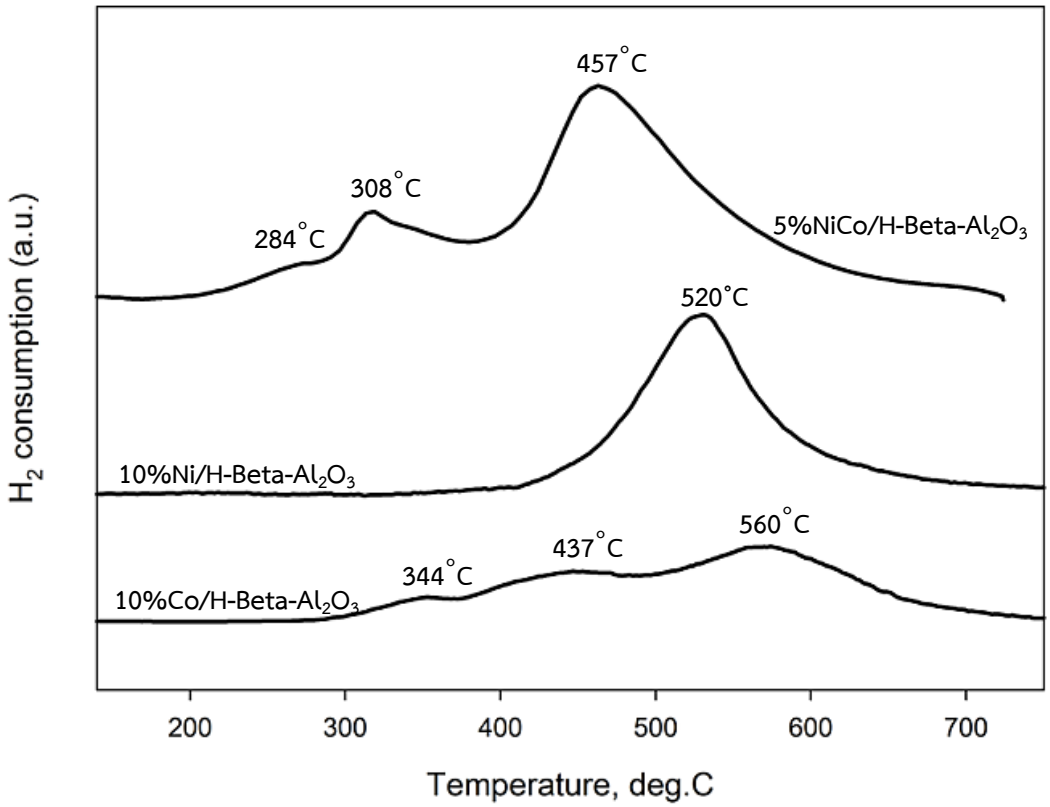

Figure 5.3 The TPR profiles of monometallic (10%wt.Ni, 10%wt.Co) and bimetallic (5%wt.Ni5%wt.Co) on H-Beta-Al_2O_3 catalysts

5.1.1.1.4 Ammonia temperature program Desorption (NH_3-TPD)

Ammonia temperature program desorption (NH_3-TPD) was a widely technique used to determine the acidity on the surface of the catalysts [62]. The strength of the acid is related to the desorption temperature [59]. In addition, the total amount of ammonia desorption corresponding to the amount of total acidity at surface of catalysts [62].

Table 5.4 Acidity form NH_3-TPD of monometallic and bimetallic on H-Beta-Al_2O_3 catalysts

Samples	Total acid site, (mmol H^+/g cat)
5%Ni5%Co/H-Beta-Al_2O_3	**0.15**
10%Ni/H-Beta-Al_2O_3	**0.14**
10%Co/H-Beta-Al_2O_3	**0.09**
H-Beta-Al_2O_3	**0.14**

The acidity on the surface of the samples monometallic and bimetallic on H-Beta-Al_2O_3 catalysts were determined by NH_3-TPD. The desorption temperature of 5%wt.Ni5%wt.Co/H-Beta-Al_2O_3, 10%wt.Ni/H-Beta-Al_2O_3 and H-Beta-Al_2O_3 support only exhibit one desorption peak (5%wt.Ni5%wt.Co/H-Beta-Al_2O_3, 10%wt.Ni/H-Beta-Al_2O_3 and H-Beta-Al_2O_3 support could be classified desorption temperature 141°C, 154°C, and 126°C, respectively) indicating the presence of weak acid sites. 10%wt.Co/H-Beta-Al_2O_3 presented a major desorption peak at 163°C and a minor desorption peak at 460°C. Generally, desorption temperature peak at temperature within 100–250°C can be ascribed to weak acid sites and the desorption peak at temperature above 250°C is associated with strong acid sites [63]. It is apparent that no strong acid sites on 5%wt.Ni5%wt.Co/H-Beta-Al_2O_3, 10%wt.Ni/H-Beta-Al_2O_3 and H-Beta-Al_2O_3 support. In contrast, the presence of desorption peaks at high temperature on 10%wt.Co/H-Beta-Al_2O_3 demonstrated the existence of strong acid sites compared with other catalysts. The desorption peak ascribed to strong acid sites on 10%wt.Co/H-Beta-Al_2O_3 shifted to a much higher temperature (460°C), indicating the increase of strong acidity. It has been known that the strong acid sites are responsible for the formation of coke and polymer on the catalyst surface [36, 46]. Moreover, the amounts of acid sites on the surface catalysts were showed in Table 5.4. The total acid sites of monometallic and bimetallic catalysts were ranged between 0.09-0.14 mol H^+/g cat. The result find the increased acidity on 5%wt.Ni5%wt.Co/H-Beta-Al_2O_3 and 10%wt.Ni/H-Beta-Al_2O_3 may hamper CO_2 adsorption and activation leading to a lower activity [36].

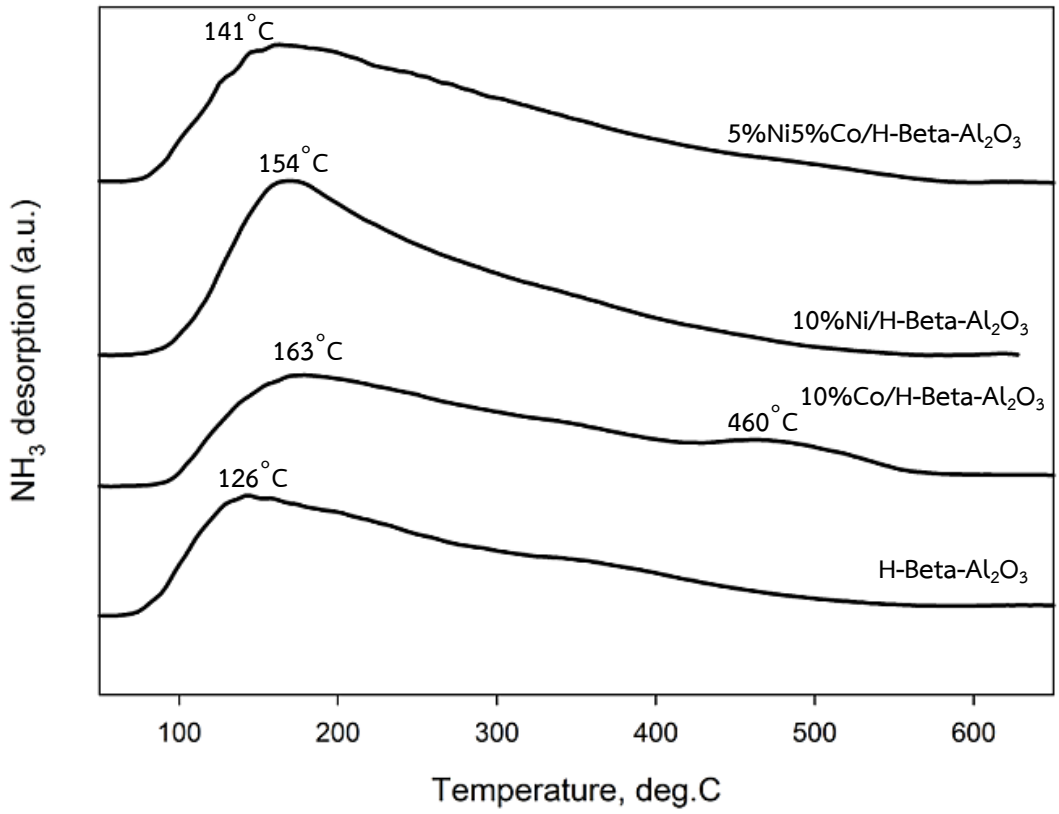

Figure 5.4 The NH_3-TPD profiles of monometallic (10%wt.Ni, 10%wt.Co) and bimetallic (5%wt.Ni5%Co) on H-Beta-Al_2O_3 catalysts

5.1.1.1.5 Scanning electron microscopy analyses (SEM)

EDX analysis was determined quantitatively the amount of composition on the catalyst surfaces [46]. In all of the EDX, the values found for composition of a given catalyst were typically found in catalysts [16]. EDX results indicate that surface composition is close to target at roughly 10%wt.Ni, 10%wt.Co and 5%wt.Ni5%wt.Co. Catalysts with monometallic and bimetallic loadings were also investigated. The adjacent from target composition may be due to adequate mixing of the catalyst materials [29].

Table 5.5 EDX Surface Composition (% Element) result of monometallic and bimetallic on H-Beta-Al_2O_3 catalysts

Samples	%Element				%Atomic			
	Al	Si	Ni	Co	Al	Si	Ni	Co
5%Ni5%Co/H-Beta-Al_2O_3	40.08	48.82	5.73	5.37	47.77	44.55	3.93	3.76
10%Ni/H-Beta-Al_2O_3	37.17	55.36	9.28	-	37.93	57.37	4.70	-
10%Co/H-Beta-Al_2O_3	36.03	53.20	-	10.77	36.03	55.33	-	8.64

5.1.1.1.6 Hydrogen chemisorption

The amount of active site of the monometallic (10%wt.Ni, 10%wt.Co) and bimetallic (5%wt.Ni5%wt.Co) on H-Beta-Al_2O_3 catalysts were analyzed by the H_2 chemisorption. Table 5.6 shows the H_2 chemisorption of the nickel and cobalt active site of the monometallic and bimetallic catalysts incurred from the incipient wetness impregnation method after calcined at 500˚C and reduction at 600˚C. The nickel and cobalt active site were ranged between 2.03-8.18 $X10^{18}$ molecules H_2/g cat in the order: 5%wt.Ni5%wt.Co/H-Beta-Al_2O_3 > 10%wt.Ni/H-Beta-Al_2O_3 > 10%wt.Co/H-Beta-Al_2O_3. Besides, the 5%wt.Ni5%wt.Co/H-Beta-Al_2O_3 shows higher H_2 chemisorption and better dispersion on support than 10%wt.Ni/H-Beta-Al_2O_3 and 10%wt.Co/H-Beta-Al_2O_3 catalysts. This suggested 5%wt.Ni5%wt.Co/H-Beta-Al_2O_3 sample exhibited higher surface area and dispersion, illustrating the homogeneous distribution of the small Ni and Co particles [5]. According to the average crystallite size as measured from XRD, the crystallite size of catalysts from the 5%wt.Ni5%wt.Co/H-Beta-Al_2O_3 was smaller than the 10%wt.Ni/H-Beta-Al_2O_3. Therefore, the crystallite size of nickel and cobalt species of 5%wt.Ni5%wt.Co/H-Beta-Al_2O_3 may be easier to reduce to nickel and cobalt active site [58].

Table 5.6 Hydrogen chemisorption result of monometallic and bimetallic on H-Beta-Al_2O_3 catalysts

Sample	H_2 chemisorption ($x10^{-18}$ molecules/g.cat)	% Dispersion
5%Ni5%Co/H-Beta-Al_2O_3	8.18	6.14
10%Ni/H-Beta-Al_2O_3	6.33	4.57
10%Co/H-Beta-Al_2O_3	2.03	3.97

5.1.1.1.7 Thermogravimetric analysis (TGA)

The amount of carbon deposited on the monometallic and bimetallic on H-Beta-Al_2O_3 catalysts samples after being used in CO_2 reforming of CH_4 was determined by TGA. The weight losses as a result of combustion of the carbon deposited on the spent catalysts are shown in Fig. 5.4. The weight losses of monometallic and bimetallic catalysts temperature were ranged between 434-505˚C. Weight losses temperature of 5%Ni5%Co/H-Beta-Al_2O_3, 10%Ni/H-Beta-Al_2O_3, and 10% Co/H-Beta-Al_2O_3 are 434˚C, 464˚C and 505˚C, respectively. However, the weight losses of monometallic and bimetallic catalysts were ranged between 24.9-56.3%. According to the TG profiles, cobalt-containing catalysts, 10%Ni/H-Beta-Al_2O_3 and 10%Co/H-Beta-Al_2O_3 catalysts, showed a weight loss about 38.8% and 56.3% respectively, whereas 5%NiCo/H-Beta-Al_2O_3 catalyst exhibited a weight loss about 24.9% revealing a lower carbon accumulation [48]. These features mirror a substantially higher resistance to carbon deposition of cobalt-containing catalysts [36, 50]. Furthermore, they demonstrate that cobalt is effective in preventing carbon deposition even if it is alloyed with nickel [16, 64].

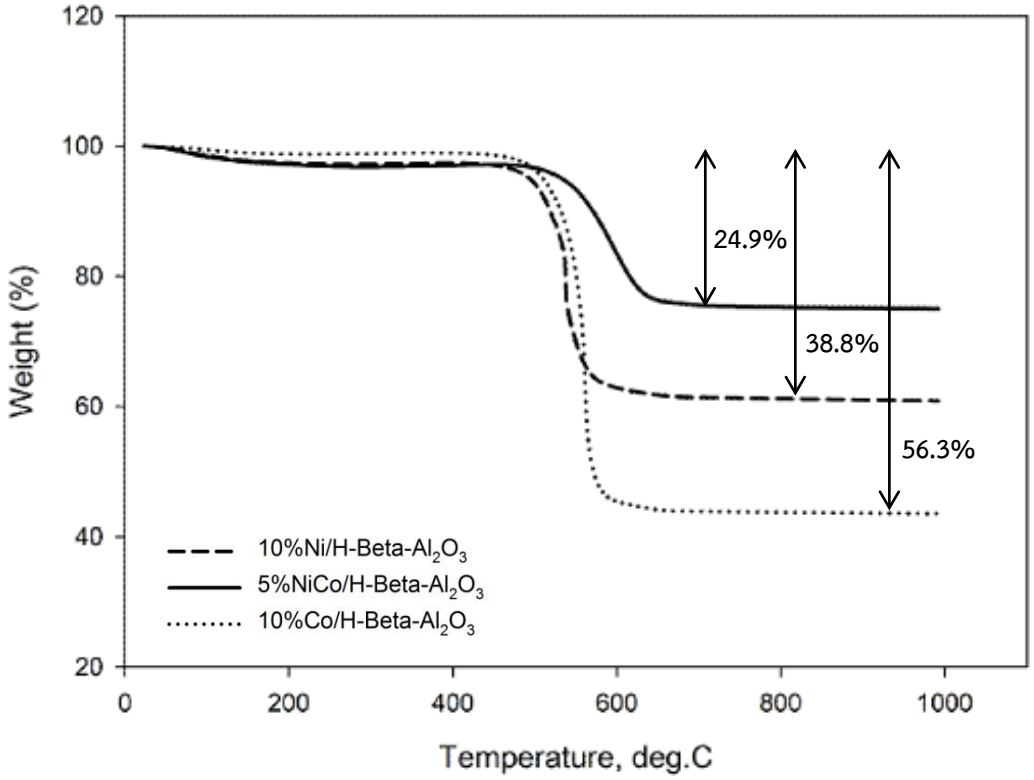

Figure 5.5 TGA curves in air atmosphere after being used in reaction at 700 °C for 5 h for the monometallic (10%wt.Ni, 10%wt.Co) and bimetallic (5%wt.Ni5%wt.Co) on H-Beta-Al_2O_3 catalysts calcined at 500˚C

5.1.1.2 The catalytic activity of the monometallic and bimetallic on H-Beta-Al_2O_3 catalysts in CO_2 reforming of methane

The overall activities of the monometallic (10%wt.Ni, 10%wt.Co) and bimetallic (5%wt.Ni5%wt.Co) on H-Beta-Al_2O_3 catalysts were studied in carbon dioxide reforming of methane reaction. Firstly, 0.2 g catalyst was packed in the quartz reactor. Total gas flow rate was 50 ml/min with the gas nitrogen. Secondly, the catalysts were reduced in flowing hydrogen at 600˚C for 1 h. Next, increase temperature to 700˚C with nitrogen. Finally, the reaction was carried out at 700˚C and 1 atm.

The conversion and product selectivity during carbon dioxide reforming of methane reaction are shown in Table 5.7. The steady state of methane and carbon dioxide conversion of carbon dioxide reforming of methane reaction of the monometallic (10%wt.Ni, 10%wt.Co) and bimetallic (5%wt.Ni5%wt.Co) on H-Beta-Al_2O_3 catalysts were ranging between 71.2-78.7% and 85.7-90.3% respectively. The CO_2 conversion was higher than the CH_4 conversion. This behavior is attributed to the occurrence of the reverse water gas shift reaction (RWGS) as is also suggested by the H_2O evidence in the outlet gas stream. The RWGS, $CO_2 + H_2 \leftrightarrow 4CO + H_2O$, is favored at high temperatures due to its endothermic nature [29, 61]. In the order methane and carbon dioxide conversion: 5%wt.Ni5%wt.Co/H-Beta-Al_2O_3 > 10%wt.Ni/H-Beta-Al_2O_3 > 10%wt.Co/H-Beta-Al_2O_3. It was found that the 5%wt.Ni5%wt.Co/H-Beta-Al_2O_3 showed the highest methane and carbon dioxide conversion among the 10%wt.Ni/H-Beta-Al_2O_3 > 10%wt.Co/H-Beta-Al_2O_3 catalysts. According to H_2 chemisorption, the amount of nickel and cobalt active sites of 5%wt.Ni5%wt.Co/H-Beta-Al_2O_3 catalysts are the highest the Ni and Co active sites although the BET surface area of 5%wt.Ni5%wt.Co/H-Beta-Al_2O_3 has high surface area and decrease pore volume which the nickel and cobalt particles may be located in the pore of H-Beta-Al_2O_3 support [42]. Comparing the monometallic (10%wt.Ni/H-Beta-Al_2O_3, 10%wt.Co/H-Beta-Al_2O_3) catalysts, the 5%wt.Ni5%wt.Co/H-Beta-Al_2O_3 exhibit slightly higher methane and carbon dioxide conversion than the 10%wt.Co/H-Beta-Al_2O_3. According to H_2 chemisorption, the amounts of active sites of 10%wt.Ni/H-Beta-Al_2O_3 are higher than 10%wt.Co/H-Beta-Al_2O_3 catalyst. However 5%wt.Ni5%wt.Co/H-Beta-Al_2O_3, cobalt addition improved nickel active catalyst which can result in higher methane and carbon dioxide conversion during the 3 h time-on-steam. The improved with cobalt catalysts performances can be attributed to better dispersion of the NiO particles, according to the smaller crystallite sizes found in the XRD patterns[16]. That is the smaller NiO and CoO may be easier to reduce to active nickel and cobalt particles. Moreover, comparing the monometallic and bimetallic catalysts, the bimetallic (5%wt.Ni5%wt.Co/H-Beta-Al_2O_3) a shift of the reduction temperature towards lower temperature than monometallic catalysts, therefore, the reduction of NiO and CoO was easier [40]. According to the crystallite sizes, the

bimetallic showed the smaller NiO crystallite size. For the bimetallic catalyst, reducibility of the catalyst was also increased with the addition of Co-promoter. Furthermore, TGA result cobalt added to promoter of nickel base catalyst which gives higher resistance to carbon deposition of cobalt-containing catalysts. Furthermore, they demonstrate that cobalt is effective in preventing carbon deposition even if it is alloyed with nickel [60].

The product selectivity is observed during carbon dioxide reforming of methane reaction. The result shows that the selectivity to CO is lower in 5%wt.Ni5%wt.Co/H-Beta-Al_2O_3 than in the 10%wt.Ni/H-Beta-Al_2O_3 and 10%wt.Co/H-Beta-Al_2O_3. In contrast, 5%wt.Ni5%wt.Co/H-Beta-Al_2O_3 showed the higher H_2 selectivity than the bimetallic. These results suggest that the high catalytic activity of the bimetallic sample is mostly related to the intrinsic nature of the Co-Ni alloy a better dispersion of the active phase in smaller particles, as recently proposed for an analogous system [65].

Table 5.7 The conversion, and product selectivity during CO_2 reforming of methane at initial and steady-state conditions of monometallic and bimetallic on H-Beta-Al_2O_3 catalysts at 600˚C

Sample	Conversion (%) [a]				Product selectivity (%) [a]			
	Initial [b]		Steady state [c]		Initial [b]		Steady state [c]	
	CH_4	CO_2	CH_4	CO_2	H_2	CO	H_2	CO
5%Ni5%Co/H-Beta-Al_2O_3	79.4	90.3	78.7	92.3	95.8	4.2	96.7	3.3
10%Ni/H-Beta-Al_2O_3	74.2	87.9	73.7	89.0	60.6	39.4	60.9	39.1
10%Co/H-Beta-Al_2O_3	71.1	85.7	71.2	86.2	56.1	43.9	56.5	43.5

[a] CO_2 reforming of methane was carried out at 600˚C, 1 atm, CH_4/CO_2= 1:1

[b] After 30 min of reaction

[b] After 3 h of reaction

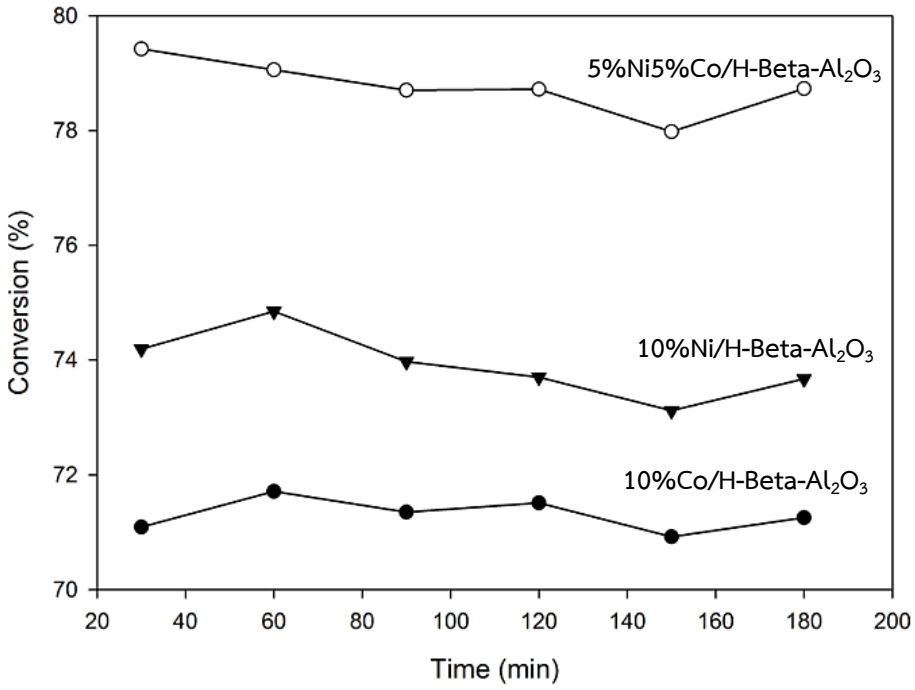

Figure 5.6 Methane conversion of monometallic and bimetallic on H-Beta-Al_2O_3 catalysts at 700˚C

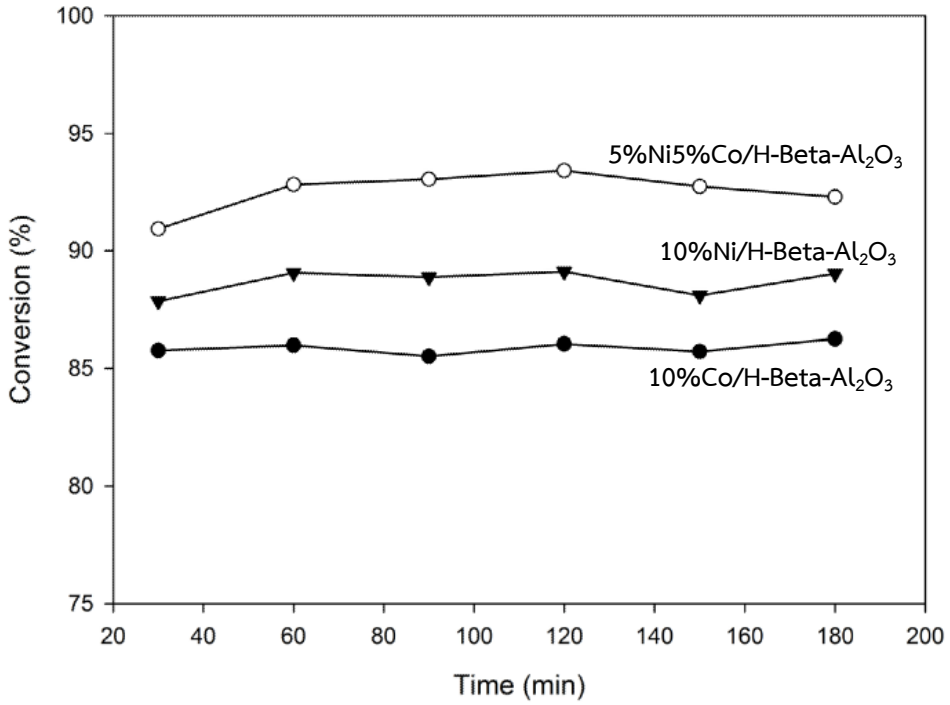

Figure 5.7 Carbon dioxide conversion of monometallic and bimetallic on H-Beta-Al_2O_3 catalysts at 700˚C

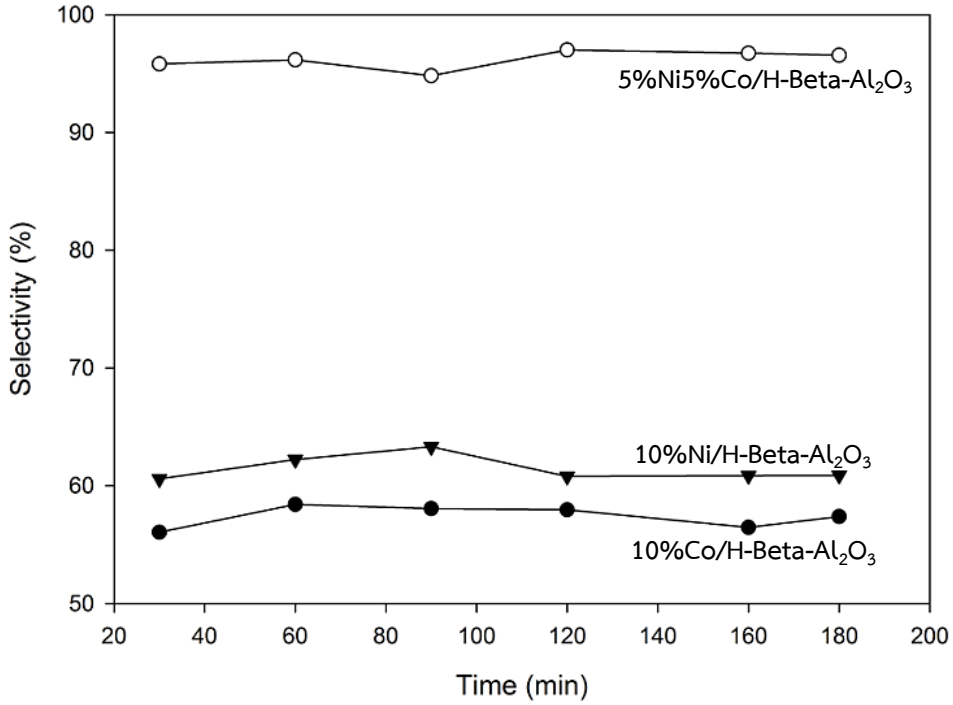

Figure 5.8 Hydrogen selectivity of monometallic and bimetallic on H-Beta-Al_2O_3 catalysts at 700˚C

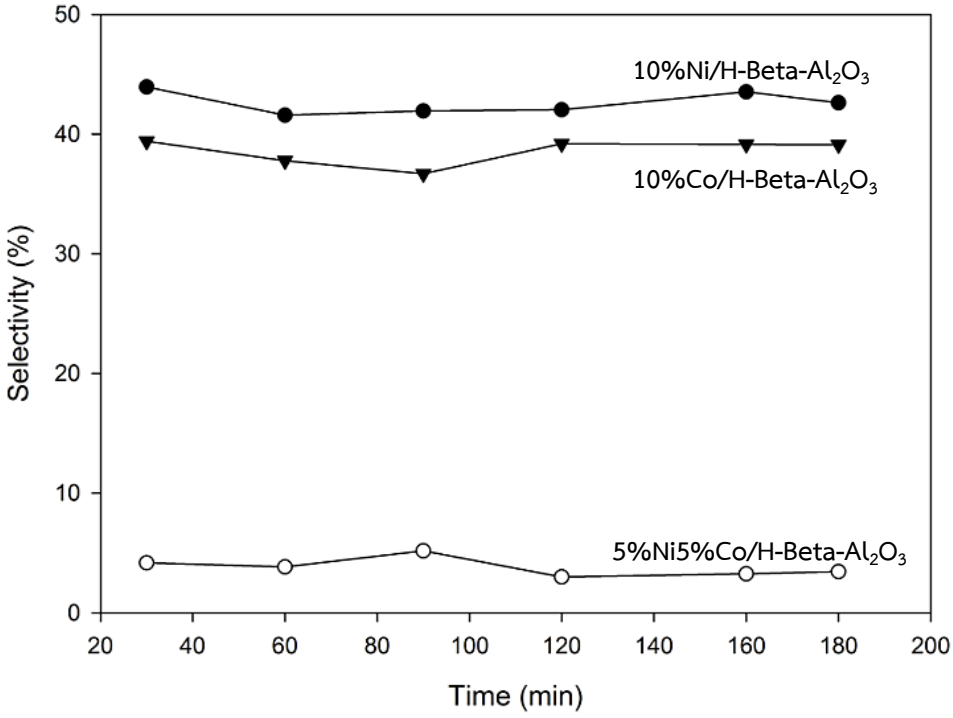

Figure 5.9 Carbon monoxide selectivity of monometallic and bimetallic on H-Beta-Al_2O_3 catalysts at 700˚C

5.1.2 Effect of monometallic (10%wt.Ni, 10%wt.Co) and bimetallic (5%wt.NiCo) on SiO_2-Al_2O_3 support

5.1.2.1 Catalysts characterization

5.1.2.1.1 X-ray diffraction (XRD)

Figure 5.9 shows the XRD patterns of the monometallic (10%wt.Ni, 10%wt.Co) and bimetallic (5%wt.Ni5%wt.Co) on SiO_2-Al_2O_3 support. For both nickel and SiO_2-Al_2O_3 supported Ni based catalysts the diffraction lines observed at 2θ degrees 30.2˚, 43.9˚, 58.3˚and 65.5˚ are attributed to the NiO [20]. While, the Co-loaded catalysts exhibited at 2θ degrees 30.2˚, 43.9˚, 58.3˚ and 64.0˚ are attributed to the Co_3O_4 [36]. In term of Ni and Co species, in all the catalysts diffraction peaks of nickel oxide and cobalt oxide crystallite phase were not detected because of their same morphology [55]. It is interesting to note that, for all catalysts, the peak intensities increase with the metal loading, which reflect the increase in crystallinity. The monometallic 10%wt.Co/SiO_2-Al_2O_3 and 10%wt.Ni/SiO_2-Al_2O_3 catalysts show characteristic peaks of SiO_2-Al_2O_3 support together are metal oxides: Co_3O_4 and NiO, respectively. Although bimetallic catalyst was reported in the literature that during the calcination Ni and Co tend to form $NiCo_2O_4$, in bimetallic catalyst 5%wt.Ni5%wt.Co/SiO_2-Al_2O_3, neither $NiCo_2O_4$ nor Co_3O_4 were detected, most likely because of their small particle sizes [14]. These features suggest the cobalt and nickel species have higher dispersion in the bimetallic system than in monometallic [56].

The Scherrer equation using the reflection at 37.9°in the XRD patterns, the crystal size of monometallic, bimetallic and catalyst support was estimated range 16.6-41.9 nm are summarized in table 5.8 As seen, only slight increase are noticed in the SiO_2-Al_2O_3 crystal size upon the addition of metals. The size of the 10%wt.Ni/ SiO_2-Al_2O_3 had the biggest size, 37.6 nm. It was reported in the literature that agglomeration of Ni particles due to low dispersion of 10%wt.Ni/ SiO_2-Al_2O_3 catalyst [40].

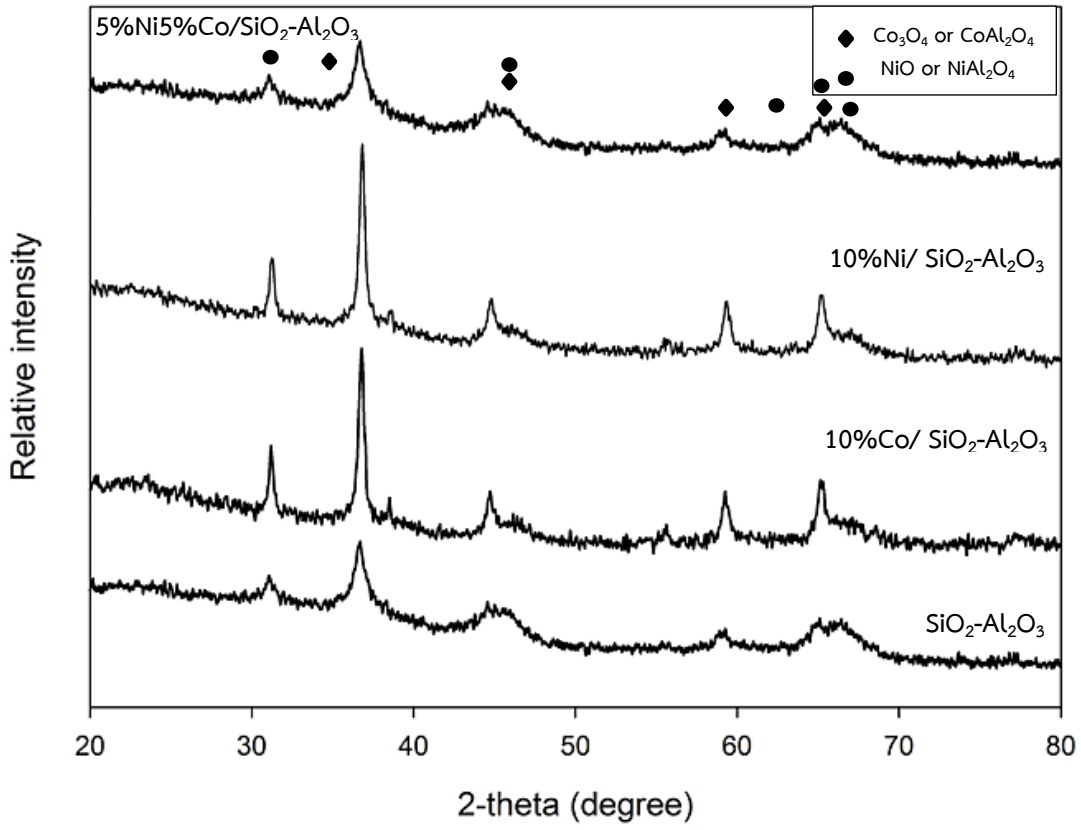

Figure 5.10 The XRD patterns to compare between monometallic (10%wt.Ni, 10%wt.Co) and bimetallic (5%wt.NiCo) on SiO_2-Al_2O_3 catalysts,

♦ = Co_3O_4 or $CoAl_2O_4$, ● = NiO or $NiAl_2O_4$.

Table 5.8 Average crystallite size of between monometallic and bimetallic on SiO_2-Al_2O_3 catalysts

Sample	Average crystallite size of catalysts from XRD (nm)
5%Ni5%Co/SiO_2-Al_2O_3	25.8
10%Ni/SiO_2-Al_2O_3	41.9
10%Co/SiO_2-Al_2O_3	24.5
SiO_2-Al_2O_3	16.6

5.1.2.1.2 Nitrogen physisorption

The nitrogen adsorption-desorption isotherm of the monometallic and bimetallic on SiO_2-Al_2O_3 catalysts are shows in Fig. 5.11. All samples exhibit type II isotherms and H2-shaped hysteresis loops that are typical of macropore structure (>50 nm) [30]. The H2-shaped hysteresis loops are associated with a more complex pore structure such as interparticle porosity or irregular tube-like porosity.

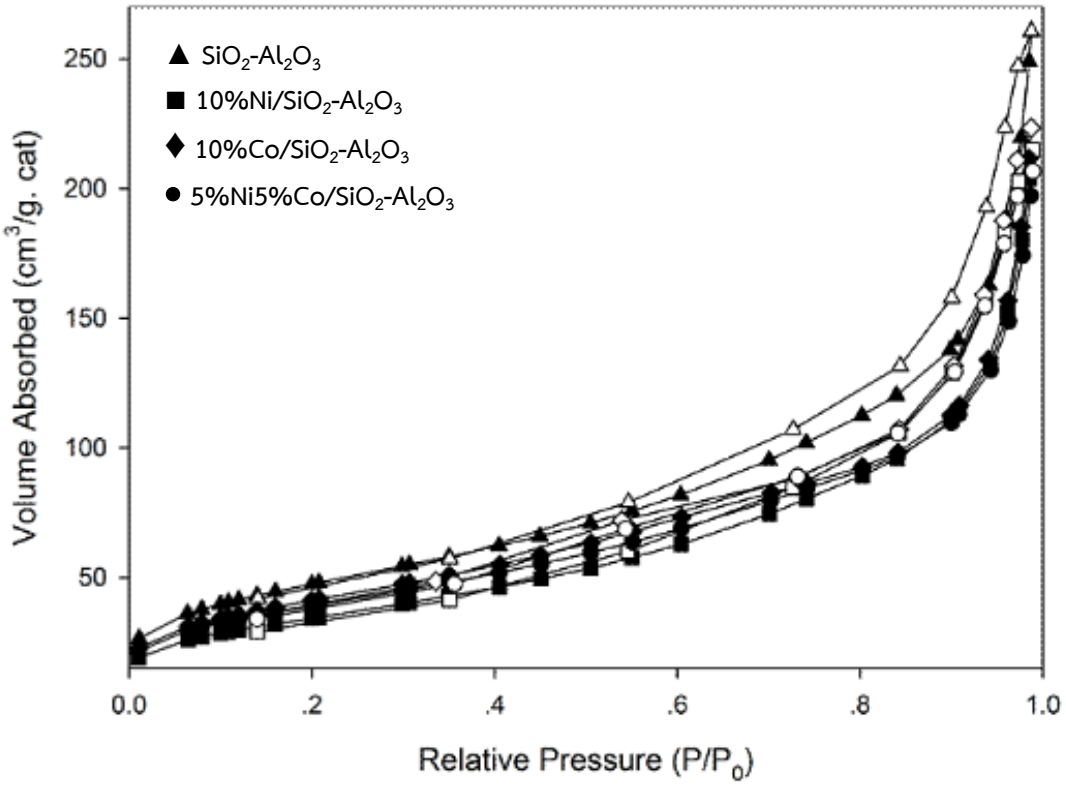

Figure 5.11 nitrogen adsorption-desorption isotherm of the monometallic and bimetallic on SiO_2-Al_2O_3 catalysts

Structural properties of the monometallic (10%wt.Ni, 10%wt.Co), bimetallic (5%wt.Ni5%wt.Co) and SiO_2-Al_2O_3 support are presented in Table 5.9. The surface areas of monometallic and bimetallic catalysts were ranged between 126-173 m^2/g, compared to no loaded metal on supports the 10%wt.Ni/SiO_2-Al_2O_3 and 10%wt.Co/SiO_2-Al_2O_3 possess lower specific surface area. The results showed that

addition of Nickel and cobalt metal of 5%wt.Ni5%wt.Co/SiO_2-Al_2O_3 do not affect BET surface areas; these features suggest the cobalt and nickel species have higher dispersion in the bimetallic system than in monometallic [23]. Pore volume of 10%wt.Ni/ SiO_2-Al_2O_3, 10%wt.Co/ SiO_2-Al_2O_3, 5%wt.Ni5%wt.Co/ SiO_2-Al_2O_3 catalysts and catalyst support were range between 0.32-0.41 cm^3/g. The pore volume of the monometallic and bimetallic catalysts decrease compared with SiO_2-Al_2O_3 support due to blocking of some nickel and cobalt metal loading of support [3]. Then, the pore size of 10%wt.Ni/SiO_2-Al_2O_3, 10%wt.Co/SiO_2-Al_2O_3, 5%wt.Ni5%wt.Co/SiO_2-Al_2O_3 catalysts and catalyst support were range between 7.83-8.80 nm. The average pore size of the bimetallic and monometallic supported on SiO_2-Al_2O_3 catalysts has no obvious change [3, 59].

Table 5.9 N_2 physisorption illustrate BET surface areas, pore volume and pore size of monometallic and bimetallic on SiO_2-Al_2O_3catalysts

Sample	BET surface area (m^2/g)	Average pore volume (cm^3/g)	Average pore size (nm)
5%Ni5%Co/SiO_2-Al_2O_3	171	0.35	7.88
10%Ni/SiO_2-Al_2O_3	151	0.32	7.94
10%Co/SiO_2-Al_2O_3	126	0.37	8.08
SiO_2-Al_2O_3	173	0.41	7.83

5.1.2.1.3 Hydrogen temperature program reduction (H_2-TPR)

Hydrogen temperature program reduction technique was carried out to determine the reduction behaviors of the monometallic (10%wt.Ni, 10%wt.Co) and bimetallic (5%wt.Ni5%wt.Co) on SiO_2-Al_2O_3 catalysts samples. In general, the TPR profiles depend on the metal support interaction, variance in metal particle size, and support porous structure which, resulted in different reducibility of nickel and cobalt species on the SiO_2-Al_2O_3 [33]. The TPR profile for the monometallic (10%wt.Ni,

10%wt.Co) and bimetallic (5%wt.Ni5%wt.Co) supported on SiO_2-Al_2O_3 catalysts samples are shown in Figure 5.10

Table 5.10 TPR data of monometallic and bimetallic on SiO_2-Al_2O_3 catalysts

Sample	T_m (°C)		
	1° peak	2° peak	3° peak
5%Ni5%Co/SiO_2-Al_2O_3	373	530	-
10%Ni/SiO_2-Al_2O_3	560	-	-
10%Co/SiO_2-Al_2O_3	459	597	-

Figure 5.10 show the TPR profiles of monometallic and bimetallic catalysts. In 10%wt.Ni/SiO_2-Al_2O_3 catalyst case, one broad reduction peak at 560°C, which is attributed to NiO species interacting with SiO_2-Al_2O_3 support, was assigned to NiO to Ni^0 species reduction that had a weak interaction with the support, implying the aggregation of NiO [12]. The TPR-profiles of 10%wt.Co/H-Beta-Al_2O_3 and 5%wt.Ni5%wt.Co/H-Beta-Al_2O_3, in both cases, two reduction peaks can be observed. The first reduction is profile of pure Co_3O_4 to CoO, the second reduction peak means the reduction of CoO to Co^0 [11]. The TPR results of the monometallic (10%wt.Ni, 10%wt.Co) and bimetallic (5%wt.Ni5%wt.Co) on SiO_2-Al_2O_3 catalysts were compared the peak temperature summarized in Table 5.10. However, the reduction temperature of 5%wt.Ni5%wt.Co/SiO_2-Al_2O_3 decreased compared to 10%wt.Ni/SiO_2-Al_2O_3 and 10%wt.Co/SiO_2-Al_2O_3 catalysts. The decreased reduction temperature means in part that Ni and Co atoms in the 5%wt.Ni5%wt.Co/SiO_2-Al_2O_3 catalyst are easier to access than that in 10%wt.Ni/SiO_2-Al_2O_3 and 10%wt.Co/SiO_2-Al_2O_3 catalysts. A shift in the reduction peaks to lower temperatures implied an easier reducibility of the catalyst [34]. This result indicates that the addition of Co improves the dispersion of Co. It is effecting to catalytic performance of carbon dioxide reforming of methane [11].

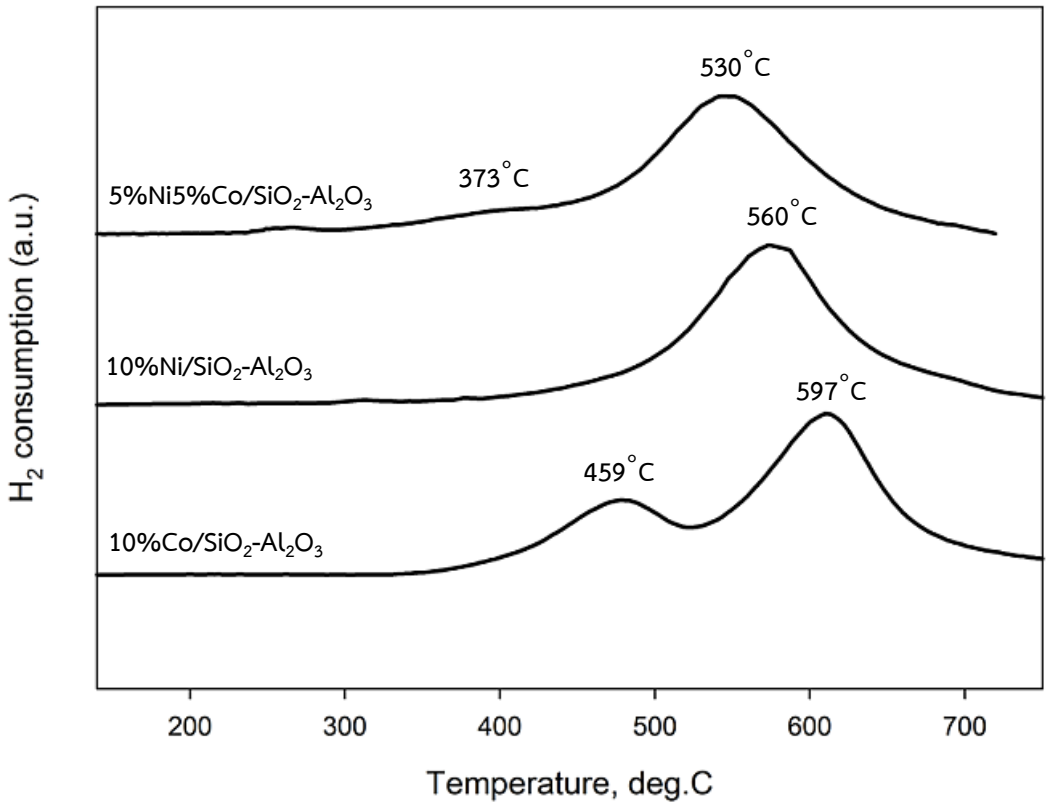

Figure 5.12 The TPR profiles of monometallic (10%wt.Ni, 10%wt.Co) and bimetallic (5%wt.Ni5%wt.Co) on SiO_2-Al_2O_3 catalysts

5.1.2.1.4 Ammonia temperature program Desorption (NH_3-TPD)

Ammonia temperature program desorption (NH_3-TPD) was a widely technique used to determine the acidity on the surface of the catalysts. The strength of the acid is related to the desorption temperature [11]. In addition, determine the total amount of ammonia desorption corresponding to the amount of total acidity at surface of catalysts [12].

Table 5.11 Acidity form NH_3-TPD of monometallic and bimetallic on SiO_2-Al_2O_3 catalysts

Samples	Total acid site, (mmol H^+/g cat)
5%Ni5%Co/SiO_2-Al_2O_3	0.12
10%Ni/SiO_2-Al_2O_3	0.11
10%Co/SiO_2-Al_2O_3	0.08
SiO_2-Al_2O_3	0.14

The acidity of the samples was determined by temperature-programmed desorption of ammonia (NH_3-TPD). Generally, desorption temperature peak within 100–250°C is ascribed to weak acid sites and the desorption peak at temperature above 250°C is associated with strong acid sites [32]. The desorption temperature of 10%wt.Ni/ SiO_2-Al_2O_3 only exhibits one desorption peak indicating the presence of weak acid sites [12]. 5%wt.Ni5%wt.Co/SiO_2-Al_2O_3, 10%wt.Co/SiO_2-Al_2O_3 and SiO_2-Al_2O_3 support presents a major desorption peak at 119°C, 126°C and 138°C, respectively and a minor desorption peak at 246°C, 241°C and 428°C, respectively. It is apparent that no strong acid site on 10%wt.Ni/SiO_2-Al_2O_3. In contrast, the presence of desorption peaks at high temperature of catalysts demonstrated the existence of strong acid sites [31]. The desorption peak ascribed to strong acid sites on 10%wt.Co/ SiO_2-Al_2O_3 and 10%wt.Ni/SiO_2-Al_2O_3 shifted to a much higher temperature (460°C), indicating the increase of strong acidity. It has been known that the strong acid sites are responsible for the formation of coke of carbon dioxide reforming of methane. Moreover, the amounts of acid sites on the surface catalysts show in Table 5.11. The total acid sites of monometallic and bimetallic catalysts were ranged between 0.08-0.14 mol H^+/g cat. The result finds the similar acidity on 5%wt.Ni5%wt.Co/SiO_2-Al_2O_3 and 10%wt.Ni/SiO_2-Al_2O_3 may be hamper CO_2 adsorption and activation leading to a lower activity of reaction [30].

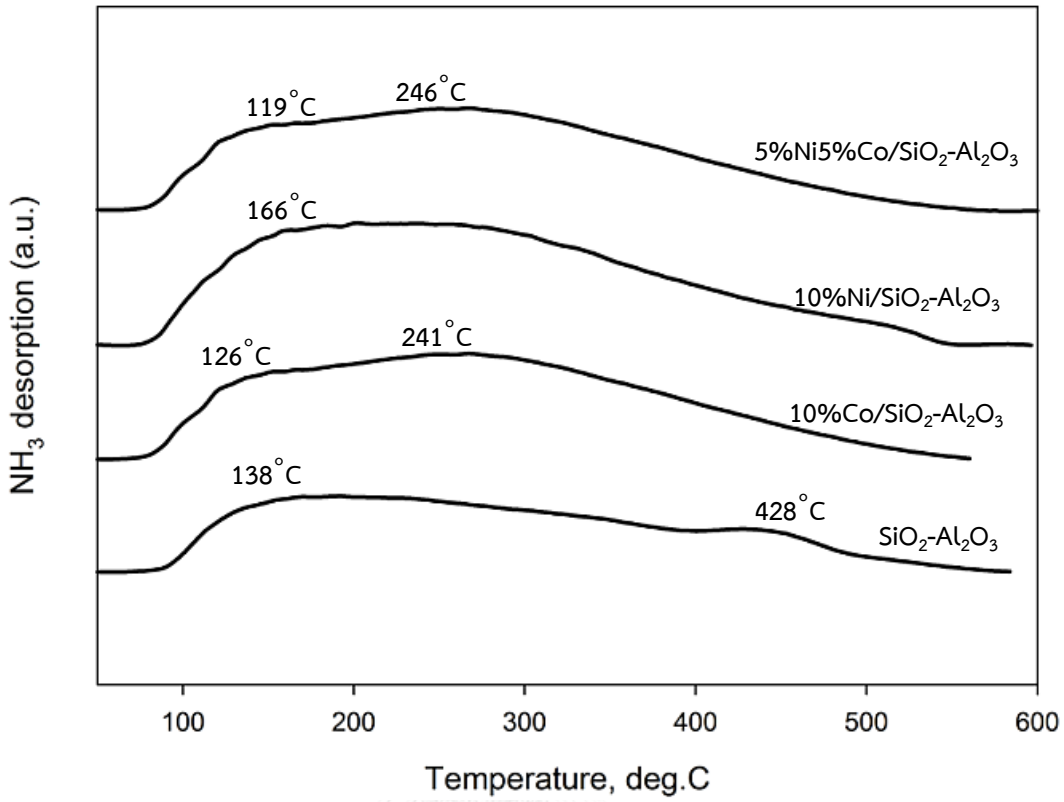

Figure 5.13 The NH_3-TPD profiles of monometallic (10%wt.Ni, 10%wt.Co) and bimetallic (5%wt.NiCo) supported on SiO_2-Al_2O_3 catalysts

5.1.2.1.5 Scanning electron microscopy analyses (SEM)

The EDX result shows for composition of a given monometallic and bimetallic on SiO_2-Al_2O_3 catalysts were typically found in catalysts. EDX results indicate that surface composition is close to target at roughly 10%wt.Ni, 10%wt.Co and 5%wt.Ni5%wt.Co. Catalysts with monometallic and bimetallic loadings were also investigated. The adjacent from target composition may be due to adequate mixing of the catalyst materials [7].

Table 5.12 EDX Surface Composition (% Element) result of monometallic and bimetallic on SiO_2-Al_2O_3 catalysts

Samples	%Element				%Atomic			
	Al	Si	Ni	Co	Al	Si	Ni	Co
5%Ni5%Co/SiO_2-Al_2O_3	50.52	38.25	4.34	4.69	62.87	28.45	4.70	3.98
10%Ni/SiO_2-Al_2O_3	48.79	40.31	10.90	-	59.98	30.49	9.53	-
10%Co/SiO_2-Al_2O_3	50.29	41.25	-	9.04	62.54	27.81	-	9.65

5.1.2.1.6 Hydrogen chemisorption

Results of H_2 chemisorption shown in Table 5.13 indicate that the monometallic (10%wt.Ni, 10%wt.Co) and bimetallic (5%wt.Ni5%wt.Co) on SiO_2-Al_2O_3 catalysts is characterized by a higher chemisorption capacity and metallic surface. The nickel and cobalt active site were ranged between 4.58-5.43 $X10^{18}$ molecules H_2/g cat in the order: 5%wt.Ni5%wt.Co/SiO_2-Al_2O_3 > 10%wt.Ni/SiO_2-Al_2O_3 > 10%wt.Co/SiO_2-Al_2O_3. This suggests that 5%wt.Ni5%wt.Co/SiO_2-Al_2O_3 sample exhibits higher surface area and dispersion, illustrating the homogeneous distribution of the small Ni and Co particles [45]. Therefore, 5%wt.Ni5%wt.Co/SiO_2-Al_2O_3 (%Dispersion: 5.43%) exhibited higher metal dispersion and larger H_2 adsorption amount than the 10%wt.Ni/SiO_2-Al_2O_3 (%Dispersion: 3.19%) and 10%wt.Co/SiO_2-Al_2O_3 (%Dispersion: 2.63%). According to the average crystallite size as measured from XRD, the crystallite size of 5%wt.Ni5%wt.Co/SiO_2-Al_2O_3 was smaller than the other catalysts. However, the crystallite size of nickel and cobalt species of 5%wt.Ni5%wt.Co/SiO_2-Al_2O_3 may be easier to reduce to nickel and cobalt active site [5]. Nickel and cobalt species were more homogeneously dispersed than 10%wt.Ni/SiO_2-Al_2O_3 and 10%wt.Co/SiO_2-Al_2O_3 catalysts, as also demonstrated in TPR result.

Table 5.13 Hydrogen chemisorption result of monometallic and bimetallic on SiO_2-Al_2O_3 catalysts

Sample	H_2 chemisorption ($x10^{-18}$ molecules/g.cat)	% Dispersion
5%Ni5%Co/SiO_2-Al_2O_3	5.43	5.63
10%Ni/SiO_2-Al_2O_3	4.96	3.19
10%Co/SiO_2-Al_2O_3	4.58	2.63

5.1.2.1.7 Thermogravimetric analysis (TGA)

For the monometallic and bimetallic on SiO_2-Al_2O_3 catalysts samples after being used in CO_2 reforming of CH_4. The weight losses of monometallic and bimetallic catalysts temperature were ranged between 400-670˚C. However, the weight losses of monometallic and bimetallic catalysts were ranged between 24.9-56.3%. In terms of % weight loss, they are 24.9%, 38.8% and 56.3% for 5%wt.Ni5%wt.Co/SiO_2-Al_2O_3, 10%wt.Ni/SiO_2-Al_2O_3 and 10%wt.Co/SiO_2-Al_2O_3, respectively. The result shows that the highest amount of carbon depositions was obtained on the 10%wt.Co/SiO_2-Al_2O_3 catalysts. Therefore, the highest amount of carbon depositions was due to lower resistance to carbon deposition of catalysts [47].

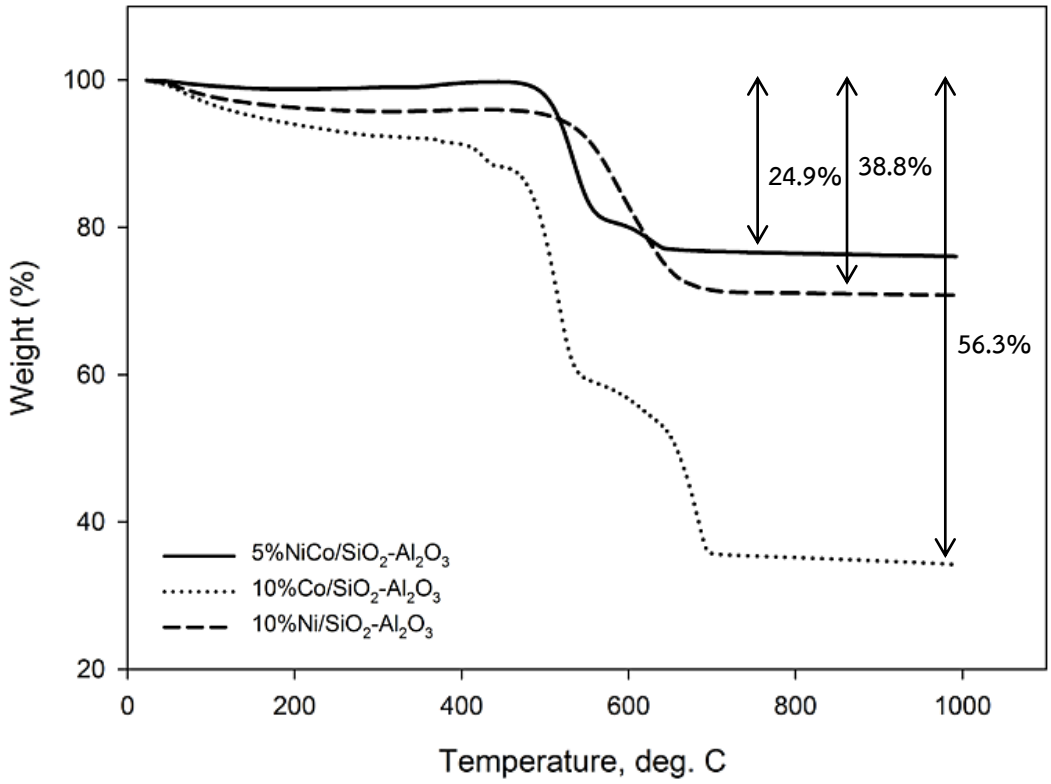

Figure 5.14 TGA curves in air atmosphere after being used in reaction at 700 °C for 5 h for the monometallic (10%wt.Ni, 10%wt.Co) and bimetallic (5%wt.Ni5%wt.Co) on SiO_2-Al_2O_3 catalysts calcined at 500˚C

5.1.2.2 The catalytic activity of the monometallic and bimetallic on SiO_2-Al_2O_3 catalysts in CO_2 reforming of methane

The overall activities of the monometallic (10%wt.Ni, 10%wt.Co) and bimetallic (5%wt.Ni5%wt.Co) on SiO_2-Al_2O_3 catalysts were studied in carbon dioxide reforming of methane reaction. Firstly, 0.2 g catalyst was packed in the quartz reactor. Total gas flow rate was 50 ml/min with the gas nitrogen. Secondly, the catalysts were reduced in flowing hydrogen at 600˚C for 1 h. Next, increase temperature to 700˚C with nitrogen. Finally, the reaction was carried out at 700˚C and 1 atm.

The conversion and product selectivity during carbon dioxide reforming of methane reaction are shown in Table 5.14. The steady state of methane and carbon dioxide conversion in carbon dioxide reforming of methane reaction of the monometallic (10%wt.Ni, 10%wt.Co) and bimetallic (5%wt.Ni5%wt.Co) on SiO_2-Al_2O_3 catalysts were methane and carbon dioxide conversion ranging between 50.1-68.0% and 83.3-87.9% respectively. Figures 5.13 and 5.14 are shows the data on catalytic activity of all catalysts, expressed as methane and carbon dioxide conversion at 700˚C. In all cases, CH_4 conversions were lower than the corresponding CO_2 conversion, probably due to the influence of the secondary reverse water-gas shift reaction [66]. In the order methane and carbon dioxide conversion: 5%wt.Ni5%wt.Co/SiO_2-Al_2O_3 > 10%wt.Ni/SiO_2-Al_2O_3 > 10%wt.Co/SiO_2-Al_2O_3. It was found that the 5%wt.Ni5%wt.Co/SiO_2-Al_2O_3 shows the highest methane and carbon dioxide conversion among other catalysts. According to H_2 chemisorption, the amount of nickel and cobalt active sites of 5%wt.Ni5%wt.Co/SiO_2-Al_2O_3 catalysts are high Ni and Co active sites, although the BET surface area of 5%wt.Ni5%wt.Co/SiO_2-Al_2O_3 are high surface area. Comparing part to 10%wt.Ni/SiO_2-Al_2O_3 and 10%wt.Co/SiO_2-Al_2O_3) catalysts, the 10%wt.Ni/SiO_2-Al_2O_3 exhibits slightly higher methane and carbon dioxide conversion than the 10%wt.Co/SiO_2-Al_2O_3 catalyst. According to H_2 chemisorption and %Dispersion, the amounts of active sites of 10%wt.Ni/SiO_2-Al_2O_3 catalyst are higher than 10%wt.Co/SiO_2-Al_2O_3 catalyst. Moreover, comparing the monometallic and bimetallic catalysts, addition of cobalt improved nickel base catalyst which result in higher methane and carbon dioxide conversion during the 3 h. The improved with cobalt catalysts performances can be attributed to better dispersion, according to the smaller crystallite sizes found in the XRD patterns [2]. That is the smaller NiO and CoO may be easier to reduce to active nickel and cobalt particles from H_2-TPR result [2]. Therefore, the reduction temperature of 5%wt.Ni5%wt.Co/H-Beta-Al_2O_3 shifts of toward lower temperature than monometallic catalysts. For the bimetallic catalyst reducibility of the catalyst are also increased with the addition of Co-promoter. According to the crystallite sizes, the bimetallic showed the smaller NiO crystallite size [67]. Furthermore, TGA result cobalt added to promoter of nickel base catalyst which higher resistance to

carbon deposition of cobalt-containing catalysts. Addition to all catalysts no deactivation has been observed during this long reaction period [29]. This means that the deposited carbon does not deactivate the catalyst active sites [29, 41]. Therefore, the catalytic activity remains constant since the active metal is still accessible to the reactants.

The product selectivity is observed during carbon dioxide reforming of methane reaction. The result was observed that the selectivity to CO is lower in 5%wt.Ni5%wt.Co/SiO_2-Al_2O_3 catalysts than in the 10%wt.Ni/SiO_2-Al_2O_3 and 10%wt.Co/SiO_2-Al_2O_3 catalysts. In contrast, 5%wt.Ni5%wt.Co/SiO_2-Al_2O_3 shows the higher H_2 selectivity than the monometallic catalysts these results suggest that the high catalytic activity of the bimetallic sample in system [40].

Table 5.14 The conversion, and product selectivity during CO_2 reforming of methane at initial and steady-state conditions of monometallic and bimetallic on SiO_2-Al_2O_3 catalysts at 600˚C

Sample	Conversion (%) [a]				Product selectivity (%) [a]			
	Initial [b]		Steady state [c]		Initial [b]		Steady state [c]	
	CH_4	CO_2	CH_4	CO_2	H_2	CO	H_2	CO
5%Ni5%Co/SiO_2-Al_2O_3	67.8	88.3	68.0	87.5	79.9	20.1	81.5	18.5
10%Ni/SiO_2-Al_2O_3	51.7	87.2	52.3	85.9	32.2	67.7	26.2	63.0
10%Co/SiO_2-Al_2O_3	47.1	83.7	50.1	83.3	32.7	67.3	35.8	64.2

[a] CO_2 reforming of methane was carried out at 600˚C, 1 atm, CH_4/CO_2

[b] After 30 min of reaction

[b] After 3 h of reaction

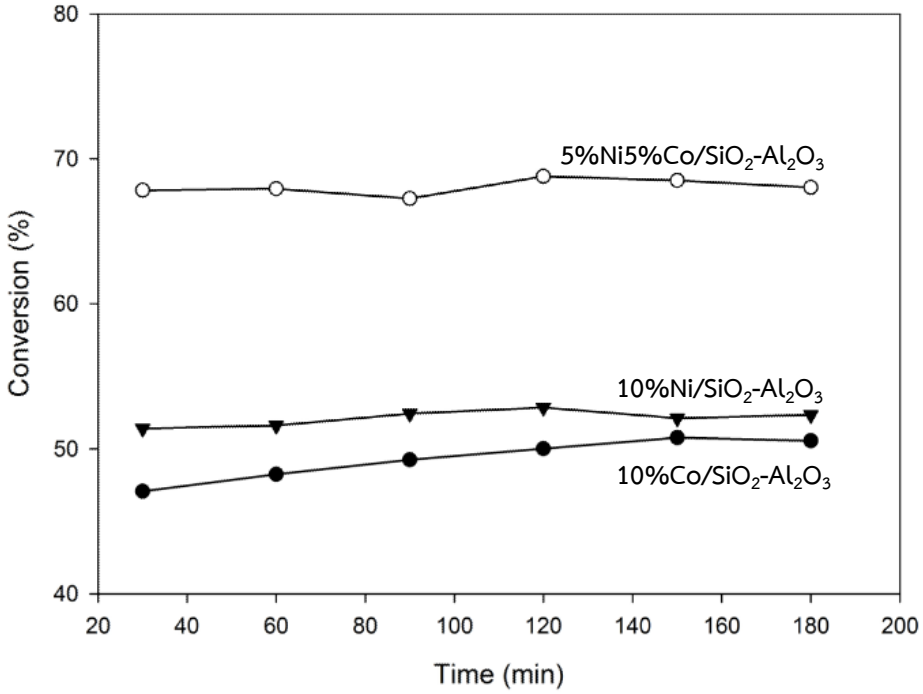

Figure 5.15 Methane conversion of monometallic and bimetallic on SiO_2-Al_2O_3 catalysts at 700˚C

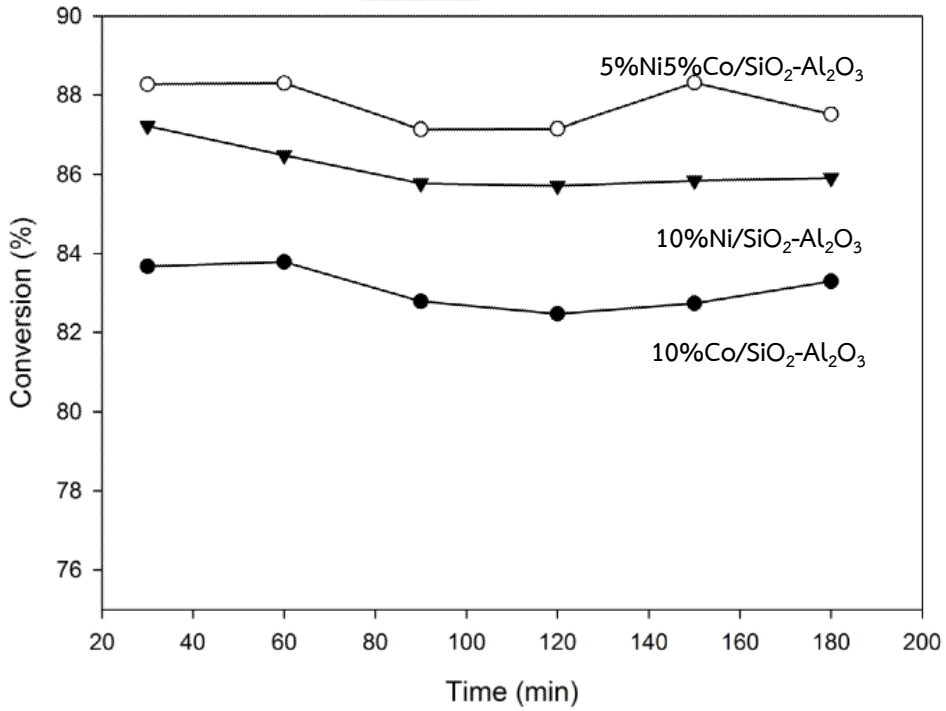

Figure 5.16 Carbon dioxide conversion of monometallic and bimetallic on SiO_2-Al_2O_3 catalysts at 700˚C

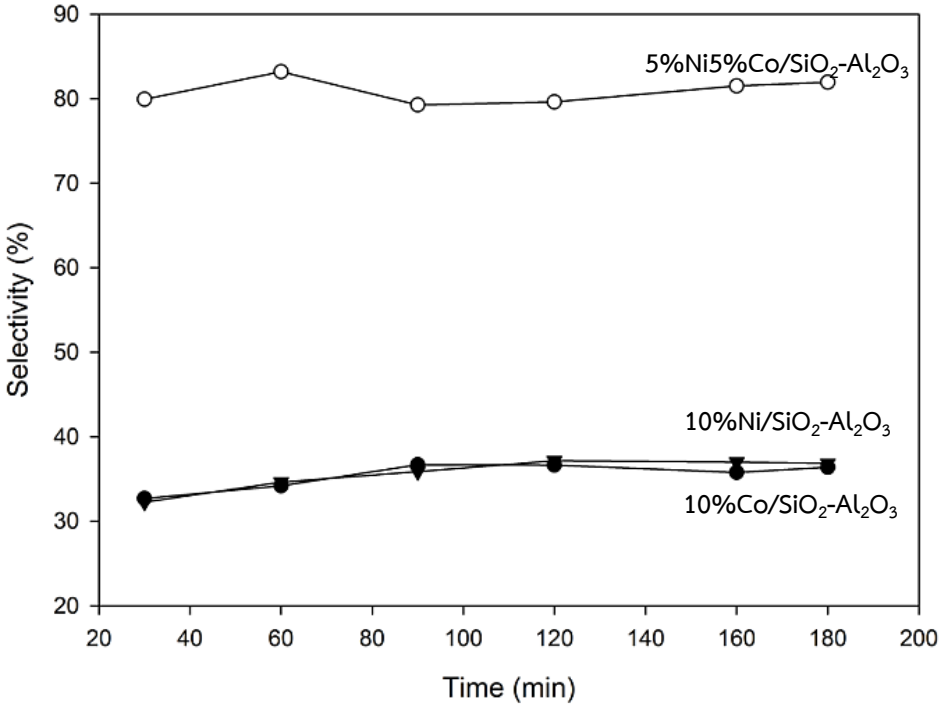

Figure 5.17 Hydrogen selectivity of monometallic and bimetallic on SiO_2-Al_2O_3 catalysts at 700˚C

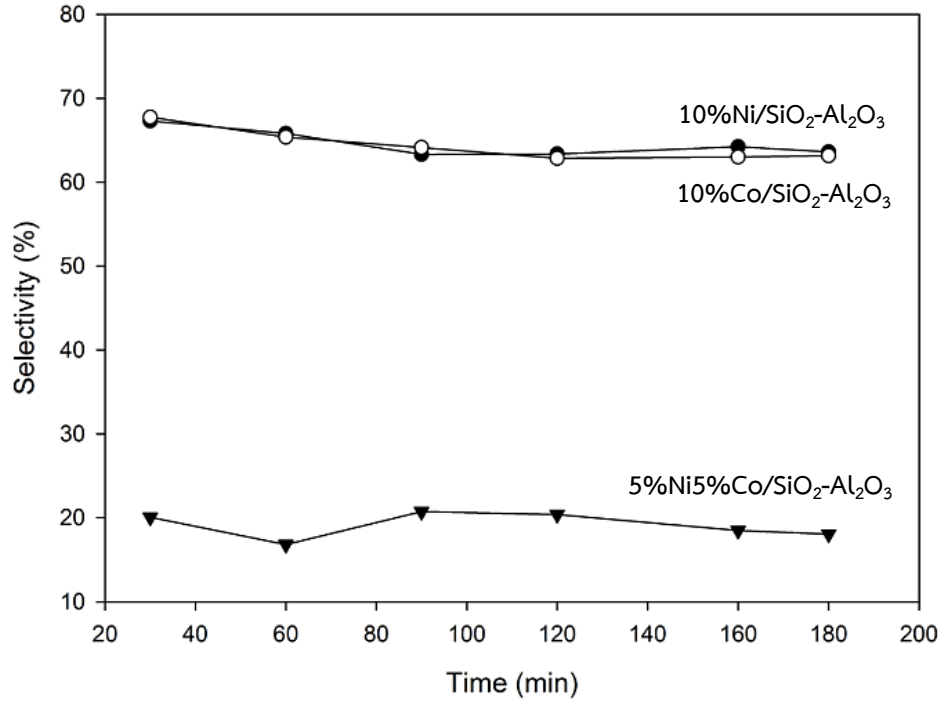

Figure 5.18 Carbon monoxide selectivity of monometallic and bimetallic on SiO_2-Al_2O_3 catalysts at 700˚C

5.1.3. Effect of monometallic and bimetallic on γ-Al_2O_3 catalysts

5.1.3.1 Catalysts characterization

5.1.3.1.1 X-ray diffraction (XRD)

The phase structure of the catalysts was analyzed using X-ray diffraction [15]. The XRD patterns shows the monometallic (10%wt.Ni, 10%wt.Co) and bimetallic (5%wt.Ni5%wt.Co) on γ-Al_2O_3 support, which γ-Al_2O_3 as commercial grade are shown in Figure 5.1. The scans were recorded in the 2θ range of 20-80°. The diffraction peaks of all the Ni-loaded exhibits at the main characteristic peaks positioned at 2θ degrees 36.2°, 43.7°and 61.6°, are correspond to the NiO or $NiAl_2O_4$ crystalline phase [28]. The Co-loaded catalysts were observed at 2θ degrees 30.6°, 36.2°, 42.9°, 58.6°, and 63.6°, are correspond to the Co_3O_4 or $CoAl_2O_4$ crystalline phase [28]. In term of Ni and Co species observes in all samples with no different Ni-Co content. This suggests that the $NiAl_2O_4$ and $CoAl_2O_4$ which are indistinguishable in XRD due to their similar morphology [17]. The result indicates that the broad peak of γ-Al_2O_3. However, the monometallic and bimetallic as the Ni-Co content increases, obvious increase in peak intensity was observed for the peaks of 2θ = 30.6°, 36.2°, 42.9° and 58.6°, indicating the increase in the amount of Ni-Co content of catalysts [53]. The XRD analysis shows that all the samples have been well-crystallized. It can also be seen from the XRD patterns that the bulk phases of the catalysts are not alternated significantly with the change of Ni-Co content [12].

The crystallite sizes of the catalysts are summarized in table 5.17 the crystallite sizes of monometallic and bimetallic were range between 24.9-37.6 nm. The 10%wt.Ni/γ-Al_2O_3 had 28.9 nm, which are larger than 10%wt.Co/γ-Al_2O_3 and 5%wt.Ni5%wt.Co/γ-Al_2O_3 catalysts. The crystallite size of the catalyst is an important factor of the activity of carbon dioxide reforming of methane reaction. Moreover, it can be concluded that there is a proper amount of Co minimizing the crystallite size and improving the catalytic activities [56].

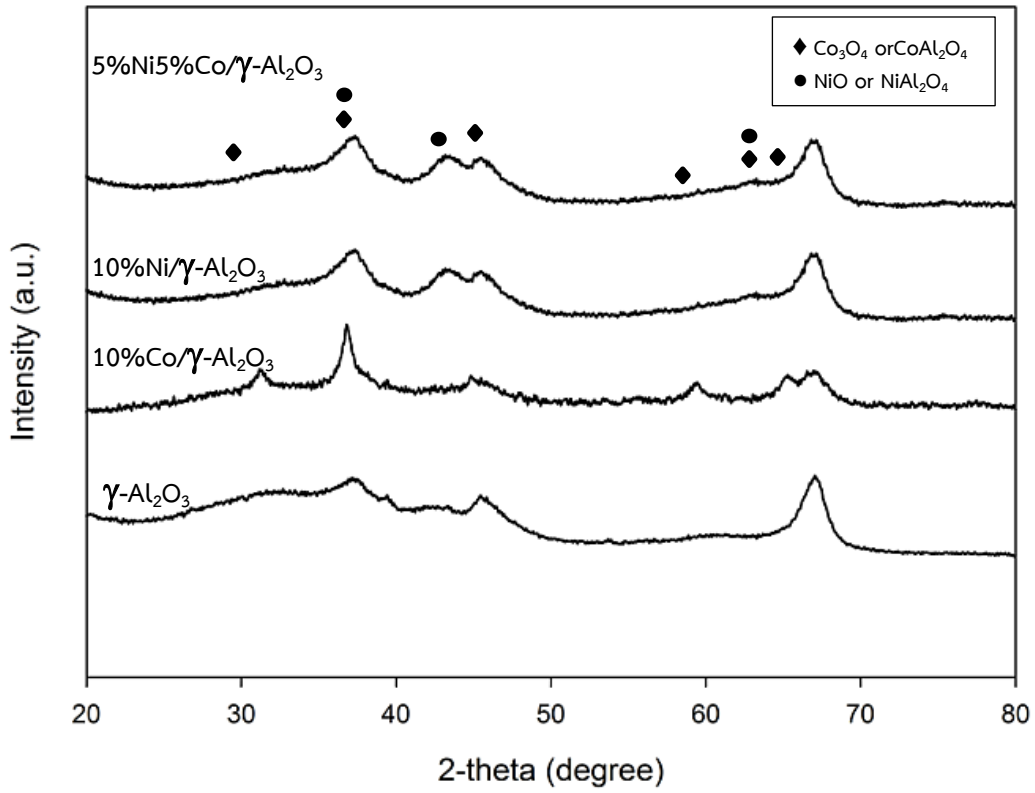

Figure 5.19 The XRD patterns to compare between monometallic (10%wt.Ni, 10%wt.Co) and bimetallic (5%wt.Ni5%wt.Co) on γ-Al_2O_3 catalysts, ♦ = Co_3O_4 or $CoAl_2O_4$, ● = NiO or $NiAl_2O_4$

Table 5.15 Average crystallite size of between monometallic and bimetallic on γ-Al_2O_3 catalysts

Sample	Average crystallite size of catalysts from XRD (nm)
5%Ni5%Co/γ-Al_2O_3	24.8
10%Ni/γ-Al_2O_3	28.9
10%Co/γ-Al_2O_3	25.2
γ-Al_2O_3	38.3

5.1.3.1.2 Nitrogen physisorption

The nitrogen adsorption-desorption isotherm of the monometallic and bimetallic on γ-Al_2O_3 catalysts are displayed in Fig. 5.20. All samples exhibited type IV isotherms and H2-shaped hysteresis loops that are typical of mesoporous structure [30]. The H2-shaped hysteresis loops are associated with a more complex pore structure such as interparticle porosity or irregular tube-like porosity.

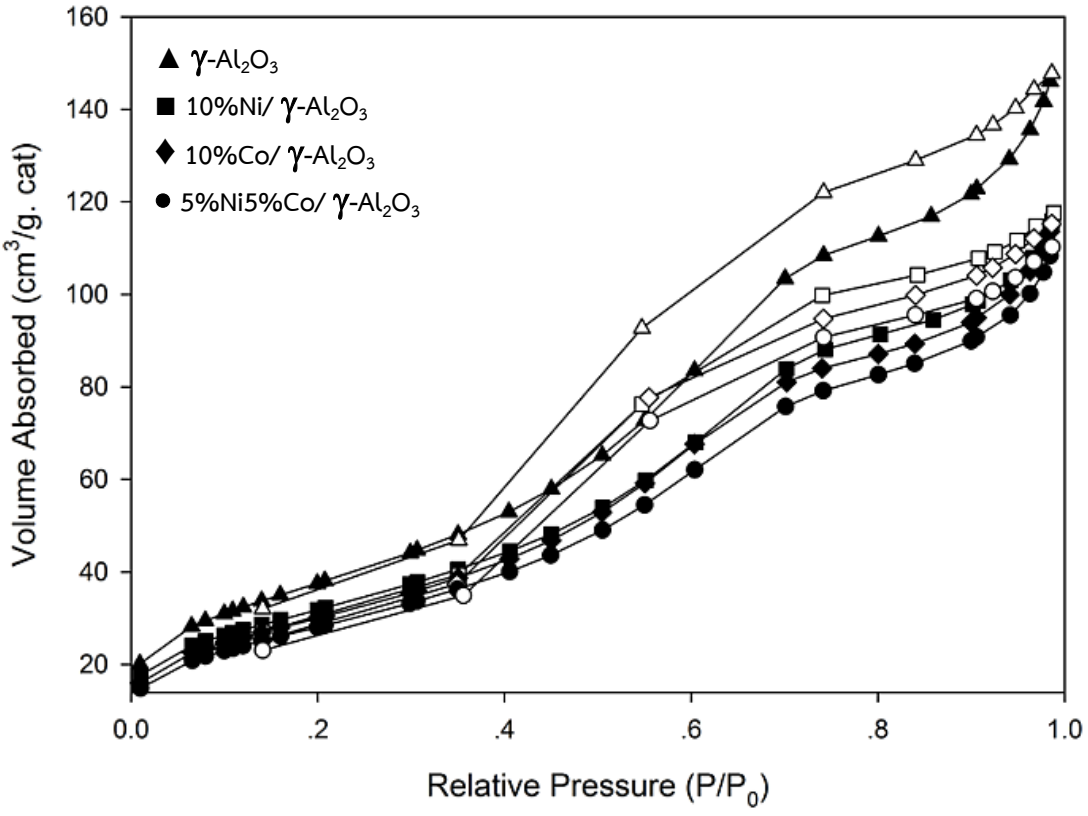

Figure 5.20 nitrogen adsorption-desorption isotherm of the monometallic and bimetallic on γ-Al_2O_3 catalysts

The physical properties of the monometallic (10%wt.Ni, 10%wt.Co), bimetallic (5%wt.Ni5%wt.Co) and catalyst support are summarized in Table 5.16. The surface areas of monometallic and bimetallic catalysts were ranged between 255-306 m^2/g.

The 10%wt.Co/γ-Al_2O_3 catalyst shows the highest BET surface areas 117m^2/g. The BET surface area of the monometallic and bimetallic catalyst decreases in the following order: 10%wt.Co/γ-Al_2O_3 (117 m^2/g) > 10%wt.Ni/γ-Al_2O_3 (110 m^2/g) > 5%wt.Ni5%wt.Co/γ-Al_2O_3 (104 m^2/g). However, the BET surface areas of metal loaded catalysts were decrease compared to γ-Al_2O_3 support, illustrating that the some pores of γ-Al_2O_3 were blocked by Ni and Co loaded particles [66]. The pore volume of 10%wt.Ni/γ-Al_2O_3, 10%wt.Co/γ-Al_2O_3, 5%wt.Ni5%wt.Co/γ-Al_2O_3, and catalyst support were range between 0.16-0.23 cm^3/g. Likewise, the pore volume of the monometallic and bimetallic catalysts decreased after loading metal. Then, the pore size of 10%wt.Ni/γ-Al_2O_3, 10%wt.Co/γ-Al_2O_3, 5%wt.Ni5%wt.Co/γ-Al_2O_3, and catalyst support were range between 3.83-4.05 nm. On the contrary, there was no change in the pore volume for all catalyst. In term of Ni and Co species, this suggests that the particles size of the Ni and Co metal may be small and dispersion on support catalysts [12].

Table 5.16 N_2 physisorption illustrate BET surface areas, pore volume and pore size of monometallic and bimetallic supported on γ-Al_2O_3 catalysts

Sample	BET surface area (m^2/g)	Average pore volume (cm^3/g)	Average pore size (nm)
5%Ni5%Co/ γ-Al_2O_3	104	0.18	3.83
10%Ni/ γ-Al_2O_3	110	0.19	3.90
10%Co/ γ-Al_2O_3	117	0.16	4.05
γ-Al_2O_3	138	0.23	4.01

5.1.3.1.3 Hydrogen temperature program reduction (H_2-TPR)

The reducibility of the catalysts samples was measured using hydrogen temperature-programmed reduction, observations from the TPR profiles. H_2-TPR and the corresponding profiles are compared between the monometallic (10%wt.Ni,

10%wt.Co) and bimetallic (5%wt.Ni5%wt.Co) on γ-Al_2O_3 catalysts samples are shown in Figure 5.18.

Table 5.17 TPR data of monometallic and bimetallic on γ-Al_2O_3 catalysts

Sample	T_m (°C)		
	1° peak	2° peak	3° peak
5%Ni5%Co/γ-Al_2O_3	366	582	-
10%Ni/γ-Al_2O_3	598	-	-
10%Co/γ-Al_2O_3	459	608	-

According to the TPR profiles, for nickel loaded samples the sharp peak seen at 598°C can be attributed to the reduction of NiO $\longrightarrow$ Ni^0 reduction [55]. It shows in literature that the reduction of pure NiO[55]. According to the literature, the reduction of pure Co_3O_4 takes place as a two-step reduction process via Co_3O_4 $\longrightarrow$ CoO $\longrightarrow$ Co° [21]. While the shoulder observed 459 °C for 10%wt.Co/γ-Al_2O_3 is attributed to the reduction of Co_3O_4 $\longrightarrow$ CoO, the main peak seen at 608 °C for 10%wt.Co/γ-Al_2O_3 attributed to the reduction of CoO $\longrightarrow$ Co° [41]. Bimetallic samples exhibit a complex reduction profile. The main reductions are observed at 366 °C for and 582 °C for 5%wt.Ni5%wt.Co/γ-Al_2O_3, are lower than the main reduction temperatures of monometallic catalyst, which may be attributed to the formation of nickel–cobalt alloy [68]. A shift in the reduction peaks to lower temperatures implied an easier reducibility of the 5%wt.Ni5%wt.Co/γ-Al_2O_3, the reduction temperature were affect catalytic activity directly [25]. TPR results of the monometallic (10%wt.Ni, 10%wt.Co) and bimetallic (5%wt.Ni5%wt.Co) on γ-Al_2O_3 catalysts were compared the peak temperature summarized in Table 5.17.

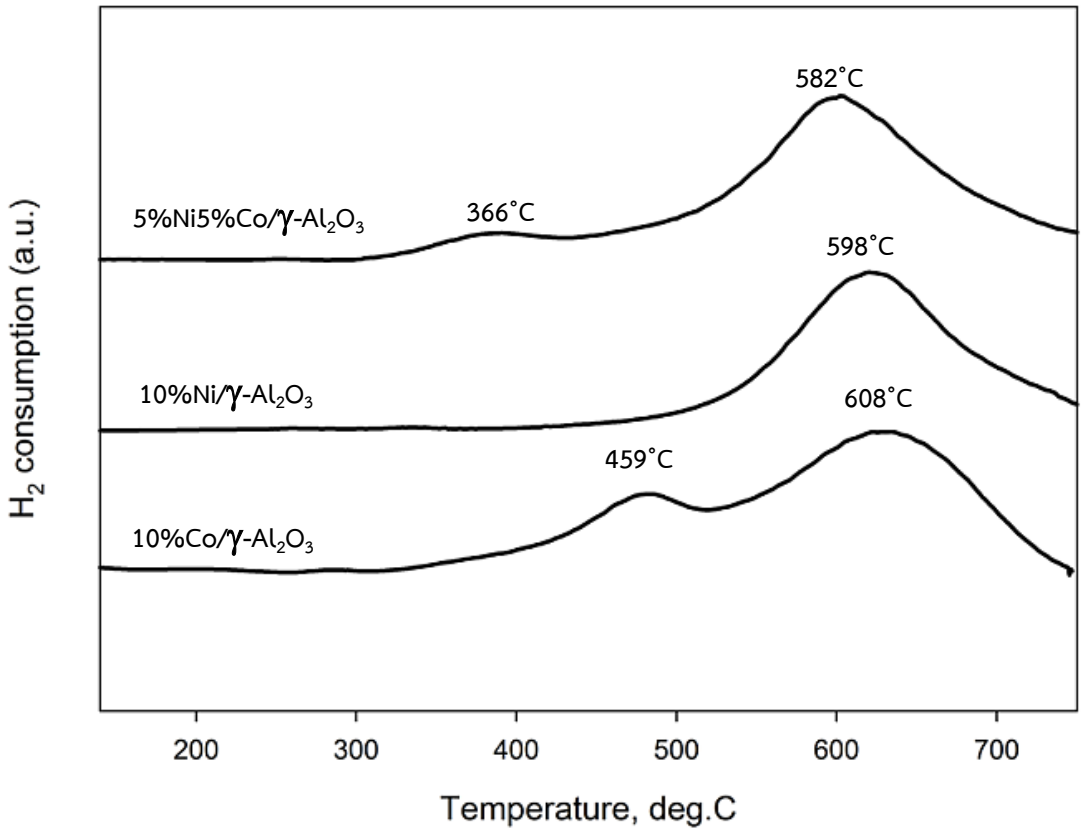

Figure 5.21 The TPR profiles of monometallic (10%wt.Ni, 10%wt.Co) and bimetallic (5%wt.Ni5%wt.Co) on γ-Al_2O_3catalysts

5.1.3.1.4 Ammonia temperature program Desorption (NH_3-TPD)

Ammonia temperature program desorption (NH_3-TPD use to determine the acidity on the surface of the monometallic (10%wt.Ni, 10%wt.Co) and bimetallic (5%wt.Ni5%wt.Co) on γ-Al_2O_3 catalysts samples. The strength of the acid is related to the desorption temperature [67].

Table 5.18 Acidity form NH_3-TPD of monometallic and bimetallic on γ-Al_2O_3 catalysts

Samples	Total acid site, (mmol H^+/g cat)
5%Ni5%Co/γ-Al_2O_3	0.11
10%Ni/γ-Al_2O_3	0.09
10%Co/γ-Al_2O_3	0.06
γ-Al_2O_3	0.07

NH_3-TPD profiles of the monometallic, bimetallic and catalyst support. NH_3 desorption peaks were detected in the tested temperature range (from 40 to 600°C), which illuminates the presence acid sites owing to NH_3 absorption energies on the samples [69]. These desorption peaks were de-convoluted and summarized total acid site in Table 5.18. The weak, medium and strong acid sites were estimated from the desorption peak in the temperature range 120–280°C, 280–450°C and 450–750°C, respectively [49]. The desorption temperature of 5%wtNi5%wtCo/γ-Al_2O_3, 10%wt.Ni/γ-Al_2O_3 , 10%wt.Co/γ-Al_2O_3 and γ-Al_2O_3 support have only one desorption peak (5%wt.Ni5%wt.Co/γ-Al_2O_3, 10%wt,Ni/γ-Al_2O_3, 10%wt.Co/γ-Al_2O_3 and γ-Al_2O_3 support could be classified desorption temperature 126°C, 207°C, 201°C and 203°C, respectively) indicating the presence of weak acid sites. In contrast, the presence of desorption peaks at lower temperature of 5%wt.Ni5%wt.Co/γ-Al_2O_3 shifts to a much low temperature compared with other catalysts. It has been known that the acid sites at high temperature are responsible for the formation of coke and polymer on the catalyst surface [70]. Moreover, the amounts of acid sites on the surface catalysts were showed in Table 5.18. The total acid sites of monometallic and bimetallic catalysts were ranged between 0.06-0.11 mol H^+/g cat. The result shows the increased acidity on 5%wt.Ni5%wt.Co/γ-Al_2O_3 may hamper CO_2 adsorption and activation leading to a lower activity [58].

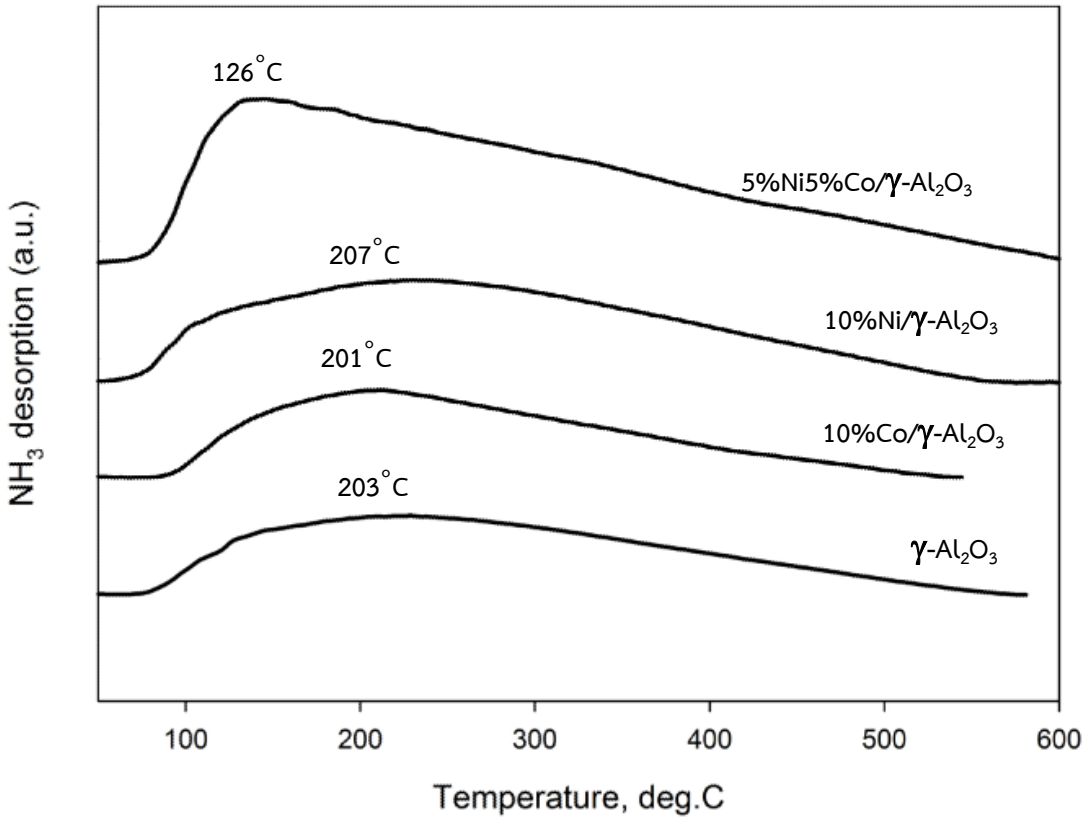

Figure 5.22 The NH_3-TPD profiles of monometallic (10%wt.Ni, 10%wt.Co) and bimetallic (5%wt.NiCo) on γ-Al_2O_3catalysts

5.1.3.1.5 Scanning electron microscopy analyses (SEM)

The EDX result showed values found for composition of a given monometallic and bimetallic on γ-Al_2O_3 catalysts were typically found in catalysts. EDX results indicate that surface composition is close to target at roughly 10%wt.Ni, 10%wt.Co and 5%wt.Ni5%wt.Co. However EDX indicates 5.84%wt.Ni, 6.04%wt.Co as 5%wt.Ni5%wt.Co/γ-Al_2O_3, 10.59%wt.Ni as 10%wt.Ni/γ-Al_2O_3 and 8.97%wt.Co as 10%wt.Co/γ-Al_2O_3. Catalysts with monometallic and bimetallic loadings were also investigated. The adjacent from target composition may be due to adequate mixing of the catalyst materials [45].

Table 5.19 EDX Surface Composition (% Element) result of monometallic and bimetallic on γ-Al_2O_3catalysts

Samples	%Element				%Atomic			
	Al	Si	Ni	Co	Al	Si	Ni	Co
5%Ni5%Co/γ-Al_2O_3	88.12	-	5.84	6.04	91.91	-	4.22	3.87
10%Ni/γ-Al_2O_3	89.41	-	10.59	-	91.35	-	8.65	-
10%Co/γ-Al_2O_3	91.03	-	-	8.97	92.53	-	-	7.43

5.1.3.1.6 Hydrogen chemisorption

H_2 pulse chemisorption results the amount of active site of over various monometallic (10%wt.Ni, 10%wt.Co) and bimetallic (5%wt.Ni5%wt.Co) on γ-Al_2O_3 catalysts are presented in Table 5.20. The nickel and cobalt active site were ranged between 1.84-8.18 $X10^{18}$ molecules H_2/g cat in the order: 5%wt.Ni5%wt.Co/γ-Al_2O_3 > 10%wt.Ni/γ-Al_2O_3 > 10%wt.Co/γ-Al_2O_3. The H_2 chemisorption of 5%wt.Ni5%wt.Co/γ-Al_2O_3 is higher than the 10%wt.Ni/γ-Al_2O_3 and 10%wt.Co/γ-Al_2O_3. Compared with 10%wt.Ni/γ-Al_2O_3 and 10%wt.Co/γ-Al_2O_3 was investigated the same amount of Ni and Co loading, the 10%wt.Ni/γ-Al_2O_3 exhibits higher Ni dispersion, illustrating the homogeneous distribution of the small Ni nanoparticles because amorphous structure and the strong interaction between Ni and γ-Al_2O_3 support [63]. The 5%wt.Ni5%wt.Co/γ-Al_2O_3 shows higher H_2 chemisorption and better dispersion on support than 10%wt.Ni/γ-Al_2O_3 and 10%wt.Co/γ-Al_2O_3 catalysts.

According to the average crystallite size as measured from XRD, the crystallite size of catalysts from the 5%wt.Ni5%wt.Co/γ-Al_2O_3 was smaller than the 10%wt.Ni/γ-Al_2O_3. Therefore, the crystallite size of nickel and cobalt species of 5%wt.Ni5%wt.Co/γ-Al_2O_3 may be easier to reduce to nickel and cobalt active site with the result of H_2-TPR [19].

Table 5.20 Hydrogen chemisorption result of monometallic and bimetallic on γ-Al_2O_3 catalysts

Sample	H_2 chemisorption ($x10^{-18}$ molecules/g.cat)	% Dispersion
5%Ni5%Co/γ-Al_2O_3	8.18	7.93
10%Ni/γ-Al_2O_3	5.43	2.63
10%Co/γ-Al_2O_3	1.84	0.89

5.1.3.1.7 Thermogravimetric analysis (TGA)

TGA analysis in Figure 5.20 showing TGA curves monometallic (10%wt.Ni, 10%wt.Co) and bimetallic (5%wt.Ni5%wt.Co) used catalysts (after 3 h reaction). In this figure, the carbon deposition can be represented by weight loss and thermal differences between the samples and the inert materials [71]. The weight losses of monometallic and bimetallic catalysts temperature were ranged between 388-495˚C. The weight loss of the spent catalysts decreased in the following order: 5%wt.Ni5%wt.Co/γ-Al_2O_3 > 10%wt.Ni/γ-Al_2O_3 > 10%wt.Co/γ-Al_2O_3. However, the weight losses of monometallic and bimetallic catalysts were ranged between 24.9-56.3%. According to the TG profiles, cobalt-containing catalysts, 10%wt.Co/γ-Al_2O_3 catalysts, showed a weight loss of about 88.7%, whereas 5%wt.NiCo/H-Beta-Al_2O_3 and 10%wt.Ni/γ-Al_2O_3 catalyst exhibits a weight loss of 40.0% and 45.6% revealing a lower carbon accumulation [3]. However, the only displayed minimal weight losses, demonstrating its higher de-coking performance of catalytic reaction [7].

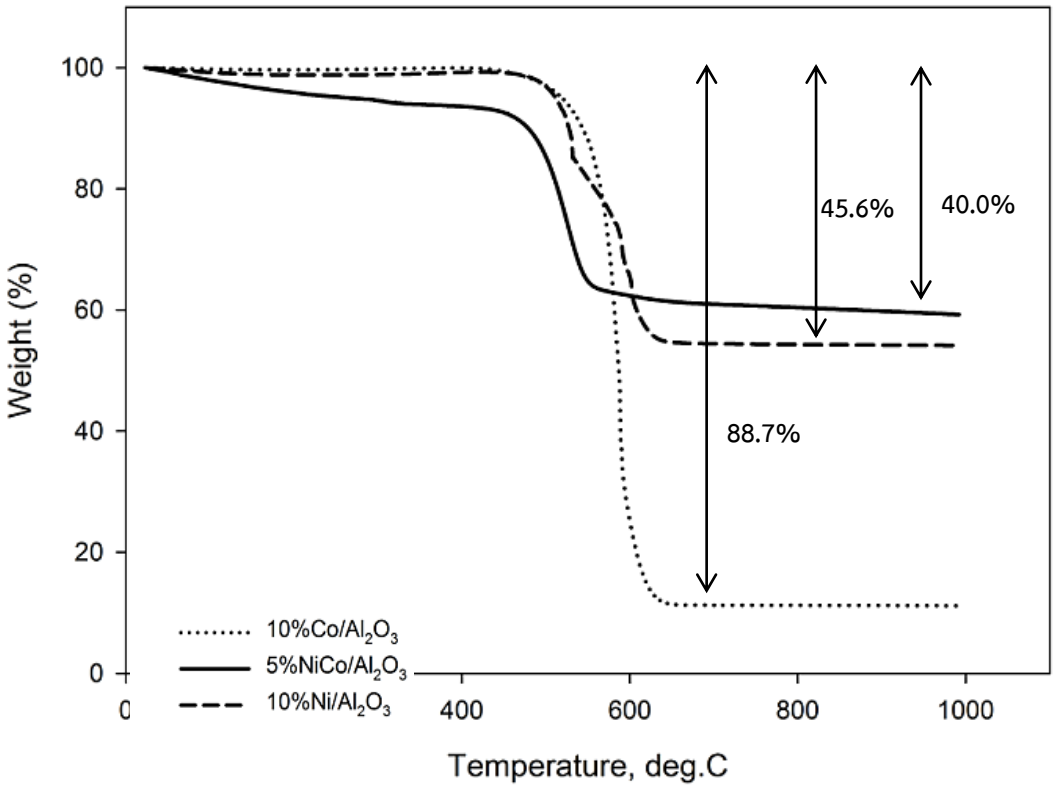

Figure 5.23 TGA curves in air atmosphere after being used in reaction at 700 °C for 5 h for the monometallic (10%wt.Ni, 10%wt.Co) and bimetallic (5%wt.NiCo) on γ-Al_2O_3 catalysts calcined at 500˚C

5.1.3.2 The catalytic activity of the monometallic and bimetallic on γ-Al_2O_3 catalyst in CO_2 reforming of methane

The overall activities of the monometallic (10%wt.Ni, 10%wt.Co) and bimetallic (5%wt.Ni5%wt.Co) on γ-Al_2O_3 catalysts were studied in carbon dioxide reforming of methane reaction. Firstly, 0.2 g catalyst was packed in the quartz reactor. Total gas flow rate was 50 ml/min with the gas nitrogen. Secondly, the catalysts were reduced in flowing hydrogen at 600˚C for 1 h. Next, increase temperature to 700˚C with nitrogen. Finally, the reaction was carried out at 700˚C and 1 atm.

The CH_4 and CO_2 conversions of monometallic and bimetallic at 700°C are shown in Figure 5.21 and Figure 5.22 the conversion and product selectivity during carbon dioxide reforming of methane reaction are shown in Table 5.21 The steady state in methane and carbon dioxide conversion of carbon dioxide reforming of methane reaction of the monometallic (10%wt.Ni, 10%wt.Co) and bimetallic (5%wt.Ni5%wt.Co) on γ-Al_2O_3 catalysts were ranged between 59.0-68.9% and 74.0-81.2% respectively. In the order: 5%wt.Ni5%wt.Co/γ-Al_2O_3 > 10%wt.Ni/γ-Al_2O_3 > 10%wt.Co/γ-Al_2O_3. The 5%wt.Ni5%wt.Co/γ-Al_2O_3 shows the highest methane and carbon dioxide conversion among the 10%wt.Ni/γ-Al_2O_3 > 10%wt.Co/γ-Al_2O_3 catalysts, evidenced H_2 chemisorption, the amount of nickel and cobalt active sites of 5%wt.Ni5%wtCo/γ-Al_2O_3 catalysts are highest. Comparing the monometallic (10%wt.Ni/γ-Al_2O_3, 10%wt.Co/γ-Al_2O_3) catalysts, the 10%wt.Ni/γ-Al_2O_3 exhibits slightly higher methane and carbon dioxide conversion than the 10%wt.Co/γ-Al_2O_3 catalyst. According to H_2 chemisorption, the amounts of active sites of 5%wt.Ni5%wt.Co/γ-Al_2O_3 catalyst are higher than 10%wt.Ni/γ-Al_2O_3 catalyst. However, the improved with added cobalt catalysts performances can be attributed to better dispersion of the NiO particles, according to the smaller crystallite sizes found in the XRD patterns [52]. That is the smaller NiO and CoO may be easier to reduce to active nickel and cobalt particles[26]. 5%wt.Ni5%wt.Co/γ-Al_2O_3 is shift of the reduction temperature towards lower temperature than monometallic catalysts. Therefore, the reduction of NiO and CoO is easier [24]. TGA result 5%NiCo/γ-Al_2O_3 has the lowest coke formation due to low deactivation of catalysts [31]. However, catalyst deactivation may be related to their lower Ni dispersion with high nickel loading that leads to the sintering of Ni particles and considerable coke accumulation [4]. Therefore, addition of cobalt to nickel catalysts improves catalytic performances of carbon dioxide reforming of methane reaction [32].

The H_2 and CO product selectivity of monometallic and bimetallic catalysts are given in Figure 5.23 and Figure 5.24. All catalysts exhibit similar performance in carbon dioxide reforming of methane. The steady state of H_2 and CO selectivity of

carbon dioxide reforming of methane reaction of the monometallic (10%wt.Ni, 10%wt.Co) and bimetallic (5%wt.Ni5%wt.Co) on γ-Al_2O_3 catalysts were ranged between 25.4-27.5% and 46.6-50.4% respectively. In terms of H_2 and CO product selectivity, CO selectivity is higher than H_2 selectivity for all the catalysts.

Table 5.21 The conversion, and product selectivity during CO_2 reforming of methane at initial and steady-state conditions of monometallic and bimetallic on γ-Al_2O_3catalysts at 600˚C

Sample	Conversion (%) [a]				Product selectivity (%) [a]			
	Initial [b]		Steady state [c]		Initial [b]		Steady state [c]	
	CH_4	CO_2	CH_4	CO_2	H_2	CO	H_2	CO
5%Ni5%Co/γ-Al_2O_3	69.1	83.8	68.9	81.2	33.8	66.2	34.7	65.3
10%Ni/γ-Al_2O_3	64.5	78.2	63.9	79.3	33.0	64.3	34.7	64.8
10%Co/γ-Al_2O_3	60.4	75.9	59.0	74.0	35.7	67.0	35.2	65.3

[a] CO_2 reforming of methane was carried out at 600˚C, 1 atm, CH_4/CO_2=1

[b] After 30 min of reaction

[b] After 3 h of reaction

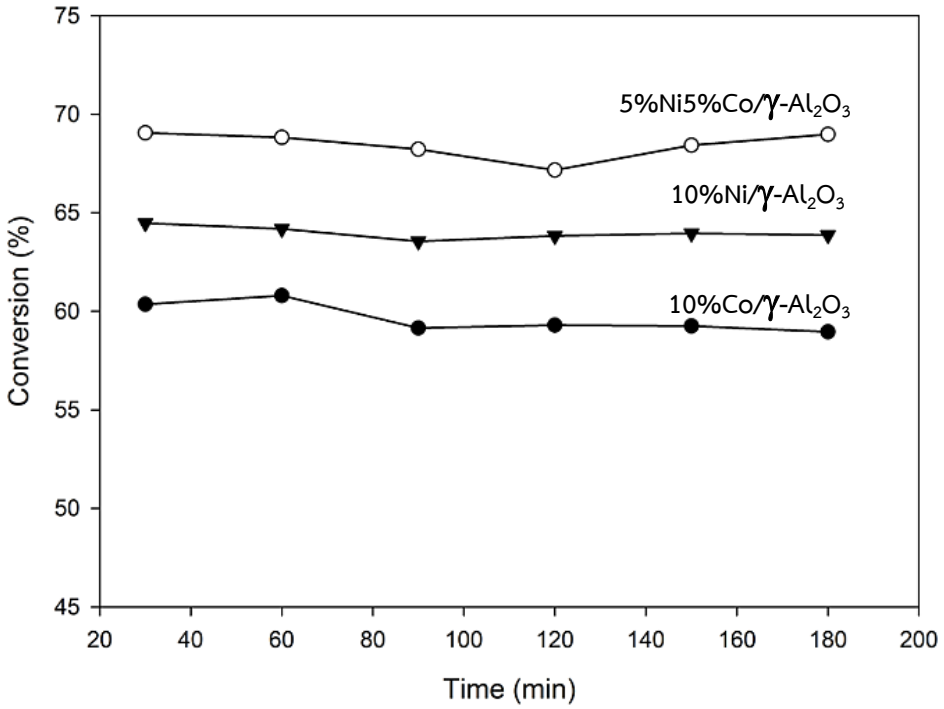

Figure 5.24 Methane conversion of monometallic and bimetallic on γ-Al_2O_3 catalysts at 700˚C

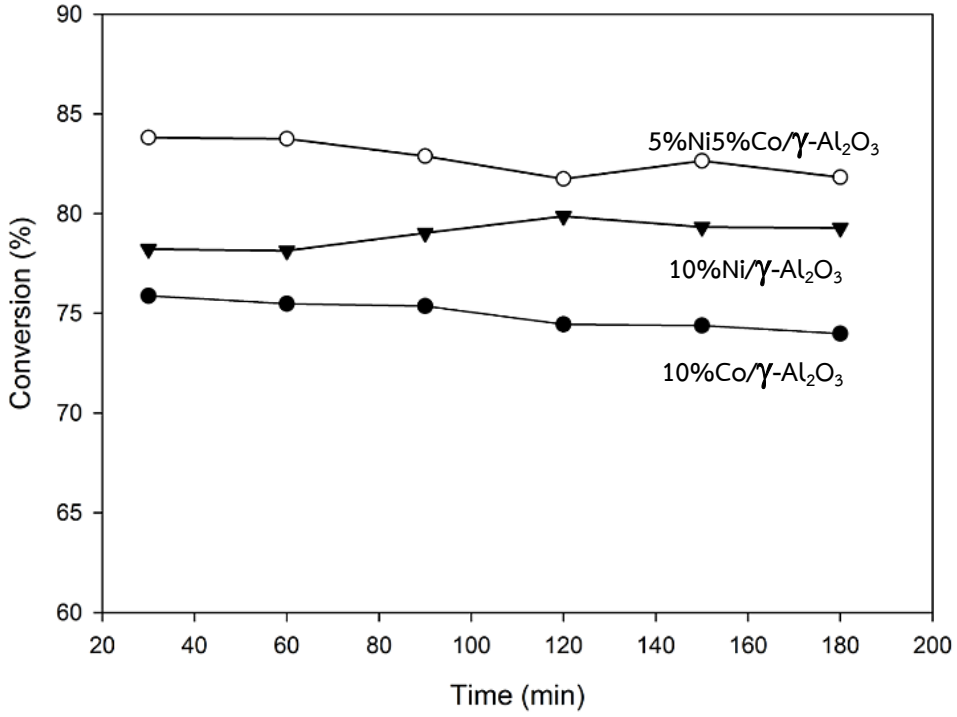

Figure 5.25 Carbon dioxide conversion of monometallic and bimetallic on γ-Al_2O_3 catalysts at 700˚C

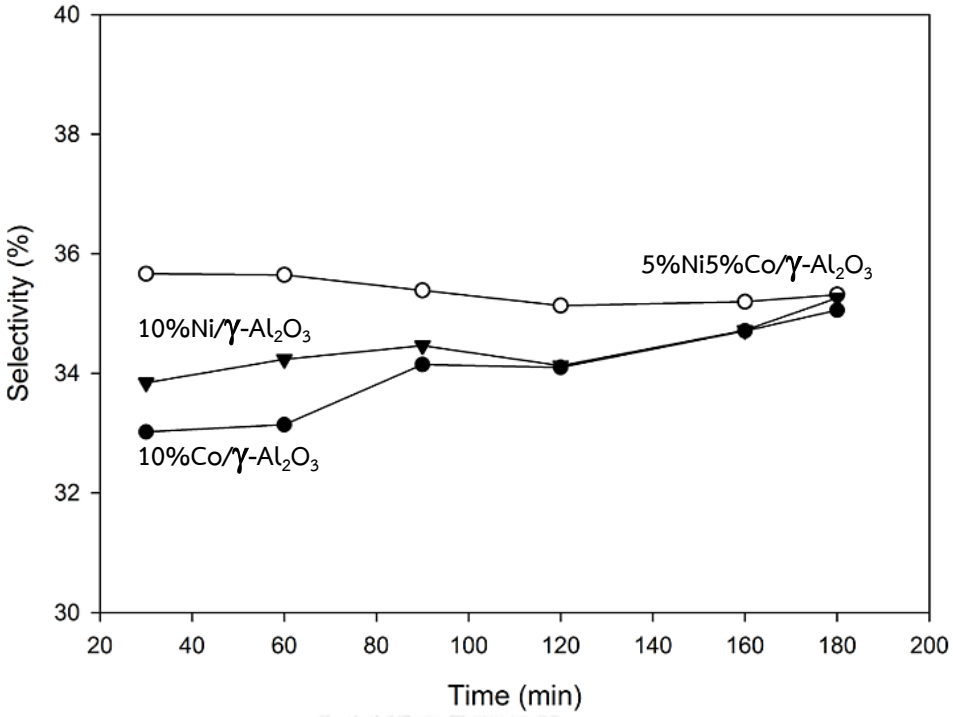

Figure 5.26 Hydrogen selectivity of monometallic and bimetallic on γ-Al_2O_3 catalysts at 700˚C

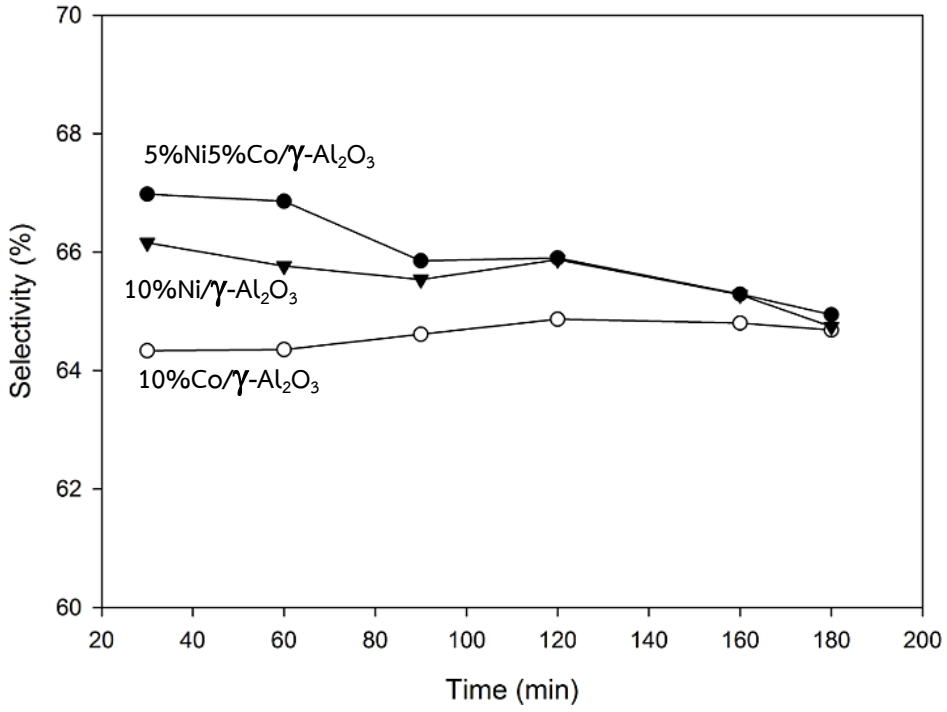

Figure 5.27 Carbon monoxide selectivity of monometallic and bimetallic on γ-Al_2O_3 catalysts at 700˚C

5.2 Effect of the bimetallic on different supports

5.2.1 Catalysts characterization

5.2.1.1 X-ray diffraction (XRD)

The crystallite sizes of the catalysts were calculated by Scherrer equation using XRD pattern [32]. The particle size of NiO and CoO species for 5%wt.Ni5%wt.Co/H-Beta-Al_2O_3 catalyst is smaller than that of the other catalysts. The small crystallite size of the NiO shows a good dispersion and better access to the active phase. H-Beta-Al_2O_3 support with the Ni and Co metal addition exhibits better metal dispersion compare to other supports [34]. Sanchez and et al [53]. reported that H-Beta has high metal dispersion of catalysts due to well-order structure, interaction between metal catalysts, and oxygen ion lattice vacancies.

Table 5.22 Average crystallite size of bimetallic catalysts on different supports

Sample	Average crystallite size of catalysts from XRD (nm)
5%Ni5%Co/H-Beta-Al_2O_3	21.9
5%Ni5%Co/SiO_2-Al_2O_3	25.8
5%Ni5%Co/γ-Al_2O_3	24.8

5.2.1.2 Nitrogen physisorption

The nitrogen adsorption-desorption isotherm of the bimetallic catalysts on different supports are display in Fig. 5.28. 5%Ni5%Co/H-Beta-Al_2O_3 and 5%Ni5%Co/γ-Al_2O_3 samples exhibit type IV isotherms. While 5%Ni5%Co/SiO_2-Al_2O_3 indicate type II isotherms and H2-shaped hysteresis loops that are typical of mesoporous structure [30]. The H2-shaped hysteresis loops are associated with a more complex pore structure such as interparticle porosity or irregular tube-like porosity.

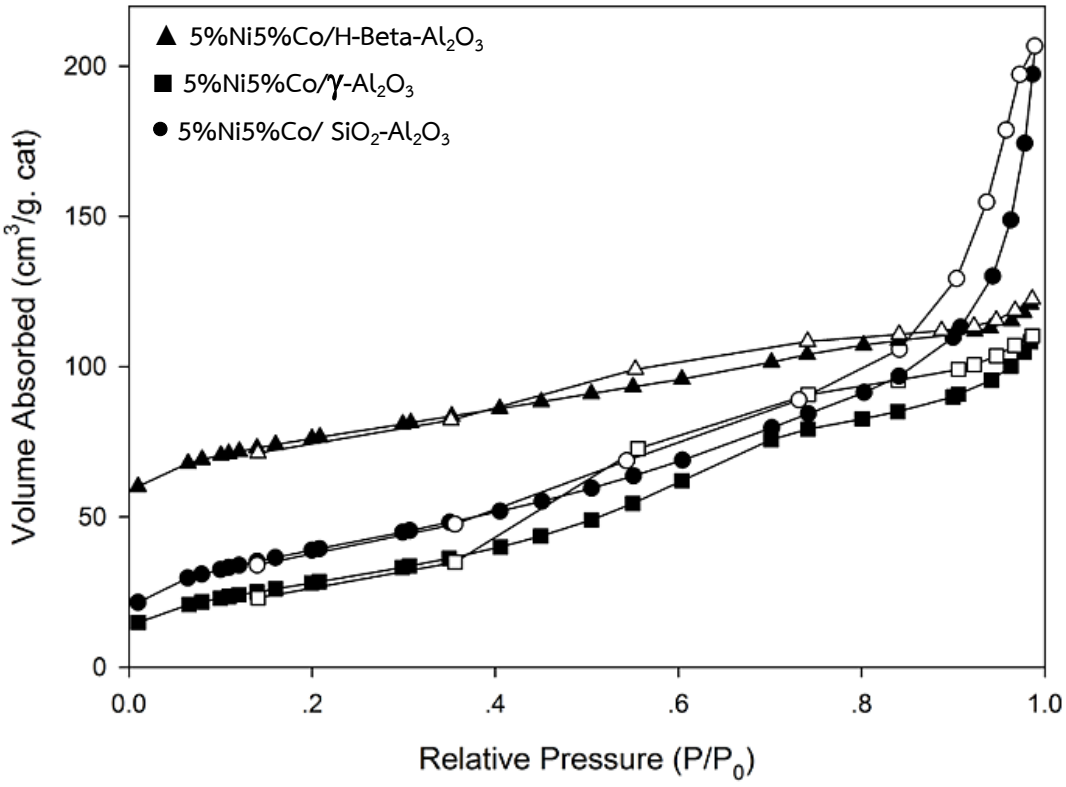

Figure 5.28 nitrogen adsorption-desorption isotherm of the bimetallic catalysts on different supports

The specific surface area of the bimetallic (5%wt.Ni5%wt.Co) on different supports which are H-Beta-Al_2O_3, Al_2O_3-SiO_2 prepared by sol-gel method and Gamma-alumina commercial are illustrated in Table 5.23. The surface areas of catalysts were characterized by BET (Brunauer-Emmett-Teller) method. BET surface areas, pore volume, and pore size are summarized in Table 5.2. The surface areas of bimetallic catalysts on different supports were ranged between 104-270 m^2/g. The modified supports with H-Beta prepared by Sol-gel method shows higher surface area than modified support with γ-Al_2O_3 and SiO_2, because H-Beta zeolite has well-defined structures, and high surface areas that improve properties of catalyst support [55]. Moreover, pore volume of the 5%wt.Ni5%wt.Co on different supports were ranged between 0.14-0.35 cm^2/g. the modified support with H-Beta prepared by Sol-gel method and γ-Al_2O_3 commercial support can result in similar pore volume and pores

size. It indicates that the modified supports do not significantly influence the textural properties of 5%wt.Ni5%wt.Co/H-Beta-Al_2O_3 and 5%wt.Ni5%wt.Co/γ-Al_2O_3 catalysts[36]. The modified supports with SiO_2 by Sol-gel method indicates the most increase of pore volume and pore size among the other catalysts [28].

Table 5.23 N_2 physisorption illustrate BET surface areas, pore volume and pore size of bimetallic catalysts on different supports

Sample	BET surface area (m^2/g)	Average pore volume (cm^3/g)	Average pore size (nm)
5%Ni5%Co/H-Beta-Al_2O_3	270	0.14	3.78
5%Ni5%Co/SiO_2-Al_2O_3	171	0.35	7.88
5%Ni5%Co/γ-Al_2O_3	104	0.18	3.83

5.2.1.2 Hydrogen temperature program reduction (H_2-TPR)

Temperature programmed reduction (TPR) analysis was used for evaluating the reduction properties of prepared catalysts. It was carried out to determine the reduction behaviors of the 5%wt.Ni5wtCo on modified catalysts supports with H-Beta-Al_2O_3, Al_2O_3-SiO_2 prepared by sol-gel method and Gamma-alumina commercial. All catalysts samples were prepared by the incipient wetness impregnation method with nickel nitrate and cobalt nitrate. In general, the TPR profiles depend on the metal support interaction, variance in metal particle size, and support porous structure which, result in different reducibility of the modified catalysts support samples are shown in Figure 5.25.

Table 5.24 TPR data of bimetallic catalysts on different supports

Sample	T_m (˚C)		
	1˚ peak	2˚ peak	3˚ peak
5%Ni5%Co/H-Beta-Al_2O_3	284	308	475
5%Ni5%Co/SiO_2-Al_2O_3	373	530	-
5%Ni5%Co/γ-Al_2O_3	366	582	-

The TPR profiles of bimetallic (5%wt.Ni5%wt.Co) on different supports which are H-Beta-Al_2O_3, Al_2O_3-SiO_2 prepared by sol-gel method and Gamma-alumina commercial catalysts. The reduction temperature can be used to manifest the metal-support interaction the reducibility [20]. TPR profile of nickel species indicates of NiO particles there is assigned to NiO to Ni^0 species reduction [38]. From TPR profiles, three reduction peaks of cobalt species can be observed. It is estimated that the first reduction peak is the bulk Co_3O_4, the second reduction peak means the reduction of Co_3O_4 to CoO and the third peak represents the reduction of CoO to metallic cobalt[1]. A similar result was also reported by Bouarab et al [14]. The TPR results of the bimetallic (5%wt.Ni5%wt.Co) on different supports which are H-Beta-Al_2O_3, Al_2O_3-SiO_2 prepared by sol-gel method and Gamma-alumina commercial catalysts are summarized in Table 5.24. However, the reduction peak of 5%wt.Ni5%wt.Co/H-Beta-Al_2O_3 is shifted to lower temperature (around 582˚C) compared with modified catalyst support by Al_2O_3-SiO_2 and γ-Al_2O_3. The addition of H-Beta modifies to catalyst support decrease the reduction temperature and increases the reducibility of bimetallic catalyst [14]. A shift in the reduction peaks to lower temperatures implied an easier reducibility of the 5%wt.Ni5%wt.Co/H-Beta-Al_2O_3 samples [57]. This result indicates that the modified support with H-Beta zeolite improves the dispersion of Ni and Co species because H-Beta-Al_2O_3 support has higher surface areas to effect of the dispersion of Ni and Co metal [21].

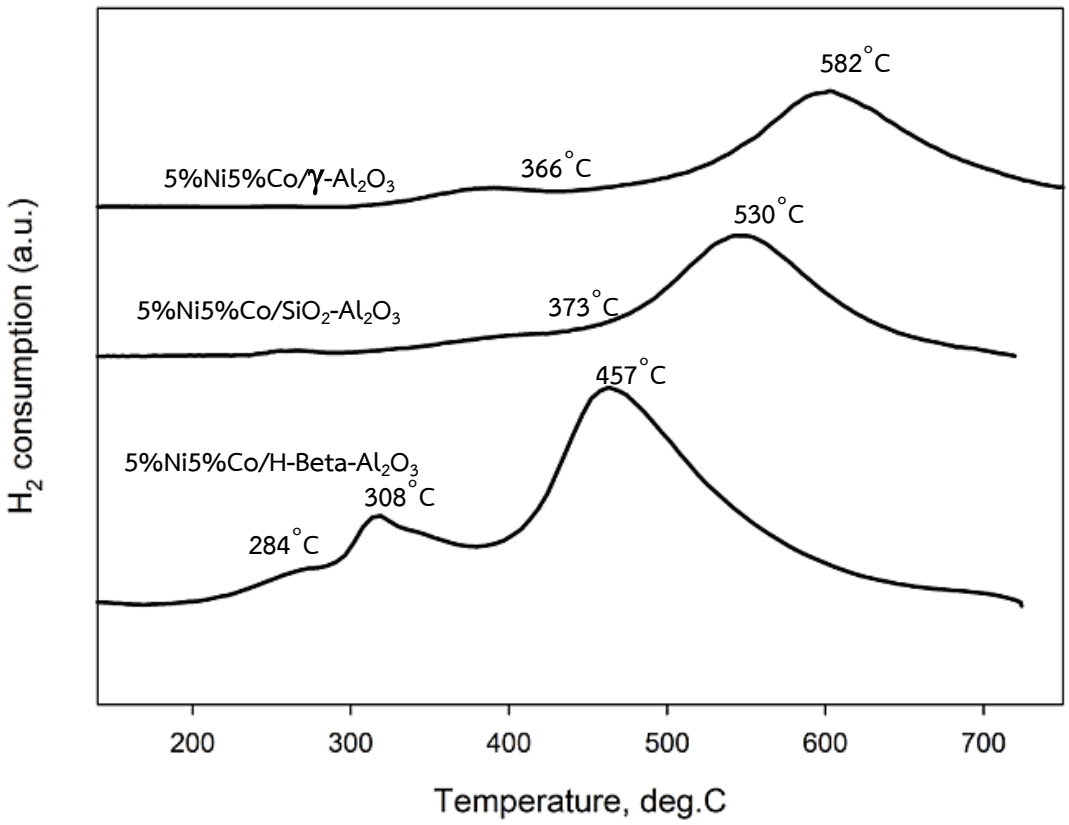

Figure 5.29 The TPR profiles of bimetallic catalysts on different supports

5.2.1.3 Ammonia temperature program Desorption (NH_3-TPD)

The surface acidity of the bimetallic (5%wt.Ni5%wt.Co) on different supports are H-Beta-Al_2O_3, Al_2O_3-SiO_2 prepared by sol-gel method and Gamma-alumina commercial catalysts samples. The strength of the acid is related to the desorption temperature [56]. The overall acidity of the samples was quantified from the adsorption step at 100 °C. Then, followed by the removal of physically bound ammonia from the surface with flowing of helium [40].

Table 5.25 Acidity form NH_3-TPD of bimetallic catalysts on different supports

Samples	Total acid site, (mmol H^+/g cat)
5%Ni5%Co/H-Beta-Al_2O_3	0.15
5%Ni5%Co/SiO_2-Al_2O_3	0.12
5%Ni5%Co/γ-Al_2O_3	0.11

NH_3-TPD profiles of the bimetallic (5%wt.Ni5%wt.Co) on different supports, which are modified Al_2O_3 by H-Beta zeolite, SiO_2 prepared by sol-gel method, and Gamma-alumina commercial catalysts, exhibit two bands corresponding to two types of acid sites. The first peak consists of a peak located at low temperatures (≤280 °C) accompanied by a second own which is much more intense feature at relatively high temperatures above 280˚C [16]. The latter are probably due to a fraction of strong acid sites present at the surface of the catalysts [10]. It can be found the desorption temperature of γ-Al_2O_3 support and modified support by H-Beta zeolite have only one desorption peak (5%wt.Ni5%wt.Co/ H-Beta-Al_2O_3 and 5%wt.Ni5%wt.Co/γ-Al_2O_3 can be classified have desorption temperature at 141˚C, 126˚C respectively) indicating the presence of weak acid sites. In contrast, the presence of desorption peaks at lower temperature on 5%wt.Ni5%wt.Co/γ-Al_2O_3 shifted to low temperature compared to other catalysts. The acid sites at high temperature are responsible for the formation of coke and polymer on the catalyst surface [41]. The result finds the modified support with SiO_2 has two peaks which locate at low temperature (5%wt.Ni5%wt.Co/SiO_2-Al_2O_3 could be classified desorption temperature 119˚C, 246˚C respectively). Moreover, these desorption peaks are de-convoluted and summarized total acid site in Table 1. The total acid sites of bimetallic (5%wt.Ni5%wt.Co) on different supports were ranged between 0.11-0.15 mol H^+/g cat. The results find the similar acidity of all cases leading to lower activity.

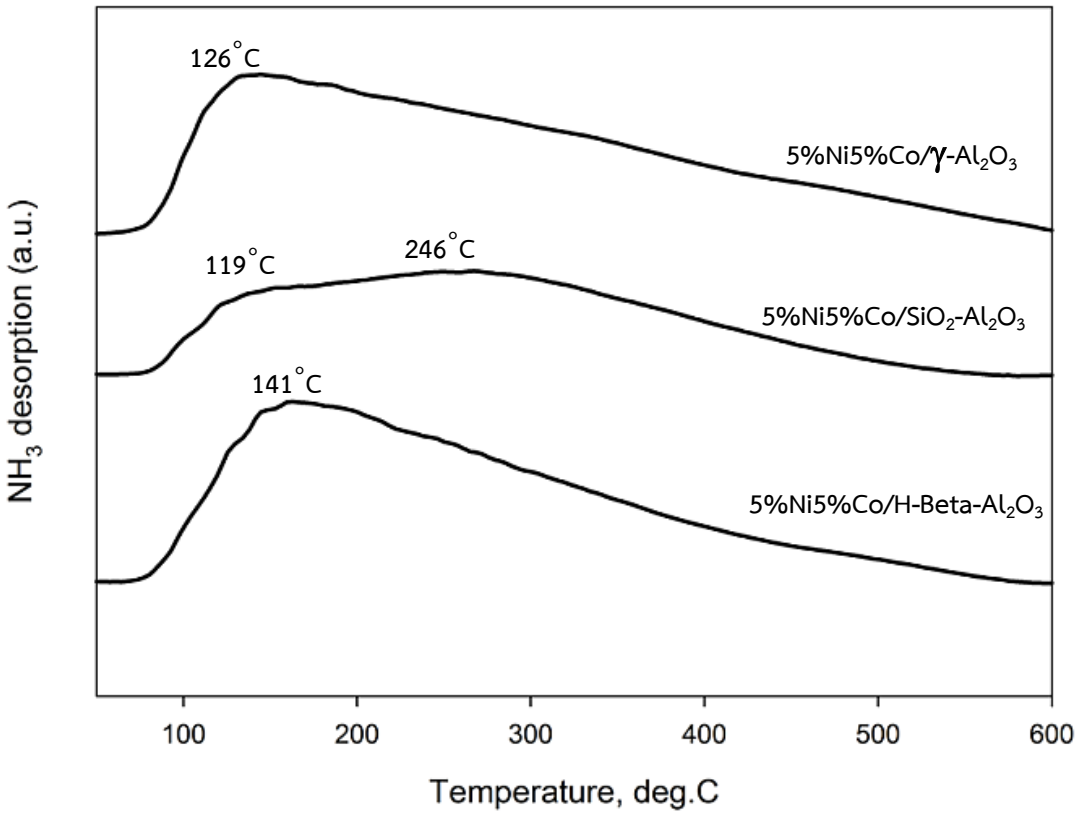

Figure 5.30 The NH_3-TPD profiles of bimetallic catalysts on different supports.

5.2.1.4 Scanning electron microscopy analyses (SEM)

EDX analyses for the bimetallic (5%wt.Ni5%wt.Co) on different supports which are modified Al_2O_3 by H-Beta zeolite, SiO_2 prepared by sol-gel method, and Gamma-alumina commercial catalysts are demonstrated in Table 5.26. All elements in the fabricating method are clearly observed in the EDX spectra [42]. EDX analysis was used to determine quantitatively the amount of composition on the catalyst surfaces [29]. From all of the samples, the surface composition is close to target at roughly 5%wt.NiCo. All catalysts were similar with target composition metal were prepared by incipient wetness impregnation.

Table 5.26 EDX Surface Composition (% Element) result of bimetallic catalysts on different supports

Samples	%Element				%Atomic			
	Al	Si	Ni	Co	Al	Si	Ni	Co
5%Ni5%Co/H-Beta-Al_2O_3	40.08	48.82	5.73	5.37	47.77	44.55	3.93	3.76
5%Ni5%Co/SiO_2-Al_2O_3	50.52	38.25	4.34	4.69	62.87	28.45	4.70	3.98
5%Ni5%Co/γ-Al_2O_3	88.12	-	5.84	6.04	91.91	-	4.22	3.87

5.2.1.5 Hydrogen chemisorption

H_2-chemisorption (metal dispersion, metal surface area and active particle size) results over bimetallic (5%wt.Ni5%wt.Co) on different supports which are modified Al_2O_3 by H-Beta zeolite, SiO_2 prepared by sol-gel method, and Gamma-alumina commercial catalysts are presented in Table 5.27. The amount of nickel and cobalt active site of modified catalysts support by H-Beta, SiO_2 and γ-Al_2O_3 were ranged between 1.84-8.18 $X10^{18}$ molecules H_2/g cat. It is found that the H_2 chemisorption of modified support with H-beta zeolite is higher than the modified support by SiO_2 and γ-Al_2O_3. Moreover, the modified support with H-Beta has the most improving metal dispersion compare to others. According to the average crystallite size as measured from XRD, the crystallite size of modified support with H-Beta is smaller than others catalysts support. Therefore, the H_2-TPR result, the crystallite size of nickel and cobalt species of 5%wt.Ni5%wt.Co/H-Beta-Al_2O_3 may be easier to reduce to nickel and cobalt active site [6]. Also, BET surface areas of modified support with H-Beta are the highest due to higher Ni and Co dispersion [68].

Table 5.27 Hydrogen chemisorption result of bimetallic catalysts on different supports

Sample	H_2 chemisorption ($x10^{-18}$ molecules/g.cat)	% Dispersion
5%Ni5%Co/H-Beta-Al_2O_3	8.18	6.14
5%Ni5%Co/SiO_2-Al_2O_3	5.43	5.63
5%Ni5%Co/γ-Al_2O_3	1.84	0.89

5.2.1.6 Thermogravimetric analysis (TGA)

The amount of carbon deposition on bimetallic (5%wt.Ni5%wt.Co) on different supports which are modified Al_2O_3 by H-Beta zeolite, SiO_2 prepared by sol-gel method, and Gamma-alumina commercial catalysts, were measured. After the prepared catalysts were used in carbon dioxide reforming of methane conducted at 700˚C, they were investigated by means of TGA in an oxidative atmosphere, as shown in Figure 5.27. The percentage of the weight loss of 5%wt.Ni5%wt.Co/H-Beta-Al_2O_3 is similar to 5%wt.Ni5%wt.Co/SiO_2-Al_2O_3. The 5%wt.Ni5%wt.Co/γ-Al_2O_3 is exhibits the largest weight loss.

It is evident that the weight loss shown by TG curves of the used catalysts was due to the burning of deposited carbon present on the catalyst [61]. The contribution from metal oxidation was negligible during temperature programmed oxidation. Therefore, the TGA results clearly show a considerable amount of coke was deposited on the surface of the used catalysts [43]. According to the higher surface areas and smaller crystallite sizes of other catalysts support, the modified support with H-Beta has the most improving metal dispersion compares to others [72]. The addition H-Beta zeolite adjusts increases dispersion of Ni and Co metal. Most probably, the high coking resistance of this catalyst stems from its very well dispersed Ni and Co sites present all over the Ni and Co covered surface due to high activity of carbon dioxide reforming of methane reaction [25].

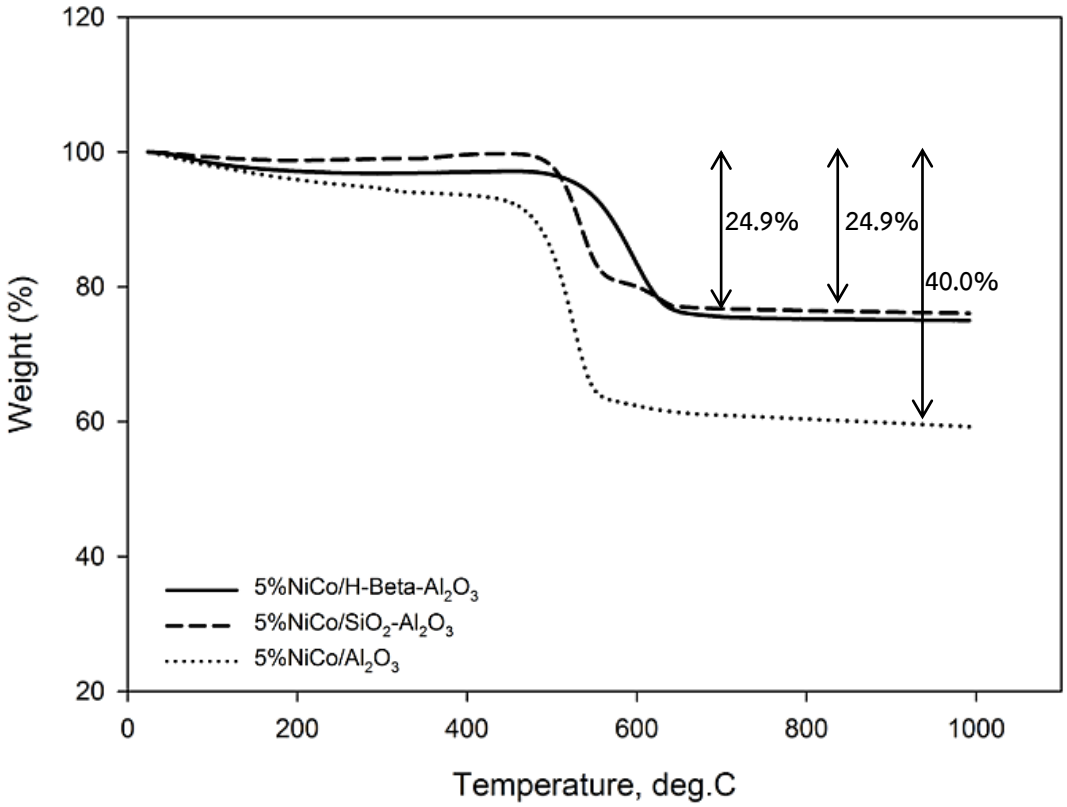

Figure 5.31 TGA curves in air atmosphere after being used in reaction at 700 °C for 5 h for bimetallic catalysts on different supports

5.2.2 The catalytic activity of bimetallic catalysts on different supports in CO_2 reforming of methane

The overall activities of bimetallic on different supports which are H-Beta-Al_2O_3, Al_2O_3-SiO_2 prepared by sol-gel method, and Gamma-alumina commercial catalysts were investigated. All catalysts were prepared by incipient wetness impregnation method and were studied in carbon dioxide reforming of methane. Firstly, 0.2 g catalyst was packed in the quartz reactor. Total gas flow rate was 50 ml/min with the gas nitrogen. Secondly, the catalysts were reduced in flowing hydrogen at 600˚C for 1 h. Next, increased temperature to 700˚C with nitrogen. Finally, the reaction was carried out at 700˚C and 1 atm.

Catalytic activity of all the samples is shown in Table 5.28. The steady state of methane and carbon dioxide conversion of carbon dioxide reforming of methane reaction of the bimetallic on different supports were ranged between 68.0-78.7% and 81.2-92.3%, respectively. It is also obvious that, CO_2 conversion is higher than CH_4 conversion due to reverse water–gas shift reaction ($CO_2 + H_2 \leftrightarrow CO + H_2O$) [73]. Compare to modified support by H-Beta zeolite, SiO_2 by Sol-gel method and γ-Al_2O_3 support of the bimetallic catalyst. In the order methane conversion: 5%wt.Ni5%wt.Co/H-Beta-Al_2O_3 > 5%wy.Ni5%wt.Co/SiO_2-Al_2O_3 ≈ 5%wt.Ni5%wt.Co/γ-Al_2O_3 and carbon dioxide conversion: 5%wt.Ni5%wt.Co/H-Beta-Al_2O_3 > 5%wt.Ni5%wt.Co/SiO_2-Al_2O_3 > 5%wt.Ni5%wt.Co/γ-Al_2O_3, respectively. The catalyst modified with H-Beta show the highest methane and carbon dioxide conversion, suggesting that this modified catalyst with H-Beta can provide sufficient Ni and Co active sites for the reactants [67]. According to H_2 chemisorption, the amount of nickel and cobalt active sites of 5%wt.Ni5%wt.Co/H-Beta-Al_2O_3 catalyst has highest nickel and cobalt active sites, although the BET surface areas of 5%wt.Ni5%wt.Co/H-Beta-Al_2O_3 catalyst had the highest surface area [69]. The well dispersion and high specific surface area of modified Al_2O_3 support with H-Beta to improve catalytic performance of carbon dioxide reforming of methane. The addition of H-Beta increased the interaction between NiO and support which influenced the reducibility, and the electronic properties of catalysts [2]. Also, H-Beta is characteristic beneficial to the absorption and activation of CO_2. Moreover, the modified support with SiO_2-Al_2O_3 displays higher methane and carbon dioxide conversion higher than γ-Al_2O_3 commercial support. Therefore, the improvement of supports by Sol-gel method enhances catalysts performance which attributed to better dispersion of the NiO and CoO particles, according to the smaller NiO and CoO crystallite size found in the XRD pattern [44]. The modified support with H-Beta, SiO_2 prepare by Sol-gel method has smaller NiO and CoO may be easier to reduce to active site nickel and cobalt particles exhibit a shift of the reduction temperature towards lower temperature than γ-Al_2O_3 commercial support [64]. TGA result shows the modified support with H-Beta has the lowest coke formation due to low deactivation of catalysts. However, catalyst deactivation may be related to their low Ni dispersion with high nickel

loading that leads to the agglomerate of Ni particles [49]. Among these support modifiers, H-Beta-Al_2O_3 by Sol-gel method has the best effect in suppressing carbon formation because it improves the activity of reaction.

Among the bimetallic on different supports, modified support with H-Beta has the best H_2 selectivity. These results in hydrogen products selectivity are related to the high specific area, small particle size, well dispersion and small crystallite size.

Table 5.28 The conversion, and product selectivity during CO_2 reforming of methane at initial and steady-state conditions of bimetallic catalysts on different support at 600˚C

Sample	Conversion (%) [a]				Product selectivity (%) [a]			
	Initial [b]		Steady state [c]		Initial [b]		Steady state [c]	
	CH_4	CO_2	CH_4	CO_2	H_2	CO	H_2	CO
5%Ni5%Co/H-Beta-Al_2O_3	79.4	90.3	78.7	92.3	95.8	4.2	96.7	3.3
5%Ni5%Co/SiO_2-Al_2O_3	67.8	88.3	68.0	87.5	79.9	20.1	81.5	18.5
5%Ni5%Co/γ-Al_2O_3	69.1	83.8	68.9	81.2	33.8	66.2	34.7	65.3

[a] CO_2 reforming of methane was carried out at 600˚C, 1 atm, CH_4/CO_2=1

[b] After 30 min of reaction

[b] After 3 h of reaction

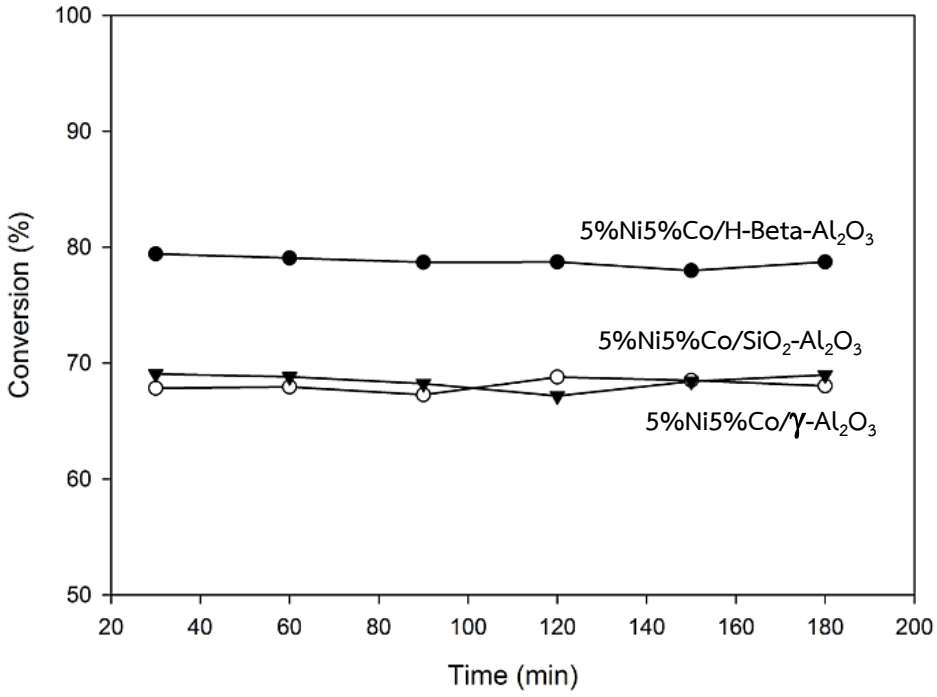

Figure 5.32 Methane conversions of bimetallic catalysts on different supports at 700˚C

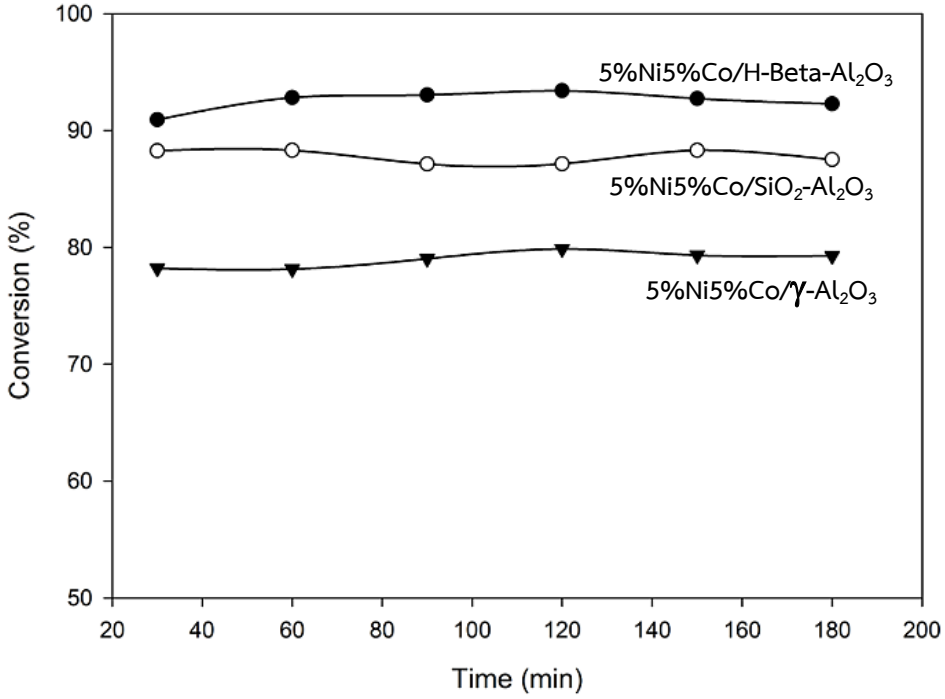

Figure 5.33 Carbon dioxide conversion conversions of catalysts on different supports at 700˚C

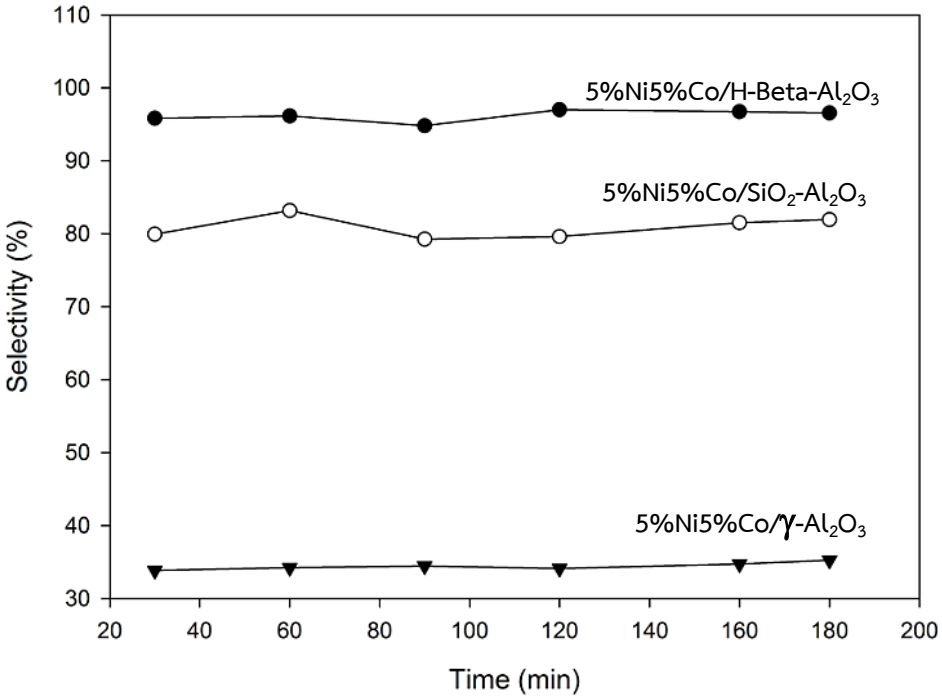

Figure 5.34 Hydrogen selectivity of bimetallic catalysts on different supports at 700˚C.

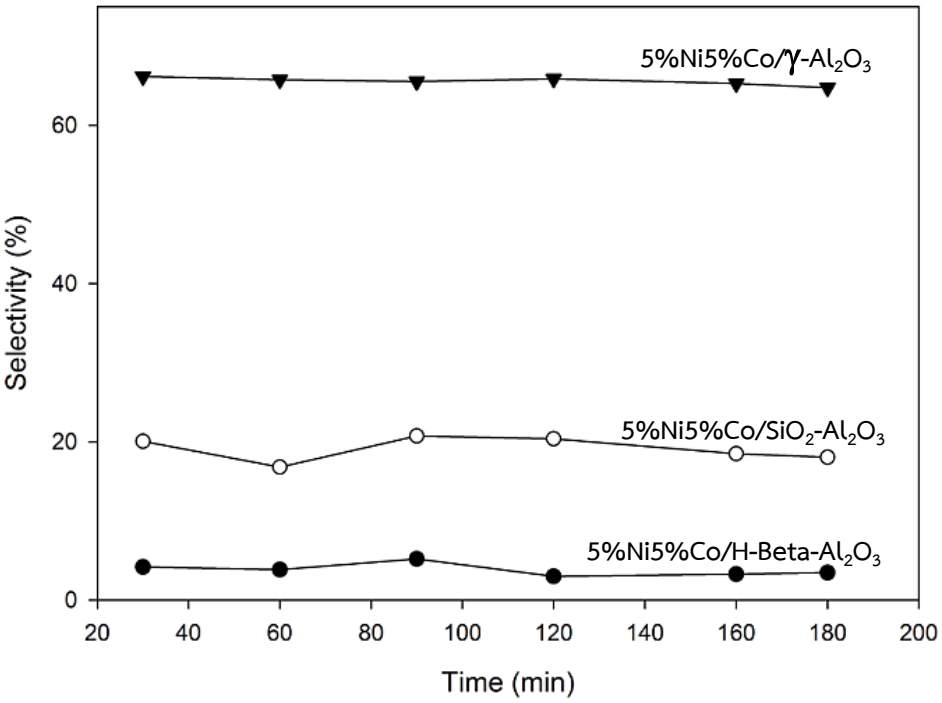

Figure 5.35 Carbon monoxide selectivity of bimetallic catalysts on different supports at 700˚C.

5.3 The effect of bimetallic catalysts with different loading ratio of nickel metal and cobalt metal on H-Beta-Al_2O_3

5.3.1 Catalysts characterization

5.3.1.1 X-ray diffraction (XRD)

The XRD pattern of the bimetallic was investigated different loading ratio of nickel metal and cobalt metal on H-Beta-Al_2O_3 supports. Loading ratios of nickel and cobalt indicates as followed 1:3, 1:1, and 3:1 which were prepared by the incipient wetness impregnation. The XRD patterns in the 20° to 80° region are shown as supplementary information in Figure 5.32. The XRD diffraction peaks at 2θ degrees 32.6°, 43.9°and 64.1°, are corresponded to NiO or $NiAl_2O_4$ crystalline phase[64]. Also, the Co-loaded catalysts exhibit at 2θ degrees 26.3°, 30.3°, 36.4°, 43.9°, 58.1° and 64.1°, are correspond to Co_3O_4 or $CoAl_2O_4$ crystalline phase [49]. In term of Ni and Co species, the XRD peaks corresponding to nickel oxide and cobalt oxide crystallite phase could not be separated because of their similar morphology [70]. While no $NiCo_2O_4$ nor Co_3O_4 were detected, most likely because of their small particle sizes. These features suggest the cobalt species have higher dispersion, for example Ni-Co alloy [66]. The result indicated that the lower Ni:Co ratio results in decreasing in the intensity of XRD patterns. It is shows the decrease crystallite phase.

The average crystallite sizes of bimetallic were investigated different loading ratio of nickel metal and cobalt metal on H-Beta-Al_2O_3 supports after calcination at 500°C are summarized in table 5.32. The crystallite sizes of catalysts with monometallic and bimetallic were ranged between 24.9-34.9 nm. The crystallite sizes of the metal in the 7.5%wt.Ni2.5%wt.Co/H-Beta-Al_2O_3 catalyst are 33.6 nm, which are larger than those sizes of the metal in the 5%wt.Ni5%wt.Co/H-Beta-Al_2O_3 and 2.5%wt.Ni7.5%wt.Co/H-Beta-Al_2O_3. The 7.5%wt.Ni2.5%wt.Co/H-Beta-Al_2O_3 had the biggest size, 33.6 nm. Cobalt addition was reported in the literature review that

to reduce agglomerate of nickel particles because cobalt to obstruct between nickel particles [48].

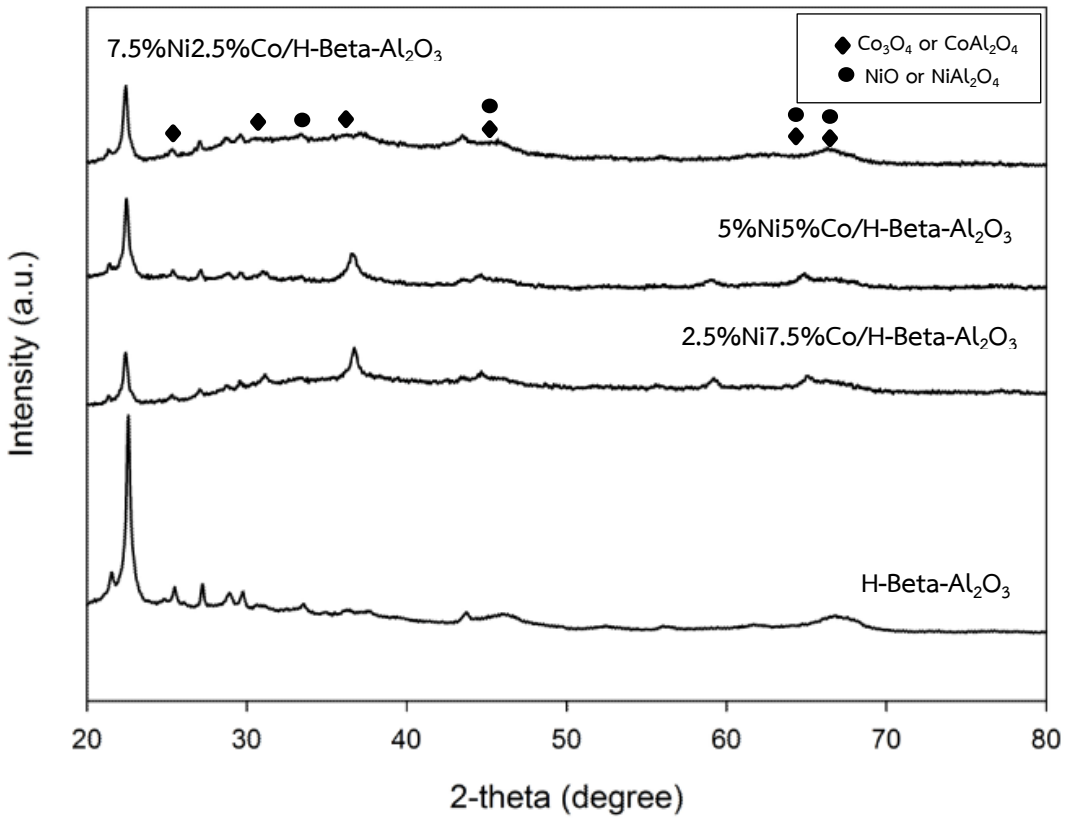

Figure 5.36 The XRD patterns of the bimetallic catalysts with different loading ratio of nickel metal and cobalt metal on H-Beta-Al_2O_3, ♦ = Co_3O_4 or $CoAl_2O_4$, ● = NiO or $NiAl_2O_4$

Table 5.29 Average crystallite size of bimetallic catalysts with different loading ratio of nickel metal and cobalt metal on H-Beta-Al_2O_3

Sample	Average crystallite size of catalysts from XRD (nm)
7.5%Ni2.5%Co/H-Beta-Al_2O_3	33.6
5%Ni5%%Co/H-Beta-Al_2O_3	27.9
2.5%Ni7.5%Co/H-Beta-Al_2O_3	24.3
H-Beta-Al_2O_3	34.9

5.3.1.2 N_2 physisorption

The nitrogen adsorption-desorption isotherm of the bimetallic catalysts with different loading ratio of nickel metal and cobalt metal on H-Beta-Al_2O_3 are display in Fig. 5.37. All samples exhibited type IV isotherms and H2-shaped hysteresis loops that are typical of mesoporous structure. The H2-shaped hysteresis loops are associated with a more complex pore structure such as interparticle porosity or irregular tube-like porosity [30].

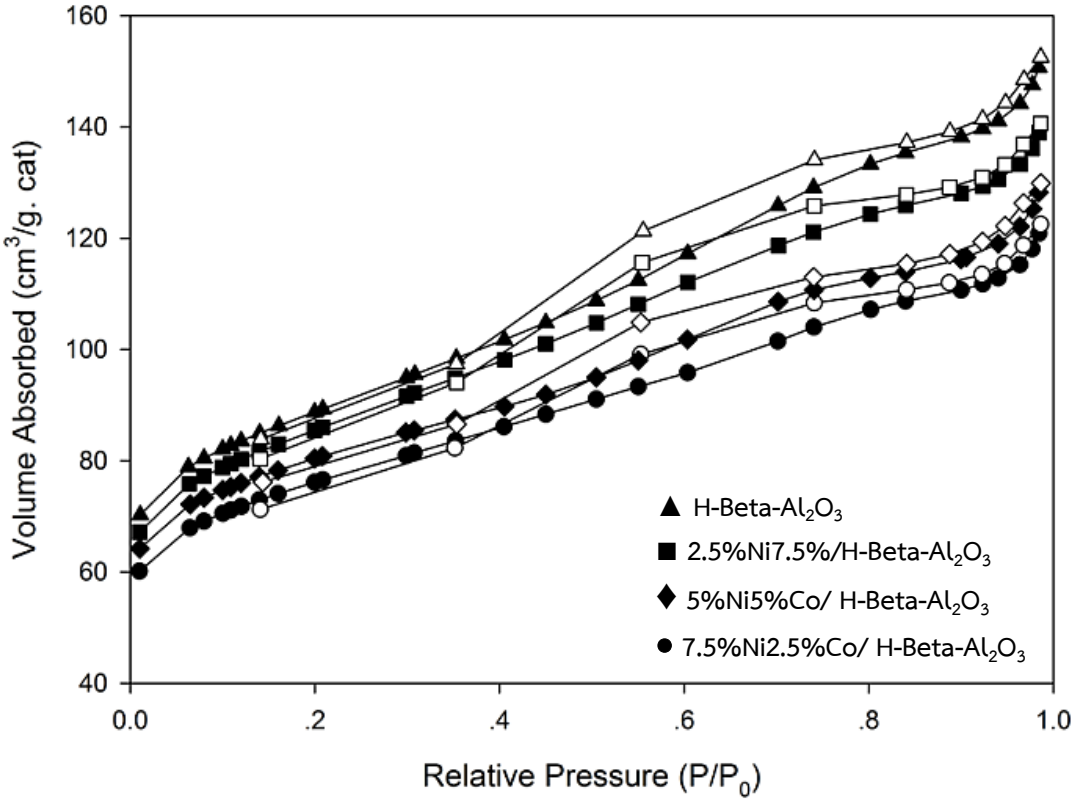

Figure 5.37 nitrogen adsorption-desorption isotherm of the bimetallic catalysts with different loading ratio of nickel metal and cobalt metal on H-Beta-Al_2O_3

The specific surface area, pore volume, and pore size of the bimetallic was investigate different loading ratio of nickel metal and cobalt metal on H-Beta-Al_2O_3 supports, loading ratios of nickel and cobalt indicates as followed 1:3, 1:1 and 3:1 are summarized tin Table 5.30. The surface areas of the varied bimetallic catalysts were

ranged between 267-295 m^2/g. The result shows surface areas of H-Beta-Al_2O_3 support are decrease. This suggests that some pore of H-Beta-Al_2O_3 support may have been blocked by Ni-metal and Co-metal loaded particles [74]. The result indicates that the decrease of ratio of Ni:Co catalysts the surface area shows increase. Because the cobalt addition promotes dispersion of active nickel may not be spread on the pore space of H-Beta-Al_2O_3 support [22]. Moreover, the pore volume and pore size of bimetallic with different loading ratio of nickel metal and cobalt metal on H-Beta-Al_2O_3 supports were ranged between 0.14-0.17 cm^3/g and 3.67-3.95 nm, respectively. It was found no significant difference between catalysts and catalyst support. In term of Ni and Co species, this suggests that the particles size of the Ni and Co metal may be small and dispersion on support catalysts [47]. Also, the addition of the varied ratio bimetallic does not have a significant effect on the structure of catalysts.

Table 5.30 N_2 physisorption illustrate BET surface areas, pore volume and pore size of bimetallic catalysts with different loading ratio of nickel metal and cobalt metal on H-Beta-Al_2O_3

Sample	BET surface area (m^2/g)	Average pore volume (cm^3/g)	Average pore size (nm)
7.5%Ni2.5%Co/H-Beta-Al_2O_3	267	0.14	3.95
5%Ni5%Co/H-Beta-Al_2O_3	270	0.14	3.78
2.5%Ni7.5%Co/H-Beta-Al_2O_3	295	0.17	3.67
H-Beta-Al_2O_3	306	0.18	3.90

5.3.1.3 Hydrogen temperature program reduction (H_2-TPR)

Hydrogen temperature program reduction technique was employed to determine the reduction behaviors of the bimetallic was investigated different loading ratio of nickel metal and cobalt metal on H-Beta-Al_2O_3 supports, loading

ratios of nickel and cobalt indicate as followed 1:3, 1:1 and 3:1 are summarized in Figure 5.33.

Table 5.31 TPR data of bimetallic catalysts with different loading ratio of nickel metal and cobalt metal on H-Beta-Al_2O_3

Sample	T_m (°C)		
	1° peak	2° peak	3° peak
7.5Ni2.5Co/H-Beta-Al_2O_3	544	-	-
5Ni5Co/H-Beta-Al_2O_3	284	308	475
2.5Ni7.5Co/H-Beta-Al_2O_3	395	519	605

The TPR results of the bimetallic with different loading ratio of nickel metal and cobalt metal on H-Beta-Al_2O_3 supports. Loading ratios of nickel and cobalt indicates as followed 1:3, 1:1 and 3:1 are summarized in Table 5.31. The H_2-TPR profiles of the 7.5%wt.Ni2.5%wt.Co/H-Beta-Al_2O_3 are appears only one peak. However, the H_2-TPR profile of the 5%wt.Ni5%wt.Co/H-Beta-Al_2O_3 and 2.5%wt.Ni7.5%wt.Co/H-Beta-Al_2O_3 sample appear to possess three distinct peaks at 284, 308, 457°C and 395, 519, 605°C respectively. The 5%wt.Ni5%wt.Co/H-Beta-Al_2O_3 and 2.5%wt.Ni7.5%wt.Co/H-Beta-Al_2O_3 sample with the peaks shifted to lower temperatures. A shift in the reduction peaks to lower temperatures implied an easier reducibility of the Ni-Co/H-Beta-Al_2O_3 samples [58]. Thus, the presence of a second reducible metal-oxide species assisted in the reduction of the Ni-Co/H-Beta-Al_2O_3 samples by lowering the reduction temperatures. The 5%wt.Ni5%wt.Co/H-Beta-Al_2O_3 catalysts are suitable for the performance of reducibility catalyst.

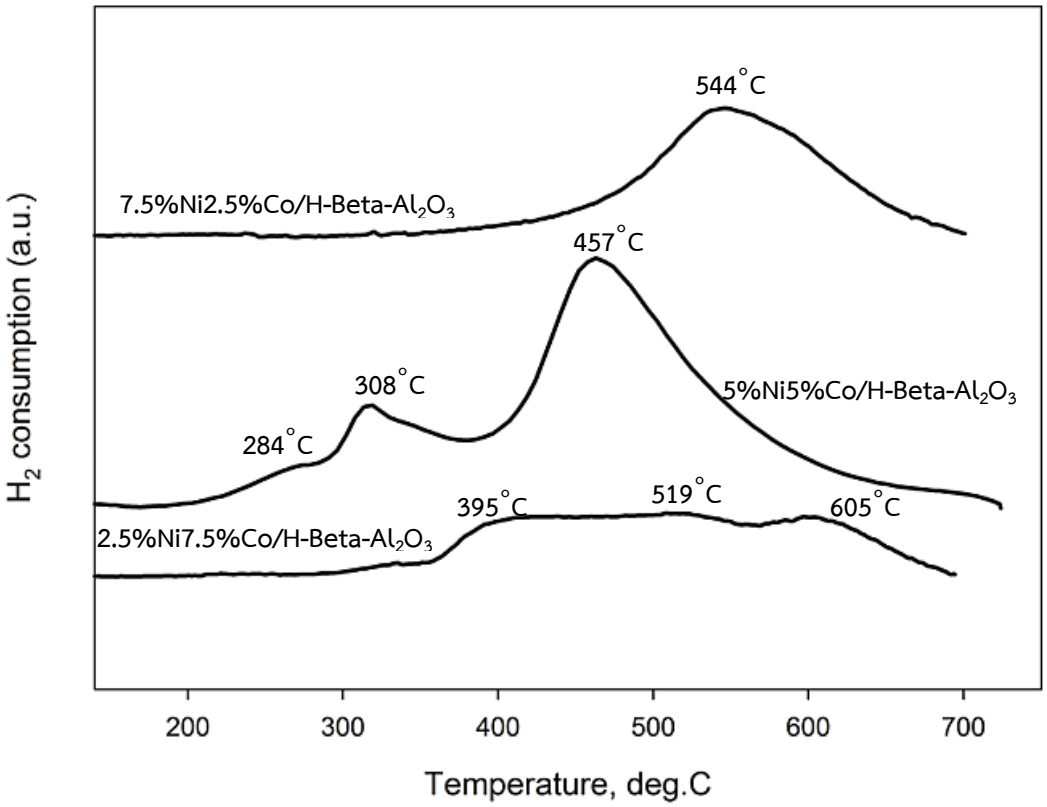

Figure 5.38 The TPR profiles of bimetallic catalysts with different loading ratio of nickel metal and cobalt metal on H-Beta-Al_2O_3

5.3.1.4 Ammonia temperature program Desorption (NH_3-TPD)

Ammonia temperature program desorption (NH_3-TPD) is widely technique used to determine the acidity on the surface of the catalysts. The strength of the acid is related to the desorption temperature [5]. In addition, the total amount of ammonia desorption correspond to the amount of total acidity at surface of catalysts [13].

Table 5.32 Acidity form NH_3-TPD of bimetallic catalysts with different loading ratio of nickel metal and cobalt metal on H-Beta-Al_2O_3

Samples	Total acid site, (mmol H^+/g cat)
7.5%Ni2.5%Co/H-Beta-Al_2O_3	0.17
5%Ni5%Co/H-Beta-Al_2O_3	0.15
2.5%Ni7.5%Co/H-Beta-Al_2O_3	0.14
H-Beta-Al_2O_3	0.14

The surface acidity of the bimetallic was investigated different loading ratio of nickel metal and cobalt metal on H-Beta-Al_2O_3 supports. Loading ratios of nickel and cobalt indicates as followed 1:3, 1:1 and 3:1 was characterized by means of temperature programmed desorption. The de-convolution of the NH_3-TPD thermograms of the 7.5%wt.Ni2.5%wt.Co/H-Beta-Al_2O_3 sample exhibit two bands corresponding to two types of acid sites. The first band consist of a peak located at low temperatures ($\leq$220°C) accompanied by a second one which is more intense feature at relatively high temperatures (250–370°C), the latter being probably due to a fraction of strong acid sites present at the surface of the catalysts [75]. However, the desorption temperature of 5%wt.Ni5%wt.Co/H-Beta-Al_2O_3, and 2.5%wt.Ni7.5%wt.Co/H-Beta-Al_2O_3 have exhibited only one desorption peak (5%wt.Ni5%wt.Co/H-Beta-Al_2O_3, 2.5%wt.Ni7.5%wt.Co/H-Beta-Al_2O_3 could be classified desorption temperature 141˚C and 133˚C, respectively) indicating the presence of weak acid sites. Moreover, the desorption peak ascribed to strong acid sites on 7.5%wt.Ni2.5%wt.Co/H-Beta-Al_2O_3 shifted to a much higher temperature (511˚C), indicating the increase of strong acidity. It has been known that the strong acid sites are responsible for the formation of coke and polymer on the catalyst surface [76]. Moreover, the amounts of acid sites on the surface catalysts are showed in Table 5.32. The total acid sites of catalysts were ranged between 0.14-0.17 mol H^+/g cat. The results find the similar acidity for all catalysts.

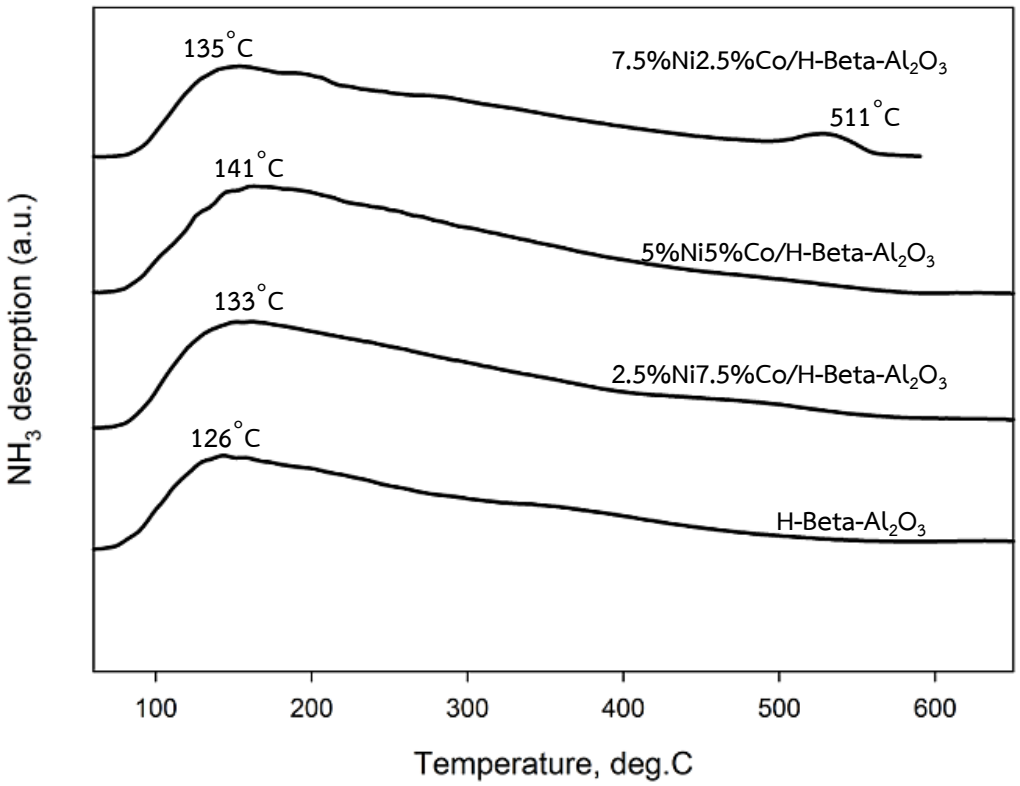

Figure 5.39 The NH_3-TPD profiles of bimetallic catalysts with different loading ratio of nickel metal and cobalt metal on H-Beta-Al_2O_3

5.3.1.5 Scanning electron microscopy analyses (SEM)

EDX analysis was used to determine quantitatively the amount of compositions on the catalyst surfaces of the bimetallic catalysts with different loading ratio of nickel metal and cobalt metal on H-Beta-Al_2O_3 supports by incipient wetness impregnation. Loading ratios of nickel and cobalt indicates as followed 1:3, 1:1 and 3:1 are summarized in Table 5.33. EDX results indicate that surface compositions were close to target at roughly 7.5%wt.Ni2.5%wt.Co, 5%wt.Ni5%wt.Co, and 2.5%wt.Ni7.5%wt.Co. The adjacent from target composition may happen due to adequate mixing of the catalyst materials [46]

.

Table 5.33 EDX Surface Composition (% Element) result of bimetallic catalysts with different loading ratio of nickel metal and cobalt metal on H-Beta-Al_2O_3

Samples	%Element				%Atomic			
	Al	Si	Ni	Co	Al	Si	Ni	Co
7.5%Ni2.5%Co/H-Beta-Al_2O_3	39.46	50.72	7.61	2.21	45.89	45.49	6.54	2.08
5%Ni5%Co/H-Beta-Al_2O_3	40.08	48.82	5.73	5.37	47.77	44.55	3.93	3.76
2.5%Ni7.5%Co/H-Beta-Al_2O_3	44.98	45.16	2.62	7.24	43.89	47.48	2.30	6.33

5.3.1.6 Hydrogen chemisorption

The amount of H_2 chemisorbed and metal dispersion on the bimetallic was investigated different loading ratio of nickel metal and cobalt metal on H-Beta-Al_2O_3 supports. Loading ratios of nickel and cobalt indicates as followed 1:3, 1:1 and 3:1 are also calculated and reported in Table 5.34. The nickel and cobalt active site were ranged between 3.04-8.18 $X10^{18}$ molecules H_2/g cat in the order: 5%wt.Ni5%wt.Co/H-Beta-Al_2O_3 > 7.5%wt.Ni2.5%wt.Co/H-Beta-Al_2O_3 > 2.5%wt.Ni7.5%wt.Co/H-Beta-Al_2O_3. The amount of active sites on 5%wt.Ni5%wt.Co/H-Beta-Al_2O_3 is more than those on 7.5%wt.Ni2.5%wt.Co/H-Beta-Al_2O_3 and 2.5%wt.Ni7.5%wt.Co/H-Beta-Al_2O_3. Furthermore, the amount of H_2 chemisorbed bimetallic catalysts decreased with an increase in Ni:Co ratio in the Ni-Co/H-Beta-Al_2O_3catalysts. The decrease amount of H_2 chemisorbed suggested a decline in the number of surface metal sites. The metal dispersion (%) given in Table 5.34. Also, the 5%wt.Ni5%wt.Co/H-Beta-Al_2O_3 has the suitable metal dispersion because Ni:Co ratio are the optimization of prepare catalysts. The amount of H_2 chemisorbed and metal dispersion (%) appears to be related to the amount of Ni and Co present in the catalyst. Furthermore, changes in the metal crystallite size (from XRD) appear to be related to the average crystallite size as measured from XRD, the crystallite size of catalysts from the 5%wt.Ni5%wt.Co/H-Beta-Al_2O_3 between 7.5%wt.Ni2.5%wt.Co/H-Beta-Al_2O_3 and 2.5%wt.Ni7.5%wt.Co/H-Beta-Al_2O_3. Therefore, the crystallite size of nickel and cobalt species of 5%wt.Ni5%wt.Co/H-Beta-Al_2O_3 may be easier to reduce to nickel and cobalt active site [45]. Besides, 5%wt.Ni5wt%Co/H-Beta-Al_2O_3 showed higher H_2

chemisorption and better dispersion on support than 7.5%wt.Ni2.5%wt.Co/H-Beta-Al_2O_3 and 2.5%wt.Ni7.5%wt.Co/H-Beta-Al_2O_3 catalysts because of the agglomerate of nickel particles of 7.5%wt.Ni2.5%wt.Co/H-Beta-Al_2O_3 [62]. While as, 2.5%wt.Ni7.5wt.Co/H-Beta-Al_2O_3 has lower bases Ni metal than others catalysts.

Table 5.34 Hydrogen chemisorption result of bimetallic catalysts with different loading ratio of nickel metal and cobalt metal on H-Beta-Al_2O_3

Sample	H_2 chemisorption ($x10^{-18}$ molecules/g.cat)	% Dispersion
7.5%Ni2.5%Co/H-Beta-Al_2O_3	5.97	3.75
5%Ni5%Co/H-Beta-Al_2O_3	8.18	6.14
2.5%Ni7.5%Co/H-Beta-Al_2O_3	3.04	3.43

5.3.1.7 Thermogravimetric analysis (TGA)

The amount of carbon deposition on the bimetallic was investigated different loading ratio of nickel metal and cobalt metal on H-Beta-Al_2O_3 supports, loading ratios of nickel and cobalt indicates as followed 1:3, 1:1 and 3:1 were measured. After the prepared catalysts were used in carbon dioxide reforming of methane conducted at 700°C, they were investigated by means of TGA in an oxidative atmosphere.

The amount of carbon deposited on the samples after being used in carbon dioxide reforming of methane was determined by TGA. The weight losses as a result of combustion of the carbon deposited on the spent catalysts are shown in Fig. 5.35. The percentage of the weight loss of 2.5%wt.Ni7.5%wt.Co/H-Beta-Al_2O_3 is the largest weight loss. It is evident that the weight loss showed by TG curves of the used catalysts was due to the burning of deposited carbon present on the catalyst [27]. Therefore, the 5%wt.Ni5%wt.Co/H-Beta-Al_2O_3 shows that a considerable amount of coke was deposited on the surface of the used catalysts. 5%wt.Ni5%wt.Co/H-Beta-Al_2O_3 is the suitable catalyst because of the higher surface areas and smaller

crystallite sizes than other catalysts support [19]. The optimization of cobalt addition has improving nickel metal dispersion of catalysts due to reduce coking of these systems [77].

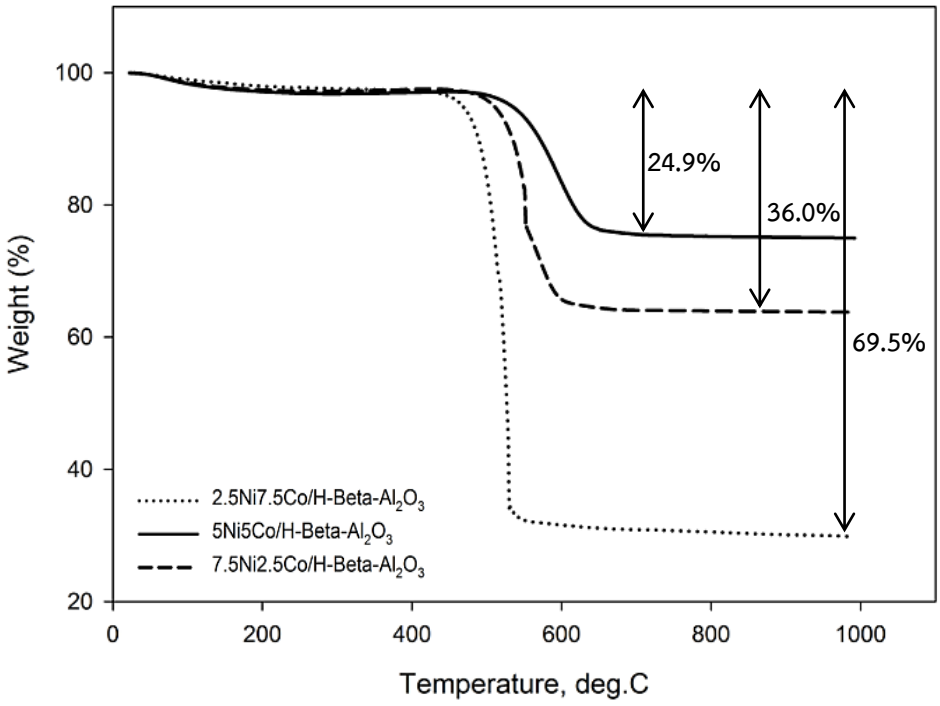

Figure 5.40 TGA curves in air atmosphere after being used in reaction at 700 °C for 5 h for of bimetallic catalysts with different loading ratio of nickel metal and cobalt metal on H-Beta-Al_2O_3

5.3.2 The catalytic activity of bimetallic catalysts with different loading ratio of nickel metal and cobalt metal on H-Beta-Al_2O_3

The overall activities of the bimetallic were investigated different loading ratio of nickel metal and cobalt metal on H-Beta-Al_2O_3 supports. Loading ratios of nickel and cobalt indicates as followed 1:3, 1:1 and 3:1 were studied in carbon dioxide reforming of methane reaction. Firstly, 0.2 g catalyst was packed in the quartz reactor. Total gas flow rate was 50 ml/min with the gas nitrogen. Secondly, the

catalysts were reduced in flowing hydrogen at 600˚C for 1 h. Next, increased temperature to 700˚C with nitrogen. Finally, the reaction was carried out at 700˚C and 1 atm.

The conversion and product selectivity during carbon dioxide reforming of methane reaction are shown in Table 5.35. The steady state of methane and carbon dioxide conversion of carbon dioxide reforming of methane reaction of the bimetallic was investigated different loading ratio of nickel metal and cobalt metal on H-Beta-Al_2O_3 supports. Loading ratios of nickel and cobalt indicates as followed 1:3, 1:1 and 3:1 were methane and carbon dioxide conversion ranging between 58.1-78.7% and 81.1-90.3% respectively. In the order: 5%wt.Ni5%wt.Co/H-Beta-Al_2O_3 > 7.5%wt.Ni2.5%wt.Co/H-Beta-Al_2O_3 > 2.5%wt.Ni7.5%wt.Co/H-Beta-Al_2O_3. The CO_2 conversions of the different catalysts were also measured and were higher than the CH_4 conversions. A higher CO_2 conversion has been attributed to the reverse water gas shift reaction (RWGS), which also occurs during the carbon dioxide reforming of methane reaction [3]. The 5%wt.Ni5%wt.Co/H-Beta-Al_2O_3 shows the highest methane and carbon dioxide conversion among the others catalysts (7.5%wt.Ni2.5%wt.Co/H-Beta-Al_2O_3 and 2.5%wt.Ni7.5%wt.Co/H-Beta-Al_2O_3). According to H_2 chemisorption, the amount of nickel and cobalt active sites of 5%wt.Ni5%wt.Co/H-Beta-Al_2O_3 catalysts had the highest. However, the optimal promotion with cobalt improved nickel active catalyst which can result in higher methane and carbon dioxide conversion during the 3 h time-on-steam. The improvement with cobalt catalysts performances can be attributed to better dispersion of the NiO particles [3,59], according to the smaller crystallite sizes that found in the XRD patterns. That is the smaller NiO and CoO may be easier to reduce to active nickel and cobalt particles [7]. The reduction temperature of 5%wt.Ni5%wt.Co/H-Beta-Al_2O_3 catalyst has shifted of towards lower temperature. Then, reducibility of the catalyst was also increased with the addition optimal of Co-promoter [51].

The product selectivity was observed during carbon dioxide reforming of methane reaction. The result shows that the selectivity to CO is lower in

5%wt.Ni5%wt.Co/H-Beta-Al_2O_3 than in the 7.5%wt.Ni2.5%wt.Co/H-Beta-Al_2O_3 and 2.5%wt.Ni7.5%wr.Co/H-Beta-Al_2O_3. In contrast, 5%wt.Ni5%wt.Co/H-Beta-Al_2O_3 shows the higher H_2 selectivity than the 7.5%wt.Ni2.5%wt.Co/H-Beta-Al_2O_3 and 2.5%wt.Ni7.5%wt.Co/H-Beta-Al_2O_3. These results suggest that the high catalytic activity of the bimetallic sample is mostly related to the optimal cobalt addition to effect intrinsic nature of the Co-Ni alloy a better dispersion of the active phase in smaller particles, as recently proposed for an analogous system [8].

Table 5.35 The conversion, and product selectivity during CO_2 reforming of bimetallic catalysts with different loading ratio of nickel metal and cobalt metal on H-Beta-Al_2O_3

Sample	Conversion (%) [a]				Product selectivity (%) [a]			
	Initial [b]		Steady state [c]		Initial [b]		Steady state [c]	
	CH_4	CO_2	CH_4	CO_2	H_2	CO	H_2	CO
7.5%Ni2.5%Co/H-Beta-Al_2O_3	61.6	82.9	60.5	81.1	69.6	30.4	72,7	72.7
5%Ni5%Co/H-Beta-Al_2O_3	74.7	90.3	78.7	92.3	95.8	4.2	67.0	96.7
2.5%Ni7.5%Co/H-Beta-Al_2O_3	59.9	80.9	58.1	81.1	44.1	55.9	31.9	46.2

[a] CO_2 reforming of methane was carried out at 600°C, 1 atm, CH_4/CO_2

[b] After 30 min of reaction

[b] After 3 h of reaction

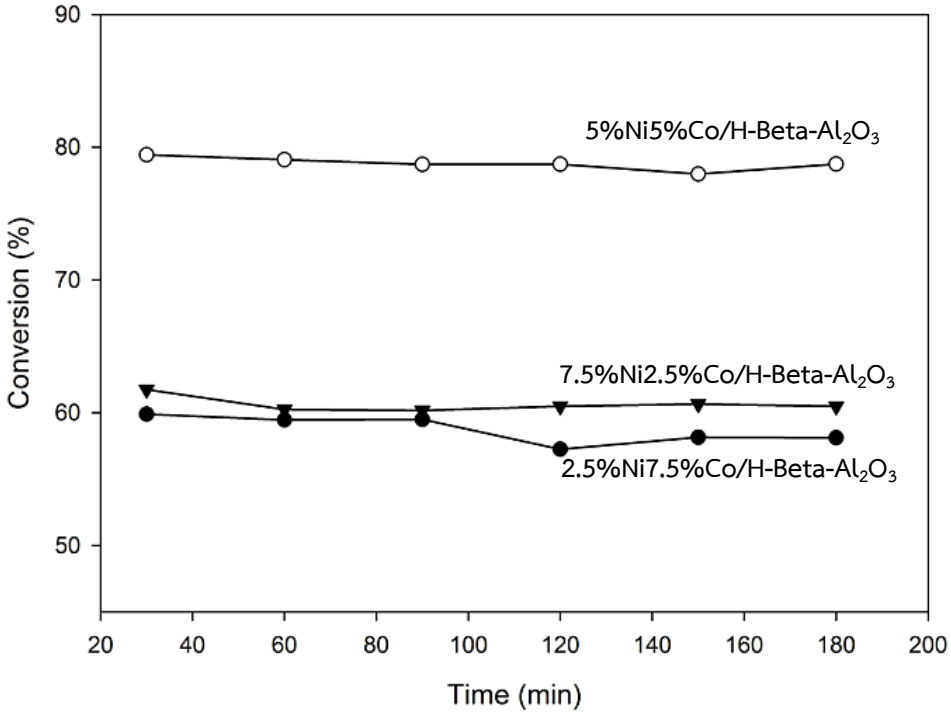

Figure 5.41 Methane conversion of bimetallic catalysts with different loading ratio of nickel metal and cobalt metal on H-Beta-Al_2O_3 at 700˚C

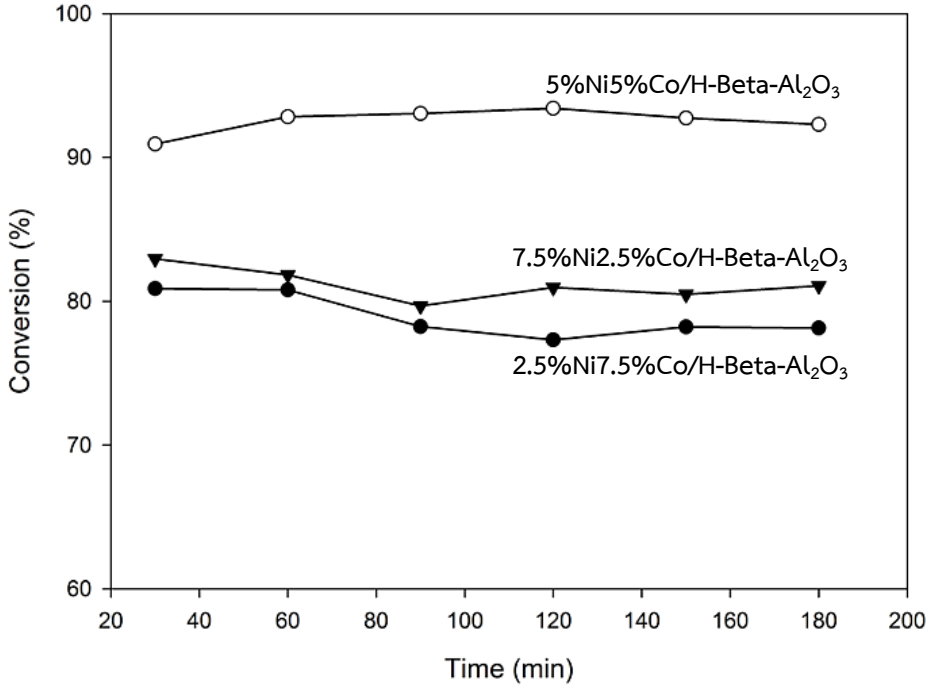

Figure 5.42 Carbon dioxide conversion of bimetallic catalysts with different loading ratio of nickel metal and cobalt metal on H-Beta-Al_2O_3 at 700˚C

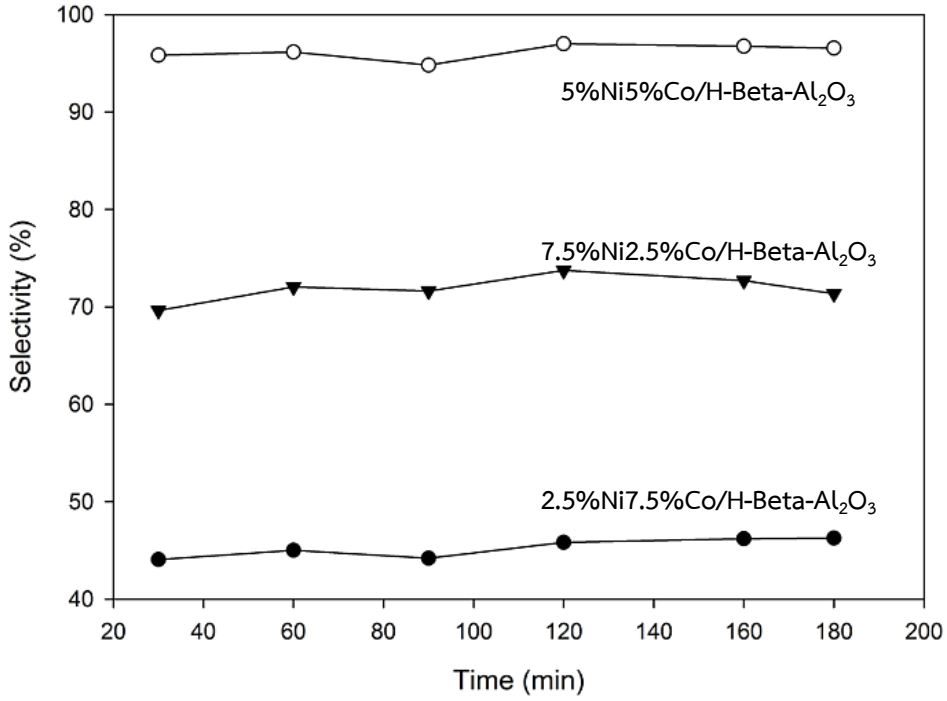

Figure 5.43 Hydrogen selectivity of bimetallic catalysts with different loading ratio of nickel metal and cobalt metal on H-Beta-Al_2O_3 at 700˚C

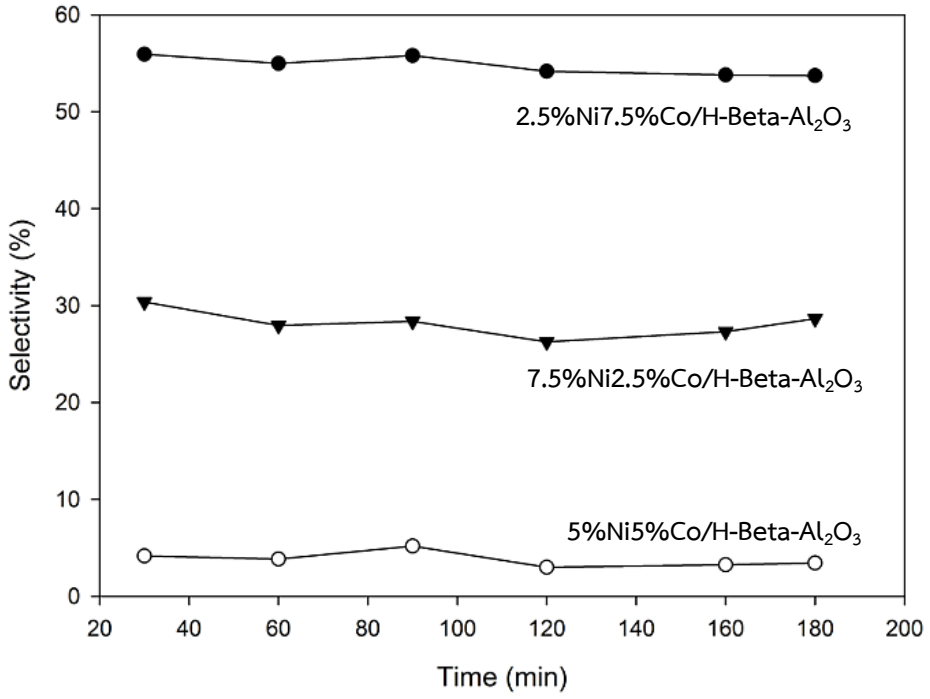

Figure 5.44 Carbon monoxide selectivity of bimetallic catalysts with different loading ratio of nickel metal and cobalt metal on H-Beta-Al_2O_3

CHARTER VI

CONCLUSIONS AND RECOMMENDATION

6.1 Conclusions

In the present work, the effect of monometallic (10%wt.Ni, 10%wt.Co) and bimetallic (5%wt.Ni5%wt.Co) on different supports are H-Beta-Al_2O_3, Al_2O_3-SiO_2 prepared by sol-gel method, and Gamma-alumina commercial catalysts was studied. Moreover, to study the effect of bimetallic catalysts with different loading ratio of nickel metal and cobalt metal on H-Beta-Al_2O_3 supports. Loading ratios of nickel and cobalt indicate as followed 1:3, 1:1, and 3:1. For comparison purpose, all catalysts were prepared by the incipient wetness impregnation method. The catalytic performances were tested in carbon dioxide reforming of methane. The results can be concluded as followed:

1. The bimetallic (5%wt.Ni5%wt.Co) on H-Beta-Al_2O_3 catalyst prepared by Sol-gel method exhibit higher methane and carbon dioxide conversion than the monometallic (10%wt.Ni, 10%wt.Co) catalysts. The better catalytic performances are explained by higher surface area, smaller crystallite size due to higher dispersion of nickel particle on the surface of support to influence a shift the reduction temperature toward lower temperature, make it easier to reduce to active nickel and cobalt particles.

2. The highest catalytic activity is achieved by the 5%wt.Ni5%wt.Co/H-Beta-Al_2O_3 catalyst, which contained Ni:Co in a ratio of 1:1. It can be explain by the optimization amount of nickel and cobalt active sites, the smaller with NiO and CoO particles due to higher dispersion of nickel particle on the surface of support implied an easier reducibility, a shift of the reduction temperature toward lower temperature.

In addition, the optimal cobalt addition has improved nickel metal dispersion of catalysts due to reduce coking of these systems.

6.2 Recommendations

1. Temperature has a major in the carbon dioxide reforming of methane. Therefore, it is investigate in the different reaction temperature which would to influence the catalytic activity.

2. The coke formation of metal on support to affect the catalytic performances, so it is interesting to investigate coke formation on catalysts using TEM technique.

3. Stability is interesting to investigate catalytic performances. Therefore, to study the effect of the long time reaction in the carbon dioxide reforming of methane reaction influences catalytic activity.

REFERENCES

[1] Cai, W.-J., Qian, L.-P., Yue, B., Chen, X.-Y., and He, H.-Y. Reforming of CH_4 with CO_2 over Co/Mg–Al oxide catalyst. Chinese Chemical Letters 24(9) (2013): 777-779.

[2] Jeong, H., Kim, K.I., Kim, D., and Song, I.K. Effect of promoters in the methane reforming with carbon dioxide to synthesis gas over Ni/HY catalysts. Journal of Molecular Catalysis A: Chemical 246(1-2) (2006): 43-48.

[3] San José-Alonso, D., Illán-Gómez, M.J., and Román-Martínez, M.C. Low metal content Co and Ni alumina supported catalysts for the CO_2 reforming of methane. International Journal of Hydrogen Energy 38(5) (2013): 2230-2239.

[4] Xu, L., et al. Catalytic CO_2 reforming of CH_4 over Cr-promoted Ni/char for H_2 production. International Journal of Hydrogen Energy 39(19) (2014): 10141-10153.

[5] Mahoney, E.G., Pusel, J.M., Stagg-Williams, S.M., and Faraji, S. The effects of Pt addition to supported Ni catalysts on dry (CO_2) reforming of methane to syngas. Journal of CO_2 Utilization 6 (2014): 40-44.

[6] Frontera, P., et al. Catalytic dry-reforming on Ni–zeolite supported catalyst. Catalysis Today 179(1) (2012): 52-60.

[7] Sengupta, S., Ray, K., and Deo, G. Effects of modifying Ni/Al_2O_3 catalyst with cobalt on the reforming of CH_4 with CO_2 and cracking of CH_4 reactions. International Journal of Hydrogen Energy 39(22) (2014): 11462-11472.

[8] Son, I.H., et al. Study on coke formation over Ni/γ-Al_2O_3, Co-Ni/γ-Al_2O_3, and Mg-Co-Ni/γ-Al_2O_3 catalysts for carbon dioxide reforming of methane. Fuel 136 (2014): 194-200.

[9] Bosko, M.L., Múnera, J.F., Lombardo, E.A., and Cornaglia, L.M. Dry reforming of methane in membrane reactors using Pd and Pd–Ag composite membranes on a NaA zeolite modified porous stainless steel support. Journal of Membrane Science 364(1-2) (2010): 17-26.

[10] Fakeeha, A.H., Naeem, M.A., Khan, W.U., and Al-Fatesh, A.S. Syngas production via CO_2 reforming of methane using Co-Sr-Al catalyst. Journal of Industrial and Engineering Chemistry 20(2) (2014): 549-557.

[11] Zhang, J., Wang, H., and Dalai, A.K. Effects of metal content on activity and stability of Ni-Co bimetallic catalysts for CO_2 reforming of CH_4. Applied Catalysis A: General 339(2) (2008): 121-129.

[12] Zhang, G., Su, A., Du, Y., Qu, J., and Xu, Y. Catalytic performance of activated carbon supported cobalt catalyst for CO_2 reforming of CH_4. J Colloid Interface Sci 433 (2014): 149-55.

[13] Mirzaei, F., Rezaei, M., Meshkani, F., and Fattah, Z. Carbon dioxide reforming of methane for syngas production over Co–MgO mixed oxide nanocatalysts. Journal of Industrial and Engineering Chemistry 21 (2015): 662-667.

[14] Castro Luna, A.E. and Iriarte, M.E. Carbon dioxide reforming of methane over a metal modified Ni-Al_2O_3 catalyst. Applied Catalysis A: General 343(1-2) (2008): 10-15.

[15] Cheng, J. and Huang, W. Effect of cobalt (nickel) content on the catalytic performance of molybdenum carbides in dry-methane reforming. Fuel Processing Technology 91(2) (2010): 185-193.

[16] Fakeeha, A.H., Khan, W.U., Al-Fatesh, A.S., and Abasaeed, A.E. Stabilities of zeolite-supported Ni catalysts for dry reforming of methane. Chinese Journal of Catalysis 34(4) (2013): 764-768.

[17] <Reforming of CH_4 with CO_2 over RhH-Beta Effect of Rhodium.pdf>.

[18] Tao, K., et al. Methane reforming with carbon dioxide over mesoporous nickel–alumina composite catalyst. Chemical Engineering Journal 221 (2013): 25-31.

[19] Rahmani, F., Haghighi, M., Vafaeian, Y., and Estifaee, P. Hydrogen production via CO_2 reforming of methane over ZrO2-Doped Ni/ZSM-5 nanostructured catalyst prepared by ultrasound assisted sequential impregnation method. Journal of Power Sources 272 (2014): 816-827.

[20] Ay, H. and Üner, D. Dry reforming of methane over CeO_2 supported Ni, Co and Ni–Co catalysts. Applied Catalysis B: Environmental 179 (2015): 128-138.

[21] Damyanova, S., Pawelec, B., Arishtirova, K., and Fierro, J.L.G. Ni-based catalysts for reforming of methane with CO_2. International Journal of Hydrogen Energy 37(21) (2012): 15966-15975.

[22] Luengnaruemitchai, A. and Kaengsilalai, A. Activity of different zeolite-supported Ni catalysts for methane reforming with carbon dioxide. Chemical Engineering Journal 144(1) (2008): 96-102.

[23] Jian Sun, X.L., Akira Taguchi,Takayuki Abe, Wenqi Niu,Peng Lu,Yoshiharu Yoneyama, and Tsubaki, a.N. Highly-Dispersed Metallic Ru Nanoparticles Sputtered on H-Beta Zeolite for Directly Converting Syngas to Middle Isoparaffins.

[24] Wang, N., Yu, X., Shen, K., Chu, W., and Qian, W. Synthesis, characterization and catalytic performance of MgO-coated Ni/SBA-15 catalysts for methane dry reforming to syngas and hydrogen. International Journal of Hydrogen Energy 38(23) (2013): 9718-9731.

[25] He, S., Wu, H., Yu, W., Mo, L., Lou, H., and Zheng, X. Combination of CO_2 reforming and partial oxidation of methane to produce syngas over Ni/SiO2 and Ni–Al_2O_3/SiO_2 catalysts with different precursors. International Journal of Hydrogen Energy 34(2) (2009): 839-843.

[26] Ulleberg, T.R.E.F.H.P.J.S.V.a.Ø. HYDROGEN PRODUCTION AND STORAGE.

[27] Rahemi, N., Haghighi, M., Babaluo, A.A., Allahyari, S., and Jafari, M.F. Syngas production from reforming of greenhouse gases CH4/CO_2 over Ni–Cu/Al_2O_3 nanocatalyst: Impregnated vs. plasma-treated catalyst. Energy Conversion and Management 84 (2014): 50-59.

[28] Alipour, Z., Rezaei, M., and Meshkani, F. Effects of support modifiers on the catalytic performance of Ni/Al_2O_3 catalyst in CO_2 reforming of methane. Fuel 129 (2014): 197-203.

[29] Frontera, P., Macario, A., Aloise, A., Antonucci, P.L., Giordano, G., and Nagy, J.B. Effect of support surface on methane dry-reforming catalyst preparation. Catalysis Today 218-219 (2013): 18-29.

[30] Sprung, C., Kechagiopoulos, P.N., Thybaut, J.W., Arstad, B., Olsbye, U., and Marin, G.B. Microkinetic evaluation of normal and inverse kinetic isotope effects during methane steam reforming to synthesis gas over a Ni/NiAl2O4 model catalyst. Applied Catalysis A: General 492 (2015): 231-242.

[31] Wang, Y., et al. Effect of Pr addition on the properties of Ni/Al_2O_3 catalysts with an application in the autothermal reforming of methane. International Journal of Hydrogen Energy 39(2) (2014): 778-787.

[32] Yao, L., Zhu, J., Peng, X., Tong, D., and Hu, C. Comparative study on the promotion effect of Mn and Zr on the stability of Ni/SiO_2 catalyst for CO_2 reforming of methane. International Journal of Hydrogen Energy 38(18) (2013): 7268-7279.

[33] Zeng, Y., Zhu, X., Mei, D., Ashford, B., and Tu, X. Plasma-catalytic dry reforming of methane over γ-Al2O3 supported metal catalysts. Catalysis Today (2015).

[34] Zhu, J., Peng, X., Yao, L., Shen, J., Tong, D., and Hu, C. The promoting effect of La, Mg, Co and Zn on the activity and stability of Ni/SiO_2 catalyst for CO_2

reforming of methane. International Journal of Hydrogen Energy 36(12) (2011): 7094-7104.

[35] Davis, K. Material Review: Alumina (Al_2O_3)

[36] Abdollahifar, M., Haghighi, M., and Babaluo, A.A. Syngas production via dry reforming of methane over Ni/Al2O3–MgO nanocatalyst synthesized using ultrasound energy. Journal of Industrial and Engineering Chemistry 20(4) (2014): 1845-1851.

[37] Sharan Shetty, S.P., Dilip G. Kanhere, Annick Goursot. Structural, electronic and bonding properties of zeolite Sn-Beta: A periodic

density functional theory study.

[38] Boukha, Z., Jiménez-González, C., de Rivas, B., González-Velasco, J.R., Gutiérrez-Ortiz, J.I., and López-Fonseca, R. Synthesis, characterisation and performance evaluation of spinel-derived Ni/Al_2O_3 catalysts for various methane reforming reactions. Applied Catalysis B: Environmental 158-159 (2014): 190-201.

[39] Jacobus C. Jansen, E.J.C., Swie Lan Njo, and Henk van Koningsvelda, H.v.B. On the remarkable behaviour of zeolite Beta in acid catalysis.

[40] Ewbank, J.L., Kovarik, L., Diallo, F.Z., and Sievers, C. Effect of metal–support interactions in Ni/Al_2O_3 catalysts with low metal loading for methane dry reforming. Applied Catalysis A: General 494 (2015): 57-67.

[41] Foo, S.Y., Cheng, C.K., Nguyen, T.-H., and Adesina, A.A. Syngas production from CH4 dry reforming over $Co–Ni/Al_2O_3$ catalyst: Coupled reaction-deactivation kinetic analysis and the effect of O_2 co-feeding on H_2:CO ratio. International Journal of Hydrogen Energy 37(22) (2012): 17019-17026.

[42] Fouskas, A., Kollia, M., Kambolis, A., Papadopoulou, C., and Matralis, H. Boron-modified Ni/Al_2O_3 catalysts for reduced carbon deposition during dry reforming of methane. Applied Catalysis A: General 474 (2014): 125-134.

[43] Guo, C., Wu, Y., Qin, H., and Zhang, J. CO methanation over ZrO_2/Al_2O_3 supported Ni catalysts: A comprehensive study. Fuel Processing Technology 124(0) (2014): 61-69.

[44] Kaengsilalai, A., Luengnaruemitchai, A., Jitkarnka, S., and Wongkasemjit, S. Potential of Ni supported on KH zeolite catalysts for carbon dioxide reforming of methane. Journal of Power Sources 165(1) (2007): 347-352.

[45] Özkara-Aydınoğlu, Ş. and Aksoylu, A.E. CO_2 reforming of methane over $Pt–Ni/Al_2O_3$ catalysts: Effects of catalyst composition, and water and oxygen

addition to the feed. International Journal of Hydrogen Energy 36(4) (2011): 2950-2959.

[46] Ocsachoque, M., Pompeo, F., and Gonzalez, G. Rh–Ni/CeO_2–Al_2O_3 catalysts for methane dry reforming. Catalysis Today 172(1) (2011): 226-231.

[47] Luisetto, I., Tuti, S., Battocchio, C., Lo Mastro, S., and Sodo, A. Ni/CeO_2–Al_2O_3 catalysts for the dry reforming of methane: The effect of $CeAlO_3$ content and nickel crystallite size on catalytic activity and coke resistance. Applied Catalysis A: General 500 (2015): 12-22.

[48] Li, X., Hu, Q., Yang, Y., Wang, Y., and He, F. Studies on stability and coking resistance of Ni/$BaTiO_3$–Al_2O_3 catalysts for lower temperature dry reforming of methane (LTDRM). Applied Catalysis A: General 413-414 (2012): 163-169.

[49] Kim, T.W., et al. The kinetics of steam methane reforming over a Ni/γ-Al_2O_3 catalyst for the development of small stationary reformers. International Journal of Hydrogen Energy 40(13) (2015): 4512-4518.

[50] Laosiripojana, N., Sutthisripok, W., and Assabumrungrat, S. Synthesis gas production from dry reforming of methane over CeO_2 doped Ni/Al_2O_3: Influence of the doping ceria on the resistance toward carbon formation. Chemical Engineering Journal 112(1-3) (2005): 13-22.

[51] Sharifi, M., Haghighi, M., Rahmani, F., and Karimipour, S. Syngas production via dry reforming of CH_4 over Co- and Cu-promoted Ni/Al_2O_3–ZrO_2 nanocatalysts synthesized via sequential impregnation and sol–gel methods. Journal of Natural Gas Science and Engineering 21 (2014): 993-1004.

[52] Therdthianwong, S. Synthesis gas production from dry reforming of methane over Ni/Al_2O_3 stabilized by ZrO_2. International Journal of Hydrogen Energy 33(3) (2008): 991-999.

[53] <CO_2 reforming of CH_4 over CoMgO solid solution catalysts effect of calcination temperature and Co loading.pdf>.

[54] <Ultrasound assisted dispersion of different amount of Ni over ZSM-5.pdf>.

[55] Abasaeed, A.E., Al-Fatesh, A.S., Naeem, M.A., Ibrahim, A.A., and Fakeeha, A.H. Catalytic performance of CeO_2 and ZrO_2 supported Co catalysts for hydrogen production via dry reforming of methane. International Journal of Hydrogen Energy 40(21) (2015): 6818-6826.

[56] Djinović, P., Osojnik Črnivec, I.G., Erjavec, B., and Pintar, A. Influence of active metal loading and oxygen mobility on coke-free dry reforming of Ni–Co bimetallic catalysts. Applied Catalysis B: Environmental 125 (2012): 259-270.

[57] Chu, B., Zhang, N., Zhai, X., Chen, X., and Cheng, Y. Improved catalytic performance of Ni catalysts for steam methane reforming in a micro-channel reactor. Journal of Energy Chemistry 23(5) (2014): 593-600.

[58] Luisetto, I., Tuti, S., and Di Bartolomeo, E. Co and Ni supported on CeO_2 as selective bimetallic catalyst for dry reforming of methane. International Journal of Hydrogen Energy 37(21) (2012): 15992-15999.

[59] San-José-Alonso, D., Juan-Juan, J., Illán-Gómez, M.J., and Román-Martínez, M.C. Ni, Co and bimetallic Ni–Co catalysts for the dry reforming of methane. Applied Catalysis A: General 371(1-2) (2009): 54-59.

[60] Boukha, Z., Kacimi, M., Pereira, M.F.R., Faria, J.L., Figueiredo, J.L., and Ziyad, M. Methane dry reforming on Ni loaded hydroxyapatite and fluoroapatite. Applied Catalysis A: General 317(2) (2007): 299-309.

[61] Gaur, S., Haynes, D.J., and Spivey, J.J. Rh, Ni, and Ca substituted pyrochlore catalysts for dry reforming of methane. Applied Catalysis A: General (2011).

[62] Pompeo, F., Nichio, N.N., González, M.G., and Montes, M. Characterization of Ni/SiO_2 and $Ni/Li\text{-}SiO_2$ catalysts for methane dry reforming. Catalysis Today 107-108 (2005): 856-862.

[63] Pinheiro, A.N., Valentini, A., Sasaki, J.M., and Oliveira, A.C. Highly stable dealuminated zeolite support for the production of hydrogen by dry reforming of methane. Applied Catalysis A: General 355(1-2) (2009): 156-168.

[64] Khajeh Talkhoncheh, S. and Haghighi, M. Syngas production via dry reforming of methane over Ni-based nanocatalyst over various supports of clinoptilolite, ceria and alumina. Journal of Natural Gas Science and Engineering 23 (2015): 16-25.

[65] Barama, S., Dupeyrat-Batiot, C., Capron, M., Bordes-Richard, E., and Bakhti-Mohammedi, O. Catalytic properties of Rh, Ni, Pd and Ce supported on Al-pillared montmorillonites in dry reforming of methane. Catalysis Today 141(3-4) (2009): 385-392.

[66] Li, L., Zhang, L.-m., Zhang, Y.-h., and Li, J.-l. Effect of Ni loadings on the catalytic properties of Ni/MgO(111) catalyst for the reforming of methane with carbon dioxide. Journal of Fuel Chemistry and Technology 43(3) (2015): 315-322.

[67] Huo, J., Jing, J., and Li, W. Reduction time effect on structure and performance of Ni–Co/MgO catalyst for carbon dioxide reforming of methane. International Journal of Hydrogen Energy 39(36) (2014): 21015-21023.

[68] Gao, J., Guo, J., Liang, D., Hou, Z., Fei, J., and Zheng, X. Production of syngas via autothermal reforming of methane in a fluidized-bed reactor over the combined CeO_2–ZrO_2/SiO_2 supported Ni catalysts. International Journal of Hydrogen Energy 33(20) (2008): 5493-5500.

[69] Izquierdo, U., et al. Ni and RhNi catalysts supported on Zeolites L for hydrogen and syngas production by biogas reforming processes. Chemical Engineering Journal 238 (2014): 178-188.

[70] Kwak, B.S., Lee, J.S., Lee, J.S., Choi, B.-H., Ji, M.J., and Kang, M. Hydrogen-rich gas production from ethanol steam reforming over Ni/Ga/Mg/Zeolite Y catalysts at mild temperature. Applied Energy 88(12) (2011): 4366-4375.

[71] Ren, H.-P., et al. High-performance Ni–SiO_2 for pressurized carbon dioxide reforming of methane. International Journal of Hydrogen Energy (2014).

[72] Halliche, D., Cherifi, O., and Auroux, A. Microcalorimetric studies and methane reforming by CO_2 on Ni-based zeolite catalysts. Thermochimica Acta 434(1-2) (2005): 125-131.

[73] Hou, Z. and Yashima, T. Meso-porous Ni/Mg/Al catalysts for methane reforming with CO_2. Applied Catalysis A: General 261(2) (2004): 205-209.

[74] Lua, A.C. and Wang, H.Y. Hydrogen production by catalytic decomposition of methane over Ni-Cu-Co alloy particles. Applied Catalysis B: Environmental 156–157(0) (2014): 84-93.

[75] Monroy, T.G., Abella, L.C., Gallardo, S.M., and Hinode, H. Catalytic Dry Reforming of Methane Using Ni/MgO-ZrO_2 Catalyst. (2010): 145-152.

[76] Ni, J., Chen, L., Lin, J., and Kawi, S. Carbon deposition on borated alumina supported nano-sized Ni catalysts for dry reforming of CH_4. Nano Energy 1(5) (2012): 674-686.

[77] San José-Alonso, D., Illán-Gómez, M.J., and Román-Martínez, M.C. K and Sr promoted Co alumina supported catalysts for the CO_2 reforming of methane. Catalysis Today 176(1) (2011): 187-190.

APPENDIX

APPENDIX A

CALCULATION FOR CATALYST PREPARATION

1. Preparation of different support which are H-Beta-Al_2O_3, Al_2O_3-SiO_2 prepared by sol-gel method and Gamma-alumina commercial catalysts samples.

The calculation shown below is H-Beta-Al_2O_3, Al_2O_3-SiO_2 and Gamma-alumina commercial catalyst. The support weight used for all preparation is 1g.

- Calculation of Al_2O_3 modified support by H-Beta zeolite by Sol-gel method.

Based on 1 g of H-Beta-Al_2O_3 support used, the composition of the H-Beta-modified Al_2O_3 supports will be follows:

Reagent: - H-Beta zeolite commercial (ratio Al:Si are 27)

- Aluminium isopropoxide ($C_9H_{21}O_3Al$) >98%

Molecular weight = 204.25 g/mol

- Ethanol (C_2H_5OH) 99%

Molecular weight = 46.07 g/mol

- Hydrochloric acid 37.7%

Molecular weight = 36.46 g/mol

For weight ratio of H-Beta/Al_2O_3 = 1:3 is shown as follow;

Base on H-Beta zeolite 5g to apply 15g of Aluminium isopropoxide

For molar ratio of H_2O/Al_2O_3 = 15:0.1 is shown as follow;

Aluminium isopropoxide	=	0.1 mol		
	=	0.1x18	=	20.4g
H_2O	=	15 mol		
	=	15X18	=	270g

Therefore, 20.4 g of Aluminium isopropoxide to apply 270 g of H_2O

15 g of Aluminium isopropoxide to apply 198.53 g of H_2O

For volume ratio of H_2O/Ethanol = 1:1 is shown as follow;

H_2O	=	198.53g
Density of H_2O (1 g/cm^3)	=	198.53 cm^3

Therefore, 198.53 cm^3 of H_2O to apply 198.53 cm^3 of Ethanol

- Calculation of Al_2O_3 modified support by SiO_2 zeolite by Sol-gel method.

Based on 1 g of SiO_2 support used, the composition of the SiO_2-modified Al_2O_3 supports will be follows:

Reagent: - Silica dioxide (SiO_2) >99%

Molecular weight = 60.08 g/mol

- Aluminium isopropoxide ($C_9H_{21}O_3Al$) >98%

Molecular weight = 204.25 g/mol

- Ethanol (C_2H_5OH) 99%

Molecular weight = 46.07 g/mol

- Hydrochloric acid 37.7%

Molecular weight = 36.46 g/mol

For weight ratio of H-Beta/Al_2O_3 = 1:3 is shown as follow;

Base on Silica dioxide 5g to apply 15g of Aluminium isopropoxide

For molar ratio of H_2O/Al_2O_3 = 15:0.1 is shown as follow;

Aluminium isopropoxide	=	0.1 mol		
	=	0.1X18	=	20.4g
H_2O	=	15 mol		
	=	15X18	=	270g

Therefore, 20.4 g of Aluminium isopropoxide to apply 270 g of H_2O

15 g of Aluminium isopropoxide to apply 198.53 g of H_2O

For volume ratio of H_2O/Ethanol = 1:1 is shown as follow;

H_2O	=	198.53g
Density of H_2O (1 g/cm^3)	=	198.53 cm^3

Therefore, 198.53 cm^3 of H_2O to apply 198.53 cm^3 of Ethanol

2. Preparation of monometallic (10%wt.Ni and 10%wt.Co) on different support catalyst by incipient wetness impregnation method

Preparation of the monometallic with percent loading of 10%wt.Ni and 10%wt.Co supported on different support catalyst by incipient wetness impregnation method, the composition of catalysts will be as follows;

Precursors: - Nickel (II) nitrate hexahydrata $Ni(NO_3)_2.6H_2O$ >98%

Molecular weight = 290.79 g/mol

- Cobalt nitrate hexahydrate, $Co(NO_3)_2.6H_2O$ >98%

Molecular weight = 290.79 g/mol

Calculation: For percent loading of 10%wt.Ni and 10%wt.Co are shown as follows: Base on 1g of monometallic supported on different supports catalyst:

100g of nickel on different supports catalyst	Consisted of nickel to 10g
1g of nickel on different supports catalyst	Consisted of nickel to 0.1g
100g of cobalt on different supports catalyst	Consisted of cobalt to 10g
1g of cobalt on different supports catalyst	Consisted of cobalt to 0.1g

The amount of nickel required 0.1g was prepares from nickel precursor as $Ni(NO_3)_2.6H_2O$ which had the molecular weight 290.79 g/mol, and the molecular weight of Ni is 58.693 g/mol. Therefore, the amount of nickel precursor can be calculated follows;

$$\text{Ni } (NO_3)_2.6H_2O \text{ required} = \frac{\text{MW of Ni } (NO_3)_2.6H_2O \text{ x nickel required x } 0.98}{\text{MW of Ni}}$$

$$= \frac{290.79 \text{ g/mol x } 0.1\text{g of Ni x } 0.98}{58.693 \text{ g Ni /mol}}$$

$$= 0.485 \text{ g of Ni } (NO_3)_2.6H_2O$$

The amount of cobalt required 0.1g was prepares from nickel precursor as $Co(NO_3)_2.6H_2O$ which had the molecular weight 290.79 g/mol, and the molecular weight of Co is 58.693 g/mol. Therefore, the amount of nickel precursor can be calculated follows;

$$\text{Co } (NO_3)_2.6H_2O \text{ required} = \frac{\text{MW of Co } (NO_3)_2.6H_2O \text{ x cobalt required x } 0.98}{\text{MW of Co}}$$

$$= \frac{290.79 \text{ g/mol} \times 0.1\text{g of Co} \times 0.98}{58.693 \text{ g Co /mol}}$$

$$= 0.485 \text{ g of Co } (NO_3)_2.6H_2O$$

3. Preparation of bimetallic (5%wt.Ni5%wt.Co) on different supports catalyst by incipient wetness impregnation method

The calculation shown below is for 5%wt.NiCo on different supports. The support weight used for all preparation is 1g. Preparation of the bimetallic with percent loading of 5%wt.NiCo catalyst by incipient wetness impregnation method, the composition of catalysts will be as follows;

Precursors: - Nickel (II) nitrate hexahydrata $Ni(NO_3)_2.6H_2O$ >98%

Molecular weight = 290.79 g/mol

- Cobalt nitrate hexahydrate, $Co(NO_3)_2.6H_2O$ >98%

Molecular weight = 290.79 g/mol

Calculation: For percent loading of 5%wt.NiCo are shown as follows:
Base on 1g of bimetallic catalyst:

100g of nickel on different supports catalyst	Consisted of nickel to 5g
1g of nickel different supports catalyst	Consisted of nickel to 0.05g
100g of cobalt on different supports catalyst	Consisted of cobalt to 5g
1g of cobalt on different supports catalyst	Consisted of cobalt to 0.05g

The amount of nickel required 0.05g was prepares from nickel precursor as Ni $(NO_3)_2.6H_2O$ which had the molecular weight 290.79 g/mol, and the molecular weight of Ni is 58.693 g/mol. Therefore, the amount of nickel precursor can be calculated follows;

$$\text{Ni } (NO_3)_2.6H_2O \text{ required} = \frac{\text{MW of Ni } (NO_3)_2.6H_2O \text{ x nickel required x } 0.98}{\text{MW of Ni}}$$

$$= \frac{290.79 \text{ g/mol x } 0.05\text{g of Ni x } 0.98}{58.693 \text{ g Ni /mol}}$$

$$= 0.243 \text{ g of Ni } (NO_3)_2.6H_2O$$

The amount of cobalt required 0.05g was prepares from nickel precursor as $Co(NO_3)_2.6H_2O$ which had the molecular weight 290.79 g/mol, and the molecular weight of Co is 58.693 g/mol. Therefore, the amount of nickel precursor can be calculated follows;

$$\text{Co } (NO_3)_2.6H_2O \text{ required} = \frac{\text{MW of Co } (NO_3)_2.6H_2O \text{ x cobalt required x } 0.98}{\text{MW of Co}}$$

$$= \frac{290.79 \text{ g/mol x } 0.05\text{g of Co x } 0.98}{58.693 \text{ g Co /mol}}$$

$$= 0.243 \text{ g of Co } (NO_3)_2.6H_2O$$

APPENDIX B

CALCULATION FOR THE CRYSTALLITE SIZES

Calculation of the crystallite sizes by Scherrer equation method

The crystallite sizes were calculates from the half-height width of the diffraction peak of X-ray diffraction pattern using the Debye-Scherrer equation.

From Debye-Scherrer equation;

$$D = \frac{\kappa\lambda}{\beta\text{Cos}\theta} \quad \text{(i)}$$

Where D = Crystallite size, Å

K = Crystallite-shape factor = 0.9

λ = X-ray wavelength, 1.54056 Å for Cu$K\alpha$

θ = Observed peak angle, degree

β = X-ray diffraction broadening, radian

The X-ray diffraction broadening (β) can be obtained by using Warren's formula.

From Warren's formula

$$\beta^2 = \beta^2_m - \beta^2_s \quad \text{(ii)}$$

Therefore $\beta = \sqrt{\beta_m^2 - \beta_s^2}$

Where β_m = the measured peak width in radians at half peak height

β_s = the corresponding width of a standard material

Example: Calculation of the crystallite size of NiO on H-Beta-Al_2O_3 support

The half-height width of peak = 0.229007° (from Figure B.1)

= 0.229007 X 0.0174

= 0.003997 radian

The corresponding half-height width of peak H-Beta standard = 0.000394

Therefore $\beta = \sqrt{\beta_m^2 - \beta_s^2}$

$= \sqrt{0.003997^2 - 0.000394^2}$

= 0.003996926 radian

β = 0.003996 radian

2θ = 22.661°

θ = 0.197755 radian

λ = 1.54056 Å

The crystallite size $= \dfrac{0.9 \text{ X } 1.54056}{(0.003996) \text{ Cos } 0.197755}$

= 353.79 Å

= 35.38 nm.

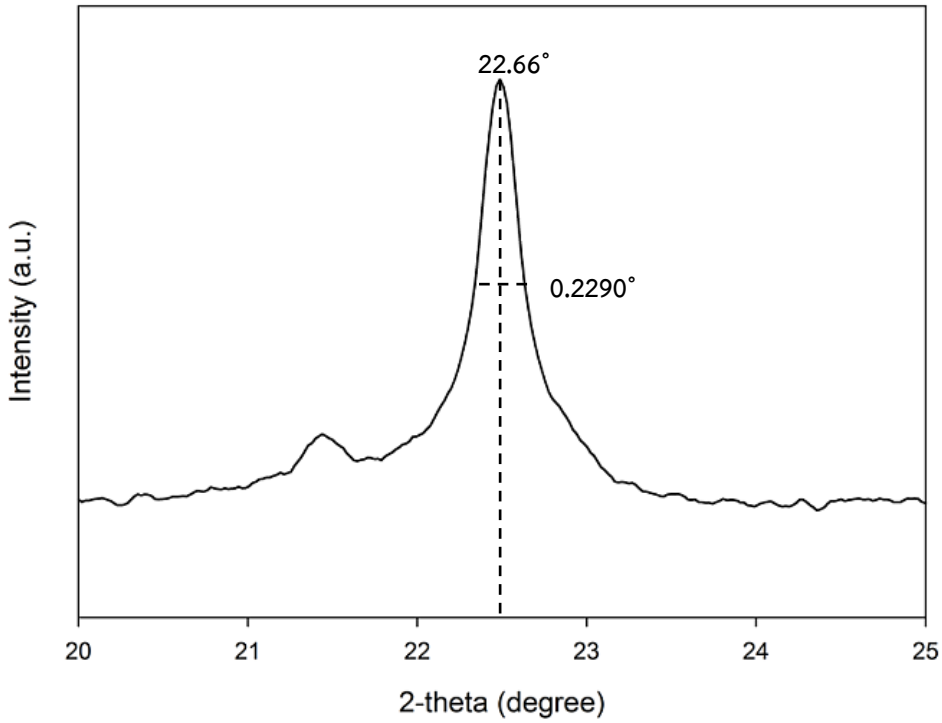

Figure B.1 The measured peak of 10%Ni/H-Beta-Al_2O_3 to calculate the crystallite size

APPENDIX C

CALCULATION FOR THE TOTAL ACID SITES OF CATALYSTS

Calculation of the total acid sites by Ammonia temperature program desorption (NH_3-TPD) is as follows;

1. Conversion of total peak area to peak volume

Conversion from Micrometrics Chemisorb 2750 is equal to 77.57016 ml/area unit. Therefore, total peak volume is derived from

Example: The H-Beta-Al_2O_3 supported has the total peak area to 1.64

Total peak volume = 77.57016 X total peak area
= 77.57016 X 1.64
= 47.30432 ml

2. Calculation for adsorbed volume of 15% NH_3

Adsorbed volume of 15% NH_3 = 0.15 X total peak volume
= 0.15 X 47.30432 ml
= 7.0956 ml

3. Total acid sites are calculated from the following equation

$$\text{Total acid site} = \frac{\text{(Adsorbed volume, ml) x 101.325 Pa}}{\text{8.314 (Pa.ml/K.mmol) x 298 K x (weight of catalyst, g)}}$$

For the H-Beta-Al_2O_3 support, used 0.1016 g of this sample was measured.

Therefore:

$$\text{Total acid site} = \frac{7.0956 \text{ ml} \times 101.325 \text{ Pa}}{8.314 \text{ (Pa.ml/K.mmol)} \times 298 \text{ K} \times 0.1016 \text{ g}}$$

$$= 0.2856 \text{ mmol } H^+/\text{g}$$

APPENDIX D

CALCULATION FOR H_2 CHEMISORPTION

Calculation of the metal active sites and metal dispersion by H_2 chemisorption is as follows;

Volume of active gas dosed from a loop (V_{inj})

$$V_{inj} = V_{loop} \times \frac{T_{std}}{T_{amb}} \times \frac{P_{amb}}{P_{std}} \times \frac{\%A}{100\%}$$

Where;

V_{loop}	=	loop volume injected	100 μL
T_{amb}	=	ambient temperature	295.15 K
T_{std}	=	standard temperature	273.15 K
P_{amb}	=	ambient pressure	760 mmHg
P_{std}	=	ambient pressure	760 mmHg
%A	=	% active gas	100%

Therefore;

$$V_{inj} = 100\ \mu L \times \frac{273.15K}{295.15K} \times \frac{760\ mmHg}{760\ mmHg} \times \frac{100\%}{100\%}$$

$$= 92.546\ \mu L$$

Volume chemisorbed (V_{ads})

$$V_{ads} = \frac{V_{inj}}{m} \times \sum_{i=1}^{n} \left[1 - \frac{A_i}{A_f}\right]$$

Example; for H_2 chemisorption on 10%wt.Ni/H-Beta-Al_2O_3 is shown as follow;

V_{inj}	=	volume injected	92.546 μL
m	=	mass of sample	0.1006 g
A_f	=	area of last peak	0.0403

Peak	A_i	A_i/A_f	1- A_i/A_f	V_{ads}
1	0.03305	0.820099	0.179901	165.4982
2	0.04042	1.002978	0.002978	2.739281
3	0.04006	0.994045	0.005955	5.478563
4	0.04038	1.001985	0.001985	1.826188
5	0.0403	1	0	0
Sum				**175.5423**

V_{ads} = 175.5423 μL/g

= 0.175542 cm^3/g

%Metal dispersion

$$\%D = S_f \times \frac{V_{ads}}{V_g} \times \frac{M.W.}{\%M} \times 100\% \times 100\%$$

Where;

S_f	=	stoichiometry factor, H_2 on Ni	2
V_{ads}	=	volume adsorbed	0.175542 cm^3/g
V_g	=	molar volume of gas at STP	22414 cm^3/mol
M.W.	=	molar weight of metal	290.79 g/mol
%M	=	weight percent of active metal	10%

$$\%D = 2 \times \frac{0.175542\ cm^3/g}{22414\ cm^3/mol} \times \frac{290.79\ g/mol}{1\%} \times 100\% \times 100\%$$

$$= 4.57\%$$

Nickel active sites

$$\text{Ni active sites} = S_f \times \frac{V_{ads}}{V_g} \times N_A$$

Where;

S_f	=	stoichiometry factor, H_2 on Ni	2
V_{ads}	=	volume adsorbed	0.175542 cm^3/g
V_g	=	molar volume of gas at STP	22414 cm^3/mol
N_A	=	Avogadro's number	6.023×10^{23} molecules/mol

$$\text{Ni active sites} = 2 \times \frac{0.175542\ cm^3/g}{22414\ cm^3/mol} \times \frac{6.023 \times 10^{23}\ \text{molecules}}{mol}$$

$$= \frac{6.33 \times 10^{23}\ H_2\ \text{molecules}}{g}$$

APPENDIX E

CALIBRATION CURVES

The calibration curves are used for calculation of the composition of reactant and product in carbon dioxide reforming of methane. The reactant are methane and carbon dioxide, the main product are hydrogen and carbon monoxide in carbon dioxide reforming of methane reaction.

The Thermal Conductivity Detector (TCD), gas chromatography Shimadzu model 8A was used to analyze the concentration of the products and reactants by molecular sieve 5A and porapack-Q column.

Mole of reagent showed y-axis and the area reported by gas chromatography showed the x-axis are exhibited in the curve. The calibration curves of methane, carbon dioxide, hydrogen and carbon monoxide are illustrated in the following figure E1-E4, respectively.

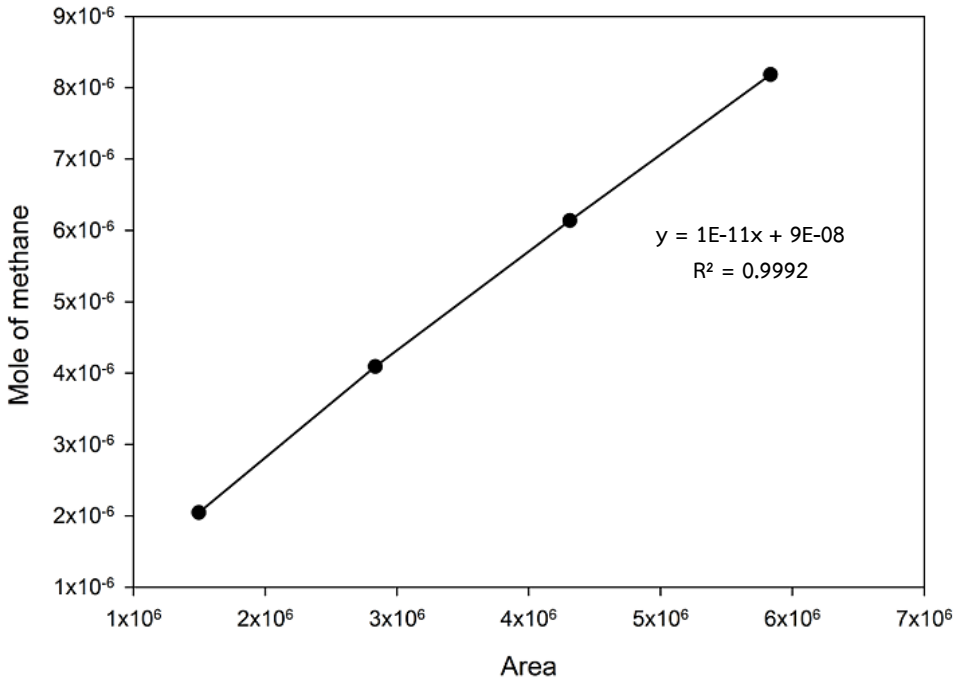

Figure E.1 The calibration curve of methane

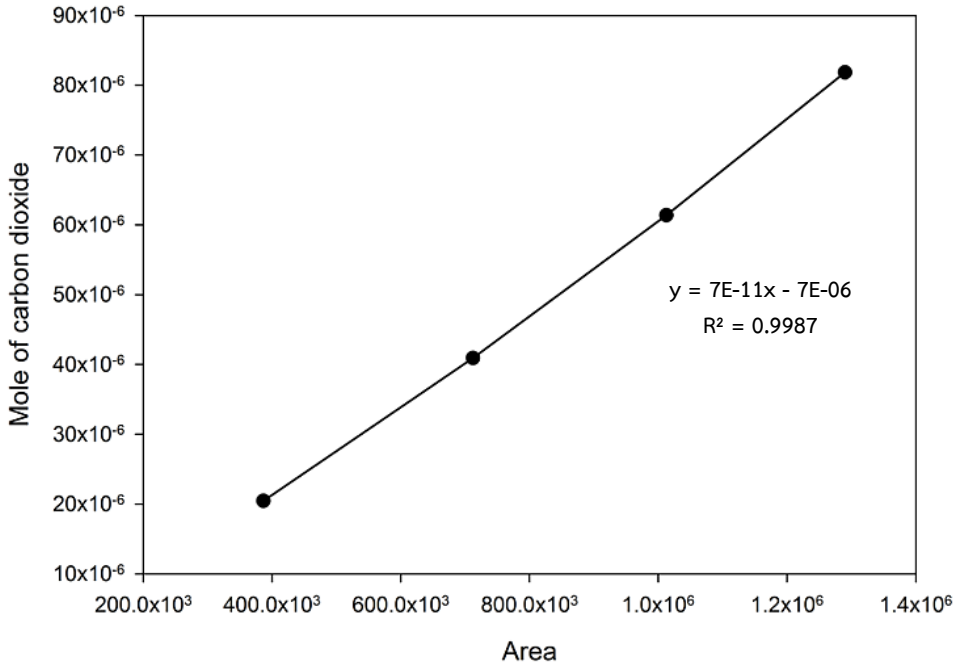

Figure E.2 The calibration curve of carbon dioxide

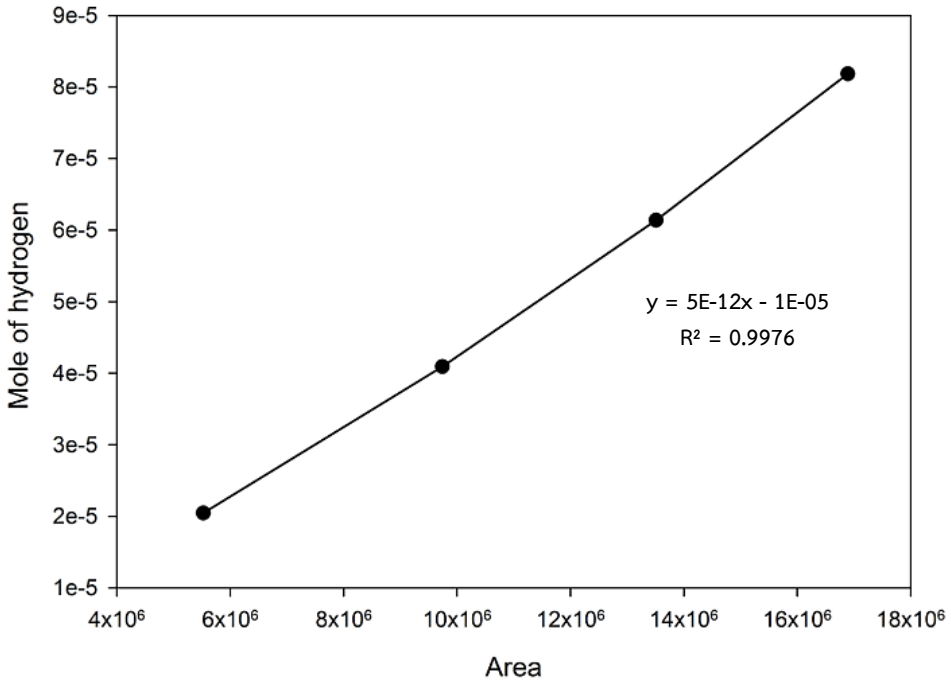

Figure E.3 The calibration curve of hydrogen

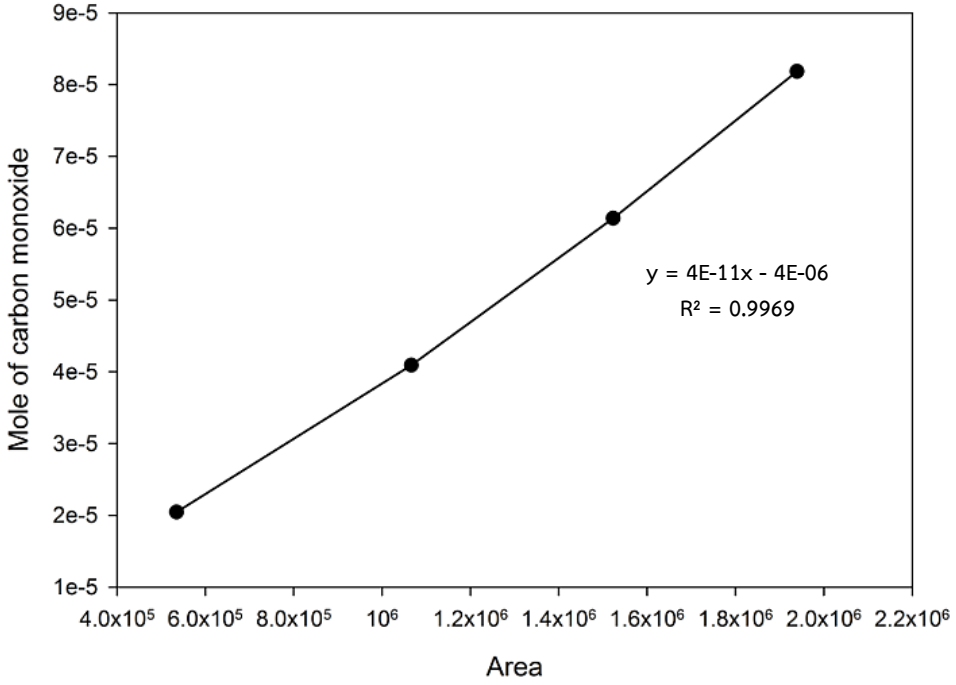

Figure E.4 The calibration curve of carbon monoxide

APPENDIX F

CALCULATION CONVERSION AND SELECTIVITY IN CARBON DIOXIDE REFORMING OF METHANE

The catalytic performance for the carbon dioxide reforming of methane was evaluated in term of activity for methane and carbon dioxide conversion.

Methane and carbon dioxide conversion are defined as moles of methane and carbon dioxide converted with respect to reactant in feed as follows:

$$CH_4 \text{ conversion (\%)} = \frac{(\text{mole of } CH_4 \text{ in feed} - \text{mole of } CH_4 \text{ in product}) \times 100}{\text{mole of } CH_4 \text{ in feed}}$$

$$CO_2 \text{ conversion (\%)} = \frac{(\text{mole of } CO_2 \text{ in feed} - \text{mole of } CO_2 \text{ in product}) \times 100}{\text{mole of } CO_2 \text{ in feed}}$$

Hydrogen and carbon monoxide selectivity are defined as moles of hydrogen and carbon monoxide converted with respect to product in out of reaction as follows:

$$H_2 \text{ selectivity (\%)} = \frac{\text{mole of } H_2 \text{ in product} \times 100}{(\text{mole of } H_2 \text{ in product} + \text{mole of CO in product})}$$

$$\text{CO selectivity (\%)} = \frac{\text{mole of CO in product} \times 100}{(\text{mole of } H_2 \text{ in product} + \text{mole of CO in product})}$$

VITA

Miss Pornthicha Katong was born in March 30th, 1991 in Lampang, Thailand. She finished high school from Assumption College Lampang, Lampang in 2009. After that, she certificate from the Bachelor's degree in Chemical Engineering, faculty of Engineering and Industrial Technology, Silpakorn University of Sanam Chandra Palace Campus, Nakhon Pathom, Thailand in April 2013. Thereafter, she continued to study in Master's degree of Chemical Engineering, department of Chemical Engineering, faculty of Engineering, Chulalongkorn University, Bangkok, Thailand since 2013 and joined of center of excellence on catalytic reaction engineering research group.

Pornthicha Katong and Suphot Phatanasri, "CO2 reforming of methane on Ni,Co-containing Al2O3-H-Beta zeolite prepared by Sol-gel method", proceeding of the Pure and Applied Chemistry International Conference 2015 (PACCON), Bangkok, Thailand, Jan. 21-23, 2015.